UNDERSTANDING FEMALE BREAST SHAPE TO IMPROVE BRA SIZING VIA 3D AND 4D BODY SCANNING TECHNOLOGY

A Dissertation

Presented to the Faculty of the Graduate School

of Cornell University

In Partial Fulfillment of the Requirements for the Degree of

Doctor of Philosophy

by

Jie Pei

May 2020

© 2020 JIE PEI

UNDERSTANDING FEMALE BREAST SHAPE TO IMPROVE BRA SIZING VIA 3D AND 4D BODY SCANNING TECHNOLOGY

Jie Pei, Ph. D.

Cornell University 2020

Due to the limitation of traditional linear body measurements in representing the complicated three-dimensional (3D) shape of female breast, in this dissertation, alternative methods to study breast shape for product development were explored. In two-dimension (2D), topographic contour maps were created and an Asymmetry Index was proposed to quantify the degree of asymmetry between the left and right breasts. This 2D system was used in the aesthetic evaluation of nude breast and the shaping effects of structured-bras and soft-bras. In 3D, two methods of handling 3D body scans were proposed, which capture data throughout the surface of the scan systematically. Both the 2D and 3D systems eliminate the need of palpation to find anatomical body landmarks, on which the accuracy of traditional measurements depend.

In four-dimension (4D), 4D body scanning technology was introduced to quantitively study breast shape under motion. Moreover, while the information of the upper boundary of the breasts is missing on 3D scans, it can be retrieved with the help of 4D scanning, by taking advantage of the time delay in the vertical displacement between the breasts and the chest wall during physical activity. This method is essential for the accurate separation of the breasts: to acquire critical anthropometric measurements such as breast volume, and to make complete the 3D breast-shape evaluation system.

Product development of bras still relies on human fit models. Aggregate-fit-loss is a concept attempting to estimate the accumulative fit-loss, resulting from the body-shape discrepancy, between the fit models and individual consumers. Based on the 3D evaluation system, a feasible solution to optimize the sizing system of bras was proposed, to minimize the aggregate-fit-loss by shape categorization and optimized selection of fit models. For the industry, the method overcomes the challenge of finding ideal fit models, filling the lack of a reliable selection criteria. For consumers, technological solutions were also presented for finding their shape-based selection of products that may best fit them. With 3D scanner becoming more accessible and the development of cellphone scanning, methods presented in this dissertation might bring revolutionary changes in apparel sizing and how bra products are made.

BIOGRAPHICAL SKETCH

Jie Pei was born and raised in Northern China. She attended Donghua University in Shanghai, China, majored in Fashion Design and Engineering, and obtained the degree of Bachelor of Engineering in 2014. She pursued her Master's degree at the Department of Fiber Science and Apparel Design, Cornell University. She was supervised by Dr. Huiju Park and obtained the degree of Master of Arts in Apparel Design in 2016. She continued her study as a PhD student at Cornell University, under the supervision of Dr. Jintu Fan. Her research interests include understanding the interactions between clothing and human body, anthropometry and body scanning technology.

I dedicate this dissertation to my dad and Duke,

the two most important men in my life

ACKNOWLEDGMENTS

I would like to express my very great appreciation to my PhD advisor Prof. Jintu Fan for all his efforts over the past four years in helping me to grow as a researcher. His valuable guidance, patience, helpfulness, and willingness to give his time generously have been very much appreciated.

I also gained great insight from my minor committee members, Prof. Edwin Kan and Prof. Robert Shepherd. I truly appreciate all their time and suggestions. I am also very grateful to Prof. Linsey Griffin from University of Minnesota, without her, I would not have access to the facility of a 4D body scanner and never be part of the research project that led to two chapters of this dissertation.

I would also like to offer my special thanks to Prof. Susan Ashdown, who has always been extremely helpful, encouraging, supportive, warm and kind throughout my six long years at Cornell. She has been an amazing mentor to me: comforts me when I feel discouraged, offers inspiring advice when I need them, connects me to the right people and resources to help me be successful. Even after she officially retired from the department, she always responds to my meeting requests and selflessly offers her time and help. I am deeply inspired by her and hope that one day I might become a caring professor just like herself.

I wish to acknowledge my parents, Jun Pei and Qianru Liu, my grandmother Yujin Wang, and my late grandfather Huancheng Pei. They have been the best family, without whose support I would never be able to finish grad school in the US.

My grateful thanks also extend to my brothers and sisters in Christ from the First Ithaca Chinese Christian Church, Twin City Chinese Christian Church, Hong Kong Mandarin Bible Church, and Canberra Chinese Christian Church, especially brothers and sisters from Cornell Chinese Christian Fellowship, Living Water Fellowship, The

Chinese University of Hong Kong Student Fellowship, and Daniel Fellowship, for their love, tolerance, support and prayers.

Last but not least, I would like to thank Jesus my God and my Lord for all His blessings in my life and for His eternal love.

TABLE OF CONTENTS

CHAPTER 1

INTRODUCTION

Background

Studies have shown that up to 85% of women have experienced bra fit issues (McGhee & Steele, 2010). Another study showed that 65% of the female participants had the experience of wearing uncomfortable bras (Nethero, 2008). The discomfort can result from insufficient support of cups, underwire pain, bra straps digging into or sliding off the shoulders, etc. (Nethero, 2008). Moreover, a bra that fits poorly can put the wearer's health and well-being at risk. Back pain, shoulder pain and neck pain are commonly reported symptoms due to the insufficient support provided by bras (Greenbaum, Heslop, Morris & Dunn, 2003). Women with severe musculoskeletal pain sometimes seek mammoplasty to be released from the symptoms (Greenbaum, Heslop, Morris & Dunn, 2003). For women who have professions that rely on personal protective equipment (PPE), such as body armor, turnout gear, fall harness systems, etc., poor fit in the bust area may cause the failure of the entire protection system (Todd, 2007). Therefore, for product designers, understanding breast shape is of great importance. For plastic surgeons, this knowledge is critical for achieving optimal surgical outcome and thus protecting patients' physical and psychological well-being (Kim et al., 2007; Kovacs et al., 2007). With breast cancer becoming a serious health concern for women nowadays, this knowledge is also extremely important for healthcare providers to establish breast care guidelines (Kim et al., 2007).

The female breast has a complex structure, composed of mammary glands, subcutaneous tissue and skin (Page & Steele, 1999). Each of these sub-structures,

especially due to the amount of adipose tissue, differs greatly among individuals, resulting in tremendous variations in the density, shape and size of the breast among individuals. Variations in breast volume were reported to range from 330 cc to 2600 cc among a group of only 101 females (Sigurdson & Kirkland, 2006). McGhee and Steele (2011) also measured the breasts of 104 females, and found a range of breast volume, from 125 to 1900 ml for the right breast, and from 100 to 1825 ml for the left breast. Moreover, breast shapes have been descriptively grouped into various types based on a variety of characteristics, for example, based on the degree of separation between two breasts, the fullness of the upper breast, the directions that the nipples point, or the relative position of the breasts on the chest, etc. (Herroom.com, n.d.). Furthermore, breast shape can be heavily influenced by hormone levels so that even for the same female, breast shape goes through many changes. Changes occur throughout a woman's life, especially pre, during, or post pregnancy, nursing, and menopause (Tiggemann, 2004; Lawrence & Lawrence, 2011). Other factors such as age and body weight can also affect her breast size (Lawrence & Lawrence, 2011).

Due to the diverse and complicated geometry of female breast and the soft, deformable nature of the breast, it is very difficult to take reproducible and accurate measurements (Westreich, 1997). Many design challenges for female wearable products also arise because of the diverse geometry of the breast (Hart & Dewsnap, 2001). The constantly changing curvature on the breast surface and the ambiguous boundary between the breast and the chest wall add to the difficulty in objectively evaluating breast shape (Lee, Hong & Kim, 2004).

Literature Review

A detailed review of literatures addressing breast shape, specifically studies of subjective and objective assessments of nude breasts, can be found in Chapter 2,

Section 2.1.

The literature review of breast shape studies that focus on the product development of bras and garments, can be found in Chapter 4, Section 1.2.

The literature review of traditional bra/breast sizing and attempts to improve the sizing of bras in recent years can be found in Chapter 6, Section 1.1.

Literature reviews of other specific topics related to breast shape can be found within each chapter (e.g. studies of breast asymmetry in Chapter 2, Section 2.2; studies of the interaction between bras and breasts in Chapter 3, Section 1). In order to keep this dissertation concise, they were not repeated in this introductory section.

Research Gaps

Based on the literature review, the following research gaps have been identified:

1) Most methods to measure the body for clothing depend on various linear body measurements such as circumferences, lengths, widths, etc. (Bye, LaBat, DeLong, 2006; Kovacs et al., 2007; Chen, LaBat & Bye, 2010; Oh & Chun, 2014). Linear measurements generally refer to the distance between two points on the three-dimensional surface of the body (Bye, LaBat & DeLong, 2006). One most traditional way of taking linear measurements is via the use of tape measure by tailors and fashion designers since the 18th century. However, the traditional 1D (linear) measurements are not sufficient to describe complicated 3D shapes, especially for the complexities of female breasts (Bye, Labat & Delong, 2006; Chen, LaBat & Bye, 2011; Ashdown, 2014; Peterson & Suh, 2019).
2) Since the reliability of traditional body measurements depends highly on the accurate placement of anatomical body landmarks, which cannot generally be achieved using automatic landmark detection (Lu & Wang, 2008; Han & Nam, 2011), the placement of landmarks still relies on manual operations, which are

time-consuming, counteracting the benefits of the rapid collection of data offered by 3D body scanning. Moreover, it is very difficult to define meaningful and reliable landmarks, other than the nipples, on the soft breast tissue.

3) Quite a few studies on the aesthetics of breast shape can be found in past studies (Hsia & Thomson, 2003; Lau, 2014; Catanuto et al., 2008). However, most of these studies rely only on the visual judgements based on photos, drawing, illustrations, and/or subjective ratings, which can be affected by individual preference and personal bias. The development of objective evaluation tools can increase the usefulness of the subjective evaluation results.
4) Very few studies that quantitatively investigate the interactions between bras and breasts were found. In these limited studies the researchers generally reported only changes in breast measurements between the nude state and when wearing a bra instead of reporting the changes in breast shape (Ashizawa, Sugane & Gunji, 1990; Scurr, Loveridge, Brown & Mills, 2015).
5) Although there has been much research into breast kinematics during physical activity (Lorentzen & Lawson, 1987; Mason, Page & Fallon, 1999; Starr et al., 2005; Scurr, White & Hedger, 2009 & 2011; Haake & Scurr, 2010; McGhee, Steele, Zealey & Takacs, 2013), most studies only report the displacement of the nipples and a few other marker points. 4D body scanning makes it possible to capture the overall shape changes of the breasts in motion, but this new technology has not yet been used to study breast shape and therefore inform bra design.
6) It is commonly believed that the existing bra sizing systems satisfy neither the manufacturers nor the consumers (McCulloch, Paal & Ashdown, 1998; Zheng, Yu & Fan, 2007; Peterson & Suh, 2019). Although attempts to classify breast shape to inform sizing have been proposed (Zheng, Yu & Fan, 2007; Liu, Wang & Istook, 2017; Coltman, Steele & McGhee, 2018), the results are difficult to put into

practice due to the lack of a solution for consumers to easily identify their own breast shape and size (Kinley, 2003; Petrova, 2007; Chun, 2007).

Research Objectives

To address the six identified research gaps, six corresponding research objectives were summarized as follows.

1) To reduce the reliance on traditional 1D (linear) body measurements and explore alternative methods to evaluate breast shape using both 2D and 3D measures.
2) To develop systems to analyze breast shape that do not rely on traditional physical placement of anatomical landmarks.
3) To use these systems to quantitatively and objectively evaluate breast shape while incorporating both visual judgements and subjective evaluations.
4) To use these systems to study the interactions between bra products and breasts.
5) To extend the use of these systems in 4D (the fourth dimension being time), to study breast kinematics and shape change of breasts during physical activity.
6) To propose a feasible solution to optimize or improve the sizing system for bras that is based on the 3D shape of natural breasts, with solutions to apply the breast-shape categorization results in practice.

Dissertation Layout

The main section of this dissertation contains five chapters: three chapters are peer-reviewed journal papers that are already published (Chapter 2, 3 and 6), while the other two chapters are manuscripts that are under review (Chapter 4 and 5). The content of each chapter is listed as follows:

Chapter 2 presents a novel way to evaluate natural breast shape via 2D topographic contour maps. An Asymmetry Index is proposed to quantify the degree of

asymmetry between the left and right breasts. The method and index can be useful in the aesthetic evaluation of nude breast shape and the shaping effects of bra products.

Chapter 3 utilizes the method and the Asymmetry Index presented in Chapter 1 to study the effects of structured-bras and soft-bras on the breast shape. Regression models are built to predict the in-bra shape given only the nude breast shape. The results can be helpful in understanding how bras interact with the breast tissue using a quantitative measure.

Chapter 4 introduces the use of 4D body scanning technology to understand breast shape under motion. A protocol to handle and analyze 4D data for application in product design is developed to inform future research. Ten breast shape related measurements are tracked in dynamic states and compared with the static state. The promises and challenges of the 4D body scanning technology are also discussed.

Chapter 5 further introduces the use of the 4D body scanning to propose a non-contact method to detect the upper boundary of the breasts, by taking advantage of the time delay in the vertical displacement between the breasts and the chest wall during physical activity. The method and results can be informative for a more accurate acquisition of anthropometric measurements such as breast volume, which is directly associated with the cup size of bras.

Chapter 6 reports on a novel and feasible method to improve the sizing system for bras based on the 3D shape of natural breasts, by minimizing the aggregate-fit-loss of the sizing system. In addition, a solution that facilitates the selection of human fit models with the most representative breast shapes is presented. Solutions to help consumers to find their best-fitting sizes are also presented.

Chapter 7 includes a condensed version of the conclusions drawn from the main chapters, summarized with respect to the research objectives. Suggestions for future work are included at the end.

REFERENCES

Ashizawa, K., Sugane, A., & Gunji, T. (1990). Breast form changes resulting from a certain brassiere. *Journal of human ergology*, *19*(1), 53-62.

Ashdown, S. P. (2014). Creation of ready-made clothing: The development and future of sizing systems. In Faust, M. E., & Carrier, S.(Eds.), *Designing Apparel for Consumers: The Impact of Body Shape and Size* (pp. 17-33). Woodhead Publishing.

Bye, E., Labat, K. L., & Delong, M. R. (2006). Analysis of body measurement systems for apparel. *Clothing and Textiles Research Journal*, *24*(2), 66-79.

Chun, J. (2007). Communication of sizing and fit. *Sizing in clothing: Developing effective sizing systems for ready-to-wear clothing*, 220-243.

Catanuto, G., Spano, A., Pennati, A., Riggio, E., Farinella, G. M., Impoco, G., ... & Nava, M. B. (2008). Experimental methodology for digital breast shape analysis and objective surgical outcome evaluation. *Journal of Plastic, Reconstructive & Aesthetic Surgery*, *61*(3), 314-318.

Chen, C. M., LaBat, K., & Bye, E. (2010). Physical characteristics related to bra fit. *Ergonomics*, *53*(4), 514-524.

Chen, C. M., LaBat, K., & Bye, E. (2011). Bust prominence related to bra fit problems. *International Journal of Consumer Studies*, *35*(6), 695-701.

Coltman, C. E., Steele, J. R., & McGhee, D. E. (2018). Effects of age and body mass index on breast characteristics: a cluster analysis. *Ergonomics*, *61*(9), 1232-1245.

Greenbaum, A. R., Heslop, T., Morris, J., & Dunn, K. W. (2003). An investigation of the suitability of bra fit in women referred for reduction mammaplasty. *British journal of plastic surgery*, *56*(3), 230-236.

Hart, C., & Dewsnap, B. (2001). An exploratory study of the consumer decision process for intimate apparel. *Journal of Fashion Marketing and Management: An International Journal*, *5*(2), 108-119.

Hsia, H. C., & Thomson, J. G. (2003). Differences in breast shape preferences between plastic surgeons and patients seeking breast augmentation. *Plastic and Reconstructive Surgery*, *112*(1), 312-320.

Haake, S., & Scurr, J. (2010). A dynamic model of the breast during exercise. *Sports engineering*, *12*(4), 189-197.

Han, H., & Nam, Y. (2011). Automatic body landmark identification for various body figures. *International Journal of Industrial Ergonomics*, *41*(6), 592-606.

Herroom.com (n.d.). Classify your breasts. Retrieved Mar 2020 from https://www.herroom.com/breast-separation,333,30.html

Kinley, T. R. (2003). Size variation in women's pants. *Clothing and Textiles Research Journal*, *21*(1), 19-31.

Kim, M. S., Reece, G. P., Beahm, E. K., Miller, M. J., Atkinson, E. N., & Markey, M. K. (2007). Objective assessment of aesthetic outcomes of breast cancer treatment: measuring ptosis from clinical photographs. *Computers in Biology and Medicine*, *37*(1), 49-59.

Kovacs, L., Eder, M., Hollweck, R., Zimmermann, A., Settles, M., Schneider, A., ... & Biemer, E. (2007). Comparison between breast volume measurement using 3D surface imaging and classical techniques. *The Breast*, *16*(2), 137-145.

Lorentzen, D. & Lawson, L. (1987). Selected Sports Bras: A Biomechanical Analysis of Breast Motion.*Physician and Sports Medicine 15*(5), 128-139.

Lee, H. Y., Hong, K., & Kim, E. A. (2004). Measurement protocol of women's nude breasts using a 3D scanning technique. *Applied Ergonomics*, *35*(4), 353-359.

Lu, J. M., & Wang, M. J. J. (2008). Automated anthropometric data collection using 3D whole body scanners. *Expert Systems with Applications, 35*(1), 407-414.

Lawrence, R. A., & Lawrence, R. M. (2011). *Breastfeeding: a guide for the medical profession*. Elsevier Health Sciences.

Lau, W. F. (2014). *Development of seamless knitted bra for optimum fit*. (Doctoral dissertation, Hong Kong Polytechnic University, Hong Kong, China). Retrieved from http://hdl.handle.net/10397/6859

Liu, Y., Wang, J., & Istook, C. L. (2017). Study of optimum parameters for Chinese female underwire bra size system by 3D virtual anthropometric measurement. *The Journal of The Textile Institute*, *108*(6), 877-882.

McCulloch, C. E., Paal, B., & Ashdown, S. P. (1998). An optimisation approach to apparel sizing. *Journal of the Operational Research Society*, *49*(5), 492-499.

Mason, B. R., Page, K. A., & Fallon, K. (1999). An analysis of movement and discomfort of the female breast during exercise and the effects of breast support in three cases. *Journal of Science and Medicine in Sport, 2*(2), 134-144.

McGhee, D. E., & Steele, J. R. (2010). Optimising breast support in female patients through correct bra fit. A cross-sectional study. *Journal of Science and Medicine in Sport*, *13*(6), 568-572.

McGhee, D. E., & Steele, J. R. (2011). Breast volume and bra size. *International Journal of Clothing Science and Technology*, *23*(5), 351-360.

McGhee, D. E., Steele, J. R., Zealey, W. J., & Takacs, G. J. (2013). Bra–breast forces generated in women with large breasts while standing and during treadmill running: Implications for sports bra design. *Applied ergonomics*, *44*(1), 112-118.

Nethero, S. (2008). *U.S. Patent Application No. 11/829,568*.

Oh, S., & Chun, J. (2014). New breast measurement technique and bra sizing

system based on 3D body scan data. *Journal of the Ergonomics Society of Korea*, *33*(4), 299–311.

Page, K. A., & Steele, J. R. (1999). Breast motion and sports brassiere design. *Sports Medicine*, *27*(4), 205-211.

Petrova, A. (2007). Creating sizing systems. *Sizing in clothing: Developing effective sizing systems for ready-to-wear clothing*, 57-87.

Peterson, A., & Suh, M. (2019). Exploratory Study on Breast Volume and Bra Cup Design. *Journal of Textile and Apparel, Technology and Management*, *11*(1).

Starr, C., Branson, D., Shehab, R., Farr, C., Ownbey, S., & Swinney, J. (2005). Biomechanical analysis of a prototype sports bra. *Journal of Textile and Apparel, Technology and management*, *4*(3), 1-14.

Sigurdson, L. J., & Kirkland, S. A. (2006). Breast volume determination in breast hypertrophy: an accurate method using two anthropomorphic measurements. *Plastic and reconstructive surgery*, *118*(2), 313-320.

Scurr, J., White, J., & Hedger, W. (2009). Breast displacement in three dimensions during the walking and running gait cycles. *Journal of Applied Biomechanics*, *25*(4), 322-329.

Scurr, J. C., White, J. L., & Hedger, W. (2011). Supported and unsupported breast displacement in three dimensions across treadmill activity levels. *Journal of sports sciences*, *29*(1), 55-61.

Scurr, J., Loveridge, A., Brown, N., & Mills, C. (2015). Acute changes in clinical breast measurements following bra removal: Implications for surgical practice. *JPRAS Open*, *3*, 22-25.

Tiggemann, M. (2004). Body image across the adult life span: Stability and change. *Body image*, *1*(1), 29-41.

Todd, W. L. (2007). Sizing for the military. In Sizing in Clothing (pp. 277-308).

Woodhead Publishing.

Westreich, M. (1997). Anthropomorphic breast measurement: protocol and results in 50 women with aesthetically perfect breasts and clinical application. *Plastic and reconstructive surgery*, *100*(2), 468-479.

Zheng, R., Yu, W., & Fan, J. (2007). Development of a new Chinese bra sizing system based on breast anthropometric measurements. *International Journal of Industrial Ergonomics*, *37*(8), 697-705.

CHAPTER 2

A NOVEL METHOD TO ASSESS BREAST SHAPE AND BREAST ASYMMETRY

Abstract

Inspired by topography, a new way of systematically extracting breast measurements is proposed and used in analyzing breast shape. Furthermore, we propose an Asymmetry Index to quantify the degree of asymmetry between left and right breasts. The nude breasts of 46 Caucasian females (BMI below 30, age range: 18-45) were 3D scanned and studied. Contour maps that depict the shape of the breast are generated by slicing the breast scans into sections that are perpendicular to the orientation of the bust point. Contour maps are then converted into a spider-web-like structures. Thirty-five measurements are extracted from the web-like structures. Four shape factors were derived from Principal Component Analysis: 1) the vertical position of the bust point, 2) the volume of the breast, 3) the horizontal position of the bust point, and 4) the fullness of the breast. Representative 3D breast shapes were found for the 46 subjects, categorizing this population into four groups. For intimate apparel designers, the representative shapes are informative for dress form construction, bra cup molding, etc. The new method and proposed index can also be useful in the aesthetic evaluation of breast shapes and improvement of bra products. Moreover, it can serve as a tool for plastic surgeons to develop optimal operation plans and to evaluate surgical outcomes.

1. Introduction

The female breast is a complex structure of skin, mammary glands and

subcutaneous tissue. It was reported that generally the breast has a diameter of 10 to 12 centimeters, and a central thickness of 5 to 7 centimeters (Yu, Fan, Ng & Harlock, 2014). However, due to the variation in the amount of adipose tissue inside a breast, breasts can vary greatly in geometry. Pregnancy and lactation can cause breasts to increase in volume. Aging and menopause can transform breast size and shape. Compared with other morphological characters, breasts generally have higher degrees of developmental instability (Møller, Soler & Thornhill,1995). The diverse geometry in breast shape makes it very hard to take accurate and reproducible measurements (Westreich, 1997). The inherent ambiguity in the boundary between breast and chest wall, as well as the constantly changing curvature on the breast surface, contribute to the difficulty in the objective evaluation of breast shape in a systematic way (Lee, Hong & Kim, 2004).

Despite the challenges, quantifying the 3D shape of breasts and their variation among the population is crucially important, especially for intimate apparel designers and plastic surgeons. Breast aesthetics can have both physical and emotional influences for women (Neto et al., 2012). The location of breasts on the chest wall, and the size and shape of breasts contribute to overall breast aesthetics (Chan et al., 2011). The shape, volume and symmetry of breasts are the most significant factors impacting patient satisfaction after cosmetic surgery (Isogai et al., 2006). A precise measurement of breast geometry is critical for achieving optimal surgical outcomes and for protecting patients' health and well-being (Kovacs et al., 2007; Kim et al., 2007). For intimate apparel design, accurate measurement of breast shape is essential to the development of bra sizing systems (Zheng, Yu & Fan, 2007). Without knowing their true breast size and shape, most women tend to select bras that are poorly fitted and uncomfortable to wear (Lee, Hong & Kim, 2004). Furthermore, the knowledge of breast measurements can help healthcare providers, governments and insurance

industry to set up appropriate breast care guidelines to benefit the vast female population (Kim et al., 2007).

Minor asymmetry in breasts can be found in the majority of female population (Edstrom, Robson & Wright, 1977). It may not be of concern for most people. However, some obvious distinctions in breast size and shape may be the result of pathological changes. For instance, giant fibroadenomas can cause one breast to be significantly larger than the other (Park, David & Argenta, 2006). The assessment of breast asymmetry can provide useful information for doctors and plastic surgeons. Scutt, Manning, Whitehouse & Leinster (1997) discovered that breast asymmetry might be one of the predictors for breast cancer. Denoel et al. (2009) suggested that breast asymmetry is an essential indicator of structural idiopathic scoliosis. Breast symmetry is also a key aesthetic requirement for postoperative breast morphology (Edstrom, Robson & Wright, 1977). Researchers also claimed that breast asymmetry has an impact on attractiveness, self-esteem, quality of life and other aspects for females (Singh, 1995; Neto et al., 2012; Chan, Mathur, Slade-Sharman & Ramakrishnan, 2011; Waljee et al., 2008). In addition, breast asymmetry can be an influential factor in bra design. Bras or garments that are designed to resolve the asymmetry issue can be found from filed patents (e.g. Davidson, 2005; Sobah-Wilhelm, 2008).

The purpose of this study is to gain further understanding of the 3D shapes of the nude breasts of the healthy, younger, non-obese Caucasian female population. Inspired by topography, a new way of systematically extracting breast measurements is proposed and used in measurement collection and data analysis. In addition, we propose an Asymmetry Index to quantify the degree of asymmetry between the left and right breast. A few research questions are as follows:

- Question 1: How can breast measurements be extracted and female breast shape be evaluated in a quantitative, systematic way?
- Question 2: How can breast asymmetry be quantitatively evaluated to detect both major and minor asymmetry?
- Question 3: How can nude breast shapes of Caucasian females be categorized and what are the representative 3D shapes for this population?
- Question 4: What are the common shape factors that can be summarized from the population of interest?

2. Literature Review

2.1. Breast shape studies

Kim et al. (2008) reported that subjective assessments on breast aesthetics have been carried out by many plastic surgeons based on a 4-point scale (with or without subscales), 5-point scale, or visual analogue scale. Breast volume, size, shape, contour, and the inframammary fold are the common parameters that are judged in these subjective assessment studies. In addition, Hsia and Thomson (2003) created a 12-scale set of lateral breast profiles for participants to rate, to study the preference in breast shape in terms of upper-pole contour. Their study suggested plastic surgeons and patients may have different opinions regarding ideal breast shape. Lau (2014) proposed a 9-point multi-dimensional breast rating scale, presented in line drawings, based on four attributes, namely, breast size, breast separation, breast projection and breast height. Statistically significant difference was found in the scores among the four attributes, indicating they could not be combined to a single parameter to describe breast shape.

Manual extraction of linear measurements between landmarked points on the body surface, was also widely adopted by researchers (Kim et al., 2008). For example,

Penn (1954) selected 20 “aesthetically perfect” breasts from 150 healthy volunteers, and reported the normative measurements of their breasts, which included nipple to sternal notch distance, nipple to nipple distance, and nipple to midclavicular point distance. Similarly, Westreich (1997) measured 50 ‘aesthetically perfect’ breasts and obtained 22 measurements from each pair of breasts. Nine of these measurements were found to be correlated with breast volume. Tsouskas and Fentiman (1990) measured the anterior breast surface length, from infra-mammary fold to the nipple, on 151 healthy volunteers and 51 patients who underwent breast irradiation treatment. They found that a 1-cm or more difference in this measurement was associated with unsatisfactory cosmetic outcome. Brown et al. (1999) obtained 12 morphometric measurements of 31 female patients who sought reduction or augmentation mammoplasty, and 60 non-patient female volunteers, using a set square, tape measure and ruler. Linear measurements are also manually extracted from photos of breasts in various perspectives, e.g. anterior-posterior view, lateral view, etc. (Kim et al. 2008). They found significant differences in most of the measurements between the patient group and the non-patient group.

Measurements were also taken from 2D images. Sacchini et al. (1991) extracted 4 measurements (e.g. nipple height, nipple to sternal notch distance, etc.) from the 2D frontal images of 148 patients after their treatment for breast cancer. Tumor location and breast size were found to have impacts on these measurements. The researchers also claimed that a conservative surgery (compared with an extensive surgery) typically resulted in more desirable aesthetic outcome. Kim et al. (2007) constructed ratios of distances, extracted from pre-operational photos (oblique views and lateral views on both sides), of 52 patients who sought breast reconstructive surgery, and investigated the relationships between the objective parameters and the subjective rating scores. A good level of consistency was found between the two.

The use of 3D scanning technology has gained popularity in breast shape studies in recent years. Lee, Hong, and Kim (2004) scanned the nude breasts of 37 Korean females, who normally wore bras of size 80A, using 3D phase shifting moirés topography. The authors suggested that radius of curvature is a useful design parameter especially for underwires. Oh and Chun (2014) analyzed the 3D body scans of 32 Korean females selected from Size Korea database, who wore bras with band size 75 (in centimeters). The scans were sliced horizontally at bust level and underbust level to create cross-section planes (i.e. transverse planes). Five measurements, including depth, width, and arc-lengths, were extracted from the planes and used for analysis. They concluded that the noncontact method, i.e. 3D scanning, was useful in measuring sensitive areas on the body. Zheng, Yu and Fan (2007) studied the breast shapes of 456 Chinese female subjects. 103 breast-shape-related measurements, including bust girths, body widths and depths, etc., were extracted from their body scans. The authors performed a Factor analysis and determined that the first factor is relevant to the overall body build, and the second factor relates to the volume of breast. Farinella et al. (2006) studied the geometric shape of female breasts by analyzing clinical cases of breast reconstructive surgery. Patients involved were scanned sitting in a chair leaning backwards. Seven points were chosen as reference points (e.g. Sternal notch point, Xiphoid point, Mid-axillary point, Nipple, etc.). An algorithm was developed to divide the breast surface into four subunits based on these reference points.

Moreover, Kovacs et al. (2007) compared the four most commonly used breast volume calculation methods, which are based on magnetic resonance imaging (MRI), 3D surface scanning, thermoplastic casting, and mathematical calculations, respectively. They concluded that 3D scanning is a promising approach for volume measurements with acceptable measurement accuracy, good participant acceptance,

low operative difficulty and relatively low cost. Kim et al. (2008) also suggested that 3D scanning is capable of generating consistent data to assist objective assessment of breast appearance. In this study, we utilized 3D scanning technology and obtained nude scans of all participants for analysis of the shapes of their breasts.

2.2. Breast asymmetry

Various methods of assessing breast asymmetry have been developed. To assess aesthetics, Singh (1995) studied the impact of breast asymmetry on female attractiveness. He adopted line drawings of female figures differing in breast asymmetry (three levels: none, low or high) as the evaluation tool, and found that both Waist-to-hip ratio and breast asymmetry affected men's judgment of female attractiveness. Waljee, Hu, Newman and Alderman (2008) asked 898 female patients who underwent lumpectomy to rate their self-perceived differences between their treated and untreated breasts, on the following aspects: breast size, breast shape, nipple appearance, breast elevation, etc. The rating was based on a 4-point Likert scale with 1 being "no difference" and 4 being "large difference". They found that higher rating in breast asymmetry was related to higher chance of desiring a reconstruction surgery. Chan, Mathur, Slade-Sharman and Ramakrishnan (2011) investigated 52 patients with developmental breast asymmetry, and evaluated the aesthetic outcome (rated by surgical personnel) after surgical correction. Only 58% of the 52 cases were evaluated as "good" in terms of breast symmetry while 75% were rated "good" in terms of aesthetics. Malata, et al. (1994) assessed the congenital breast asymmetry of 24 patients who received corrective surgery. Two panels of observers, as well as patients themselves, were asked to rate the symmetry score on the scale of 1 to 5. They concluded that subjective evaluation could be biased despite of the lack of evidence of significant errors observed.

Many objective assessments of breast asymmetry involve anthropometric measurements. In addition to subjective rating, Malata, et al. (1994) obtained several linear measurements that relate to bust point position and breast volume (e.g. nipple to sternal notch, center of nipple to inframammary fold, etc.) through stereophotogrammetry. They assigned symmetry scores to the linear measurements to further investigate breast asymmetry. However, they found that breast shape was too complex to be assessed merely by the linear and volume measurements. Møller, Soler and Thornhill (1995) had doctors to manually measure the circumferences (from the midpoint of the sternum to the meeting point between the Musculus pectoralis and the ribs) of both breasts. They also measured the distance from the suprasternal notch to the bust point using frontal perspective photos. They regarded the circumference difference or the distance difference between two breasts as a breast asymmetry indicator, and found that higher degree of asymmetry was observed for large breasts, and for women without children. They also claimed that breast symmetry was a predictor of fecundity and associated with sexual selection. Manning, Scutt, Whitehouse and Leinster (1997) assessed breast asymmetry of 500 women by the volume difference between left and right breasts. Volume was calculated by estimating each breast as a cone, where cone height and radius were obtained from mammograms. They found that breast asymmetry was related to breast volume, age at first childbirth and number of offspring, and claimed that large and symmetric breasts were indicators of high phenotypic quality in women. Grolleau, et al. (1999) reported that 70% of the plastic surgery patients that they had studied had a difference in weight between the two breasts of over 100 grams. Denoel et al. (2009) evaluated breast asymmetry using five manually measured parameters (e.g. suprasternal notch-to-nipple distance, inframammary crease length, etc.) and one parameter, i.e. breast volume, obtained through 3D scan processing software. Strong correlation was found

between the anthropometric measurements and the clinical parameters. Liu, Luan, Mu and Ji (2010) extracted many anthropometric measurements, including nipple to midline distance, breast width, breast volume, etc., from the 3D body scans of 100 female patients who sought breast augmentation surgery, to investigate breast asymmetry. They concluded that 3D scanning could be a useful tool for implant selection to correct breast asymmetry.

Losken et al. (2005) proposed a more sophisticated method using 3D scanning technology. They obtained 3D surface images of the breasts of 87 healthy female volunteers. The mirror image of the left breast was superimposed with the image of the right breast to generate a color histogram showing differences. The averaged distance and the root mean square distance between the two layers were calculated. The degree of asymmetry was judged by the root mean square distance. They found breast asymmetry commonly existed, and on average left breast was larger than the right. Isogai et al. (2006) adopted a similar method, where 51 patients were scanned using a laser light scanner after breast reconstruction. The mirror image of the untreated breast was superimposed on the image of the reconstructed breast; four layers of Moire patterns were then obtained (Moire topography was first used to evaluate breast asymmetry in 1991, by Noguchi et al.). The differences in the corresponding layers were used to judge breast symmetry. The degree of asymmetry was determined by the area difference in transverse and sagittal cross-sections. Using their method, they found the best surgical strategies, in terms of breast symmetry, following a total or partial mastectomy. Inspired by Losken et al. and Isogai et al., in this study, we propose a similar, yet more standardized, repeatable and automatic method to objectively evaluate breast asymmetry.

3. Methodology

With approval of the study obtained from the Institutional Review Board, 46 Caucasian females (non-obese, i.e. BMI below 30, age range: 18-45) were recruited for 3D body scanning. None of them reported having plastic surgery or surgery of any kind on their breasts. They were scanned with their upper body nude in the upright standing posture, using a Human Solutions scanner.

The original scans were in an .STL format. They were imported into Matlab® and converted to .M files, where about 2,000,000 of 3D coordinates of the surface points were stored for each participant. The head, neck and limbs of each scan were then removed, keeping only the torso. The central axis of the torso was determined by averaging the x-coordinates and y-coordinates respectively of all the points on the torso. The scans were shifted so that their central axis was at x = 0 and y = 0 (Cartesian coordinate system). The locations of nipples, regarded as bust points, and underbust level (the level right below the swell of the breast) were identified visually. Breast shape was the focus of this study, thus only the section above underbust level was kept from the torso (see Figure 1).

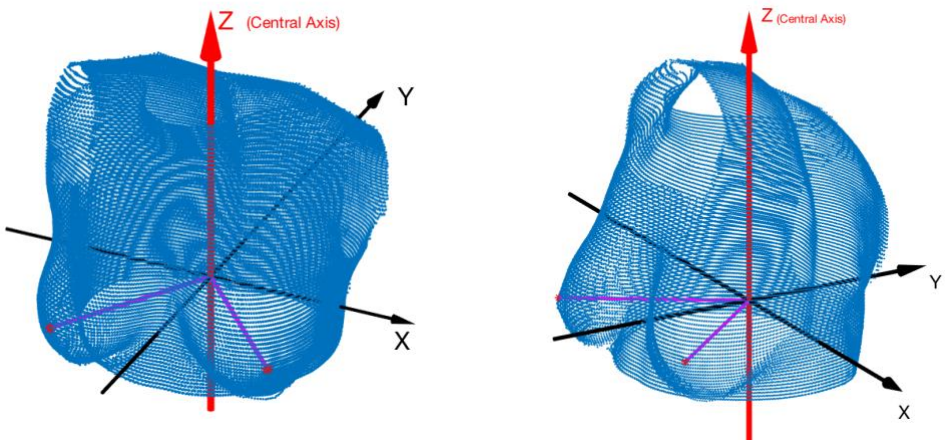

Figure 1. The processed scan

3.1. Slicing of breast and creation of contour map

As demonstrated in Figure 2, the black arrow which starts from the origin (where the central axis is located) and passes through each of the bust points, observed from the top view of breasts, indicates the pointing orientations of the bust points. Slicing was done perpendicular to this bust point to central axis line, starting from the origin towards the anterior of the breast. The parallel lines in Figure 2 represent the lines of slice. Each breast was sliced 30 times, creating 31 slices with equal thickness. However, only the last 11 slices, shown by the red lines in Figure 2 were kept for the creation of the contour map. The thickness of the slices can vary among participants (range: 4.4-7.6 mm, median: 5.5mm). Trivial differences can be observed in the thickness of the slices between the left and right breasts (maximum: 0.48 mm, median: 0.016mm). The breast could be sliced fewer times or more times, depending on the level of precision required. The 11-to-31 ratio was chosen as it insures the inclusion of the whole breast and a small portion of the chest wall for most of the participants. Although a larger portion of the chest wall will be included for participants whose underbust to full-bust ratio is smaller and vice versa, it is essential to fix the total number of slices and the number of slices that are kept from all scans for analysis, to ensure systematicity and reliability in the measurement collection process.

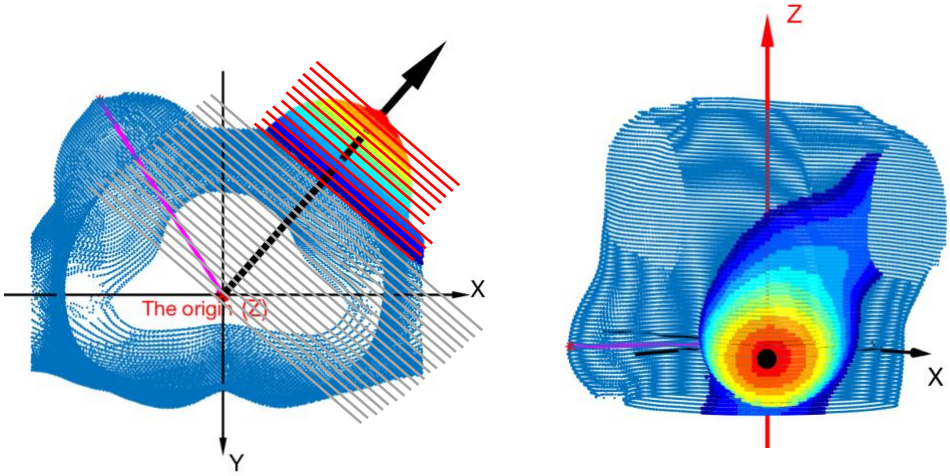

Figure 2. Illustration of the slicing of breast

Figure 3 shows the contour maps of the left breasts of six randomly selected participants. The 11 slices are colored differently: colors red and orange indicate higher altitudes, i.e. farther away from the origin (0, 0), while the blue colors indicate lower altitudes, i.e. closer to the origin. The intersection of the four black auxiliary lines is the location of the bust point. The contour map of the right breast can be created in the same way.

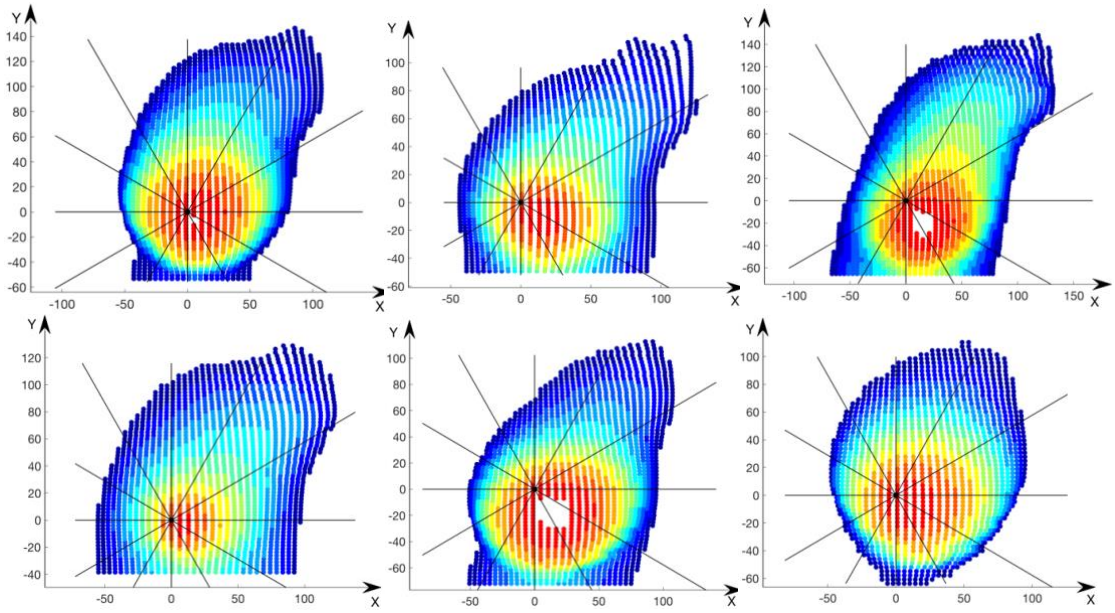

Figure 3. Contour maps of left breasts

3.2. Spider web structure

In order to strike a balance in simplifying the data clouds for further analysis and to preserve the essential shape information of the breasts, the colored contour maps were transformed into the spider web structure shown in Figure 4. The procedure is as follows. Firstly, each point on the sliced layers (each layer shapes like an irregular ring

for most cases, see Figure 3) was converted into polar coordinates, i.e. the combination of radial coordinate (the distance from the origin) and angular coordinate (the angle with respect to the x-axis). Because of the width of the irregular ring, which depends on the thickness of the slice, there are multiple points with various radial distances at the same angle on the same ring/layer. Among those points, the point that has median radial distance can be found, and can be considered as the vertex point at this angle on this layer. Hence, the vertex points at the following angles were found for each layer: 0°, 30°, 60°, 90°, 120°, 150°, 180°, 210°, 240°, 270°, 300°, and 330°. As shown in Figure 4, these vertex points lie on the designated auxiliary lines. Lastly, the adjacent vertex points on the same layer were connected except for missing points due to the fact that the body contour drops away from the lower slices at certain locations for some participants.

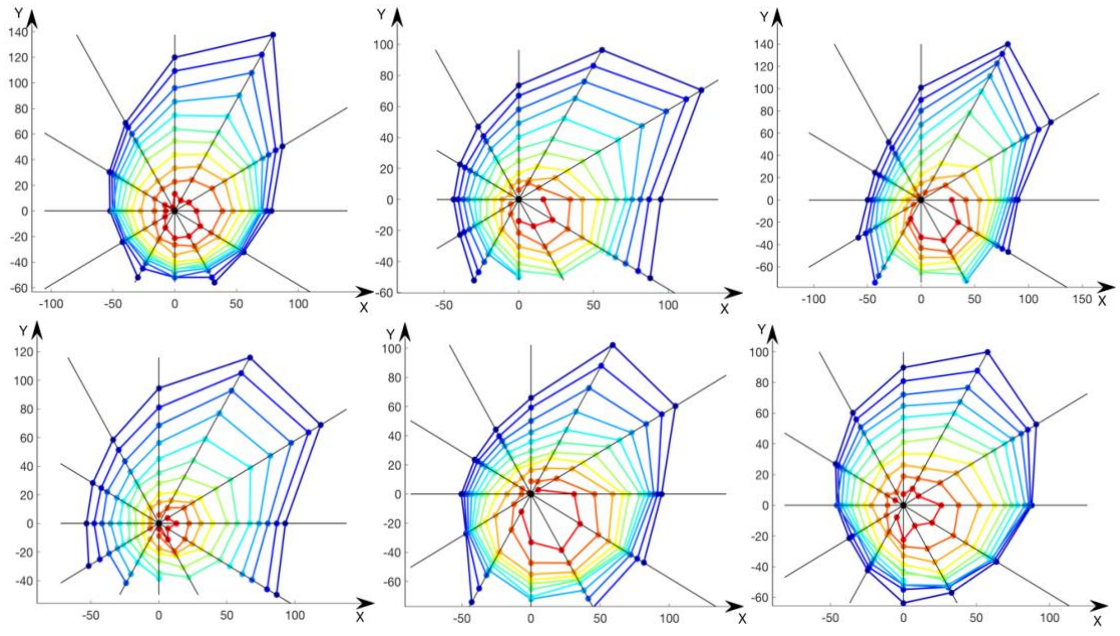

Figure 4. Left breasts presented by the spider web structure corresponding to the contour maps in Figure 3

3.3. Averaging breast shapes on both sides and assessment of breast asymmetry

All scans were scaled proportionally to have the same bust circumference of 90 cm (35.4 inches, a common band size) so that only the breast shape is quantified regardless of the band size (which is associated with breast size). The bust circumference of 90 cm was chosen arbitrarily. Changing it to another value will not affect the analysis result. After scaling, the same algorithm that creates contour maps and spider webs was applied to the right breast and left breast separately and then plotted together. The right and left bust points were shifted apart horizontally until the distance between them matched with the distance between bust points measured from their scaled 3D scan.

Subsequently, an averaged web was created for each subject by averaging every pair of corresponding vertex points on the web structures of the right and left breasts. One spider web can contain a maximum of 132 points (11 slices, 12 angles). Therefore, there is a maximum of 132 pairs of points (null points can exist). Before averaging, the right breasts were flipped horizontally, so that they have the same orientation with the left breasts. In addition, both breasts had been shifted to make their bust points centered at the origin. The averaged webs were used in measurement extraction.

The methodology developed for this study also provides a way to quantitatively evaluate the degree of asymmetry between the left and right breast. Once the webs have been processed such that both the left and right breasts have the same orientation, with their bust points centered at the origin, an Asymmetry Index can be calculated using the following formula:

$$\text{Asymmetry Index} = \frac{1}{2 \times N} \sum_{i=1}^{N} \sqrt{\frac{(X_{i\_right} - \bar{X}_i)^2 + (Y_{i\_right} - \bar{Y}_i)^2 + (X_{i\_left} - \bar{X}_i)^2 + (Y_{i\_left} - \bar{Y}_i)^2}{\bar{X}_i^{\,2} + \bar{Y}_i^{\,2}}} \qquad (1)$$

where N is the number of non-null points, ($\bar{X}_i$, $\bar{Y}_i$) is the averaged location of the i_{th} pair of non-null points, with (X_{i_right} , Y_{i_right}) being the right-side point and (X_{i_left} , Y_{i_left}) being the left-side point. (In this calculation, the Cartesian coordinate system is used.)

A larger Asymmetry Index implies greater differences in shapes between the two breasts. An Asymmetry Index of 0, though practically not achievable, implies perfect symmetry. This can only happen when every point on the right breast lies exactly at the same location as its corresponding point on the left breast. The Index is dimensionless and can never exceed 1.

3.4. Statistical Analysis

A total of 35 measurements that are relevant to the geometric shape of the spider webs (i.e. the 11-layer superimposed polygons) were extracted from the averaged webs, including:

- the overall median radius (N=1);
- the anglewise radius (the median value among all slices at one same angle). Angles include 0°, 30°, 60°, 90°, 120°, 150°, 180°, 210°, 240°, 270°, 300°, and 330° (N=12);
- the anglewise radius increment (the median value among all pairs of adjacent slices at one same angle), divided by its corresponding anglewise radius (N=12);
- the median perimeter of all 11 polygons (or 11 slices) (N=1);
- the median value of the perimeter ratios between any two adjacent polygons (outer polygon over inner polygon) (N=1);
- the median area that each polygon encloses (N=1);

- the median value of the area ratios between any two adjacent polygons (outer polygon over inner polygon) (N=1) and
- The median diagonal radius difference: (1) radius at 30˚minus radius at -150˚; (2) radius at 60˚minus radius at -120˚; (3) radius at 90˚minus radius at -90˚; (4) radius at 120˚minus radius at -60˚; (5) radius at 150˚minus radius at -30˚; and (6) radius at 180˚minus radius at 0˚(first compute the difference at each slice, then compute the median among all 11 slices) (N=6).

Principal component analysis (PCA) was applied to the data. The variances of the principal components (PC's) were studied. Moreover, K-medoids clustering method was used to categorize the breast shapes into a few groups. The Partitioning Around Medoids (PAM) algorithm, one of the most commonly used algorithms for K-medoids clustering, was adopted. Furthermore, Random Forest (RF) was conducted to examine the clustering results. Its cross-validation results, i.e. the estimations on the misclassification rates, were used as the main reference to determine the appropriate number of clusters. Lastly, MANOVA (Multivariate Analysis of Variance) was performed to check whether the multivariate means are significantly different among clusters. A small p-value indicates the difference is statistically significant. All statistical analysis was done in R.

4. Results

4.1. The Asymmetry Index

Table 1 lists four randomly selected examples to demonstrate the averaging results and their calculated Asymmetry Index. The histogram of the Asymmetry Index is also included in the table. The Asymmetry Index of the 46 subjects has a minimum value of 0.0264 and a maximum value of 0.103. The mean value was found to be

0.0548, with a standard deviation of 0.0167. The 25, 50 and 75 Percentile values are 0.0434, 0.0536 and 0.0647 respectively. As shown in Table 1, the averaged web can be considered as a sufficient representation of either breast, and the Asymmetry Index can reflect the difference in shape between the right and left breasts.

Table 1. Four examples to demonstrate the averaging result and asymmetry index

Contour Map	Spider Webs from both sides	Averaged Web	Asymmetry Index
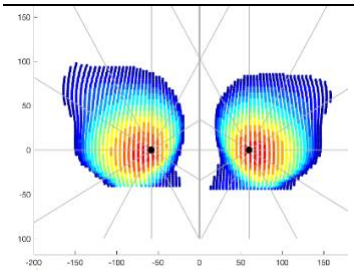	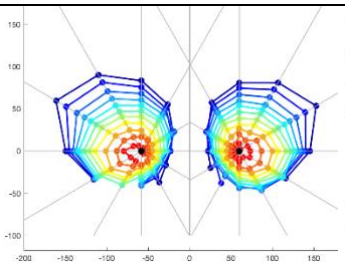	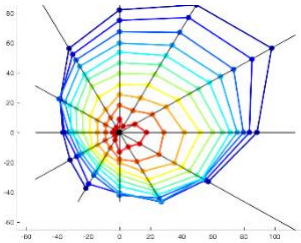	0.0433
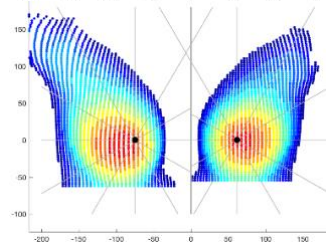	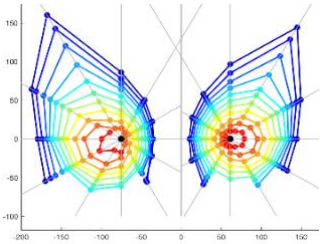	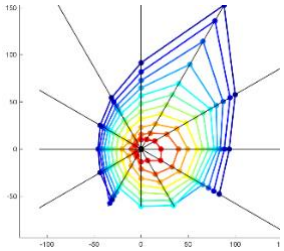	0.0822
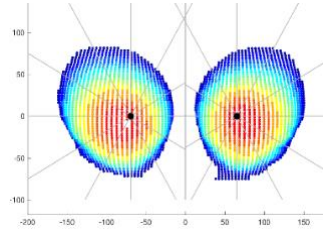	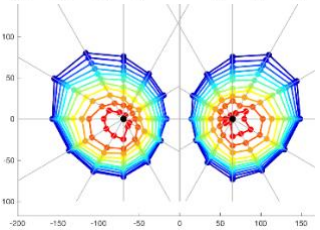	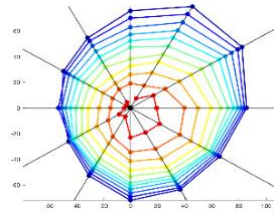	0.0280
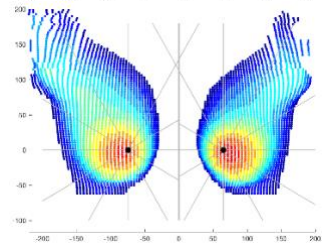	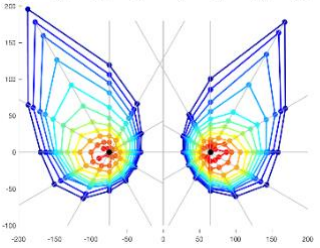	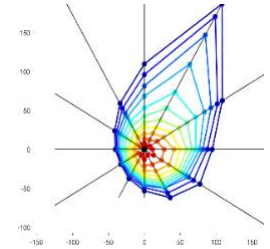	0.0536
Histogram of the Asymmetry Index			

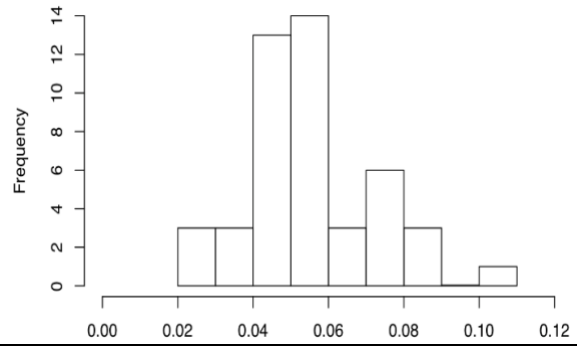

Note. A larger Asymmetry Index implies higher difference in shapes between the two breasts

4.2. Principal Component Analysis

Each datapoint was standardized, by subtracting the mean and then dividing the result by the standard deviation, before the PCA was applied. A total of 35 PC's were obtained. The summary statistics of the first 10 PC's and the scree plot of all 35 PC's can be found in Table 2. Clearly, the first four PC's can explain more than 80% of the total variance. In other words, the first four PC's dominate the majority of the variance in the data, while the rest of the PC's are not as important.

Table 2. PCA Summary Table (Partial) and the Scree Plot

	PC1	PC2	PC3	PC4	PC5
Standard deviation	3.1206	2.8051	2.6247	1.9809	1.1505
Proportion of Variance	0.2782	0.2248	0.1968	0.1121	0.0378
Cumulative Proportion	0.2782	0.5030	0.6999	**0.8120**	0.8498
	PC6	PC7	PC8	PC9	PC10
Standard deviation	1.0746	0.9191	0.7400	0.6968	0.6749
Proportion of Variance	0.0330	0.0241	0.0156	0.0139	0.0130
Cumulative Proportion	0.8828	0.9070	0.9226	0.9365	0.9495
The Scree Plot					

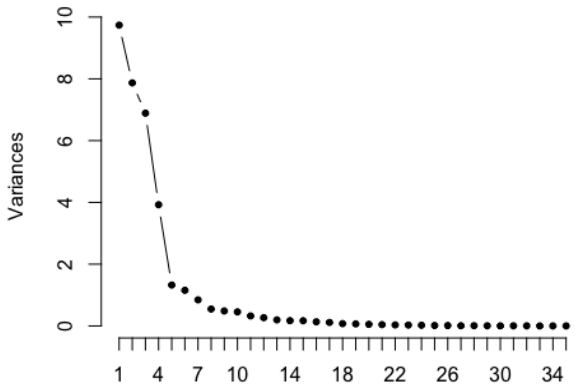

Each PC is a linear combination of the 35 measurements, with a different loading factor for each measurement. Measurements that have larger loading factors have larger impact on the PC scores. On the other hand, some measurements are correlated with each other, and those that are highly correlated could correspond to the same shape factor. Therefore, for each PC, there is usually more than one measurement that has significant loading factors. The loading factors of the first 4 PC's were investigated and summarized to describe what these four PC's stand for as shape factors. The four breast shape factors are listed in Table 3, and for each of the 4 PC's, the highest and lowest scored subjects were selected and are regarded as the extreme cases for the corresponding shape factor. The shape factors and their dominating measurements (i.e. measurements which have outstanding loading factors) are as follows:

- the vertical position of the bust point (dominating measurements: the radii at 90°, 240°, 270° and 300°; the diagonal radius difference between 90° and 270°);
- the volume of the breast (dominating measurements: the overall radius; the perimeter ratio between adjacent polygons; and the area ratio between adjacent polygons);

- the horizontal position of the bust point (dominating measurements: the radii at 0°, 30°and 330°; the diagonal radius difference between 0° and 180°) and
- the fullness of the breast (dominating measurements: the overall radius; a few anglewise radius increments).

Although PC2 (the volume of the breast) and PC4 (the fullness of the breast) both depend highly on the overall radius and the measurements that are associated with the inter-slice shape differences, PC2 has a negative loading factor for the overall radius that is outstanding, while PC4 has a positive loading factor for this measurement. This is how we differentiate fullness from volume.

Table 3. Extreme cases by breast shape factors

Factor 1 (PC1) Vertical position of bust point		Factor 2 (PC2) Volume of breast	
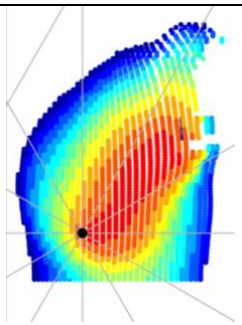	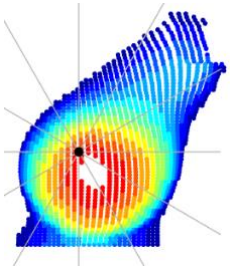	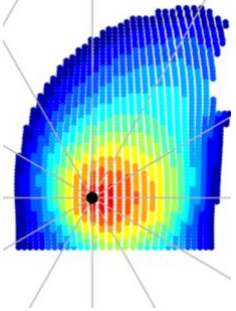	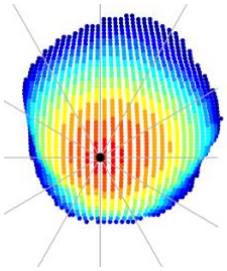
Low	High	Flat	Full
Factor 3 (PC3) Horizontal position of bust point		Factor 4 (PC4) Fullness of breast	

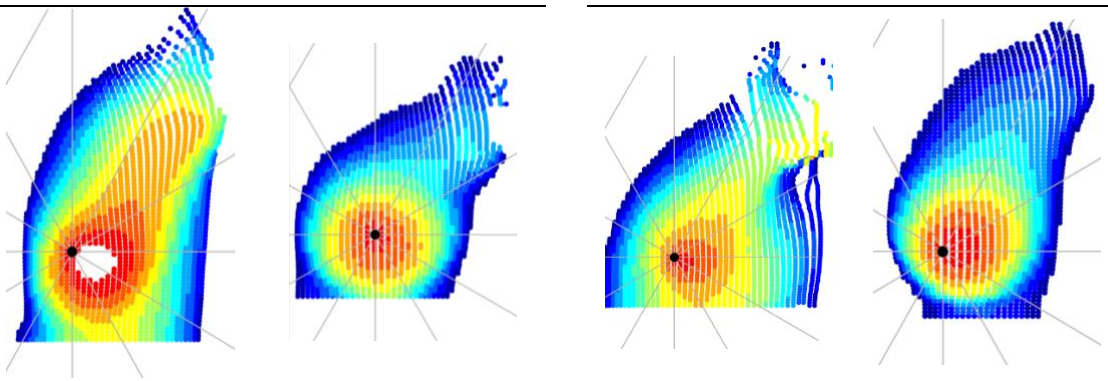

Abducted | Centered | Pointed (Conical) | Round (Hemisphere)

4.3. K-medoids Clustering Results

With K (the number of clusters) set to be 2, 3, 4, 5 or 6, the 46 subjects were categorized into 2 to 6 groups, respectively. The clustering assignments, as well as the medoid cases, were recorded. Then MANOVA was performed for each K (see Table 4). Pillai's Trace was used in approximating F-values and calculating p-values. It can be seen that all p-values are smaller than 0.05. Therefore, at a 0.05 significance level, the multivariate means of different clusters can be considered statistically significantly different for all K's. For K=4 and above, the p-values are smaller than 0.001, indicating that the means are different at an even stricter significance level.

Table 4. MANOVA Results and RF Estimation of Misclassification Rate

K-medoids Clustering	MANOVA				Misclassification Rate
	Df	Pillai's Trace	Approximate F-value	P-value	
K = 2	1	0.914	3.021	0.03334	13.04%
K = 3	2	1.850	3.521	0.00131	15.22%
K = 4	**3**	**2.727**	**2.857**	**< 0.001**	**10.87%**
K = 5	4	3.673	3.206	< 0.001	13.04%
K = 6	5	4.531	2.761	< 0.001	15.22%

Unlike clustering, classification refers to the process of allocating new cases into previously defined groups (Rencher, 2003). Random Forest (RF) is one of the machine learning techniques that perform classification. To use RF, the clustering outcomes were considered as the known groups. The algorithm randomly separates the data into a training set and a testing set, and uses the training set to build discriminant rules while regarding the testing set as the new cases to be allocated. A case is considered misclassified when its allocated group is different from the initial cluster that it belongs to. The estimated misclassification rates are also included in Table 4. According to the table, the smallest misclassification rate appears when K=4. Therefore, 4 is considered as the most appropriate number of clusters, and chosen as the final group number.

Moreover, for K-medoids clustering, the medoids are constrained to be actual observations (Kaufman & Rousseeuw, 2009). Hence, the medoid cases can be regarded as the representative breast shapes for the groups. Figure 5 presents the final medoids used by the algorithm for the 4-cluster case, and the four breast shapes are the shape representatives for the 46 subjects: Subject 1 in Figure 5a represents the group (or cluster, N=9) that has a little bit of breast ptosis (relatively low bust point); Subject 2 (Figure 5b) represents the group (N=21) that has relatively high bust points, and has relatively (as compared with Group 3) conical breasts; Subject 3 (Figure 5c) also has relatively high bust points, but has relatively round breasts (N=12), while Subject 4 (Figure 5d) represents the flat chest group (N=4). Note that Subject 1 through 4 are the central cases of each cluster, rather than the extreme cases, therefore their shape characteristics are not as prominent as those in Table 3.

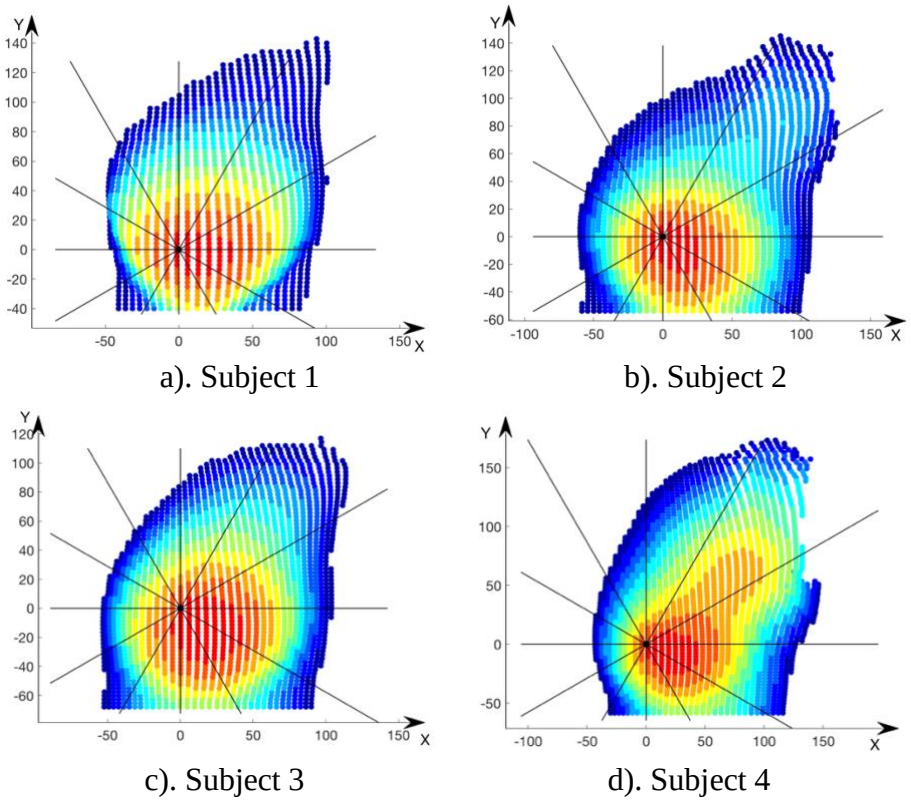

Figure 5. The final medoids for the 4-cluster case

5. Discussion and Conclusion

To answer Research Question 1, in this study we propose a new way of extracting breast shape measurements. By slicing a breast along the lines that are perpendicular to the pointing direction of its bust point, a contour map that depicts the shape of the breast can be generated. The altitudes of slices (the distance of each slice from the central axis, i.e. the Z axis) are differentiated by colors for ease of visualization. The bust point is typically on the slice of the highest altitude, and is regarded as an important reference point on the map: therefore the map is shifted so that the bust point can lie exactly at Point (0, 0). To reduce the number of points on the slices, and to simplify calculations, the contour maps were converted into spider web structures: points that do not lie on the auxiliary lines were removed. Accuracy and precision in

shape can be improved by adding more auxiliary lines pointing at intermediate angles, or by increasing the number of slices. We adopted a structure with 11 slices and 12 angles after conducting multiple trials with a different choice of the number of slices and/or the number of angles each time. Fewer slices or angles may not be able to capture the complex geometry of the breast, while more slices or angles could result in a heavier calculation load without gaining much benefit in terms of precision. By applying the same rules of slicing and simplification, we were able to systematically extract 35 measurements (radial distances or ratios/differences of radii, etc.) for all of our scans.

To answer Research Question 2, the web structure makes it possible to quantify the asymmetry between left and right breasts. A new parameter, the Asymmetry Index, is proposed to quantitatively evaluate the degree of asymmetry. The calculation of the Asymmetry Index requires knowing the locations of the vertex points on the webs of both breasts for comparison. The distribution of the Asymmetry Index for the 46 subjects is roughly normal (see Table 1). A larger sample size could help to distinguish distribution in the population more reliably. Nevertheless, the examples in Section 3.1 show that subjects with larger values of Asymmetry Index tend to have less symmetric breasts as judged visually. The Asymmetry Index is able to not only detect major asymmetry easily perceived by the eye, but also minor asymmetry not so visible. Therefore, it can be a useful objective tool in the evaluation of breast asymmetry.

To answer Research Question 3, the nude breasts of the 46 Caucasian females were studied. Based on the 35 measurements, their breast shapes were categorized into 2 to 6 groups via K-medoids clustering analysis. MANOVA results suggest that the multivariate means of different clusters are significantly different for all cases, especially for K= 4, 5 and 6. The misclassification rate obtained through Random

Forest analysis was used as the main reference to determine the appropriate number of clusters (groups). Four was chosen to be the final group number, because the 4-cluster case has the lowest misclassification rate, compared with other cases. In the end, four representative breast shapes were obtained based on the medoids of the 4 clusters. The corresponding subjects, whose breast shapes were found to be representative, can be regarded as fit models. The 3D scans of their breasts can be useful in building dress forms (particularly the new forms being produced with materials with densities and compression properties of breasts, as they represent the nude breast, not the bra shape (Yu et al., 2004)), evaluating bra products, and for bra cup molding.

To answer Research Question 4, several multivariate analysis methods were applied to the standardized measurement data. Results from Principal component analysis shows that the first 4 PC's account for more than 80% of the total variance. In the end, four shape factors were summarized from the 4 PC's, by referring to the extreme cases (in terms of PC scores) and the influential measurements (those that have relatively large loading factors). The four factors are 1) the vertical position of the bust point; 2) the volume of the breast; 3) the horizontal position of the bust point, and 4) the fullness of the breast.

Although all scans involved in this study were nude breast scans, the creation of web structures and the calculation of an Asymmetry Index are not limited to nude breasts. This method can be applied to in-bra scans as well. Future studies can compare the shape of nude breasts with the shapes of breasts with different types of bras on. Because contour maps, as in geography, are a precise measure of surface topography, the contour maps of breasts, and the reduced version- the web structures- can capture slight changes in shape and in breast asymmetry. Some of those changes can be so small that traditional measurements might not be able to detect them.

There are several limitations in this study. Firstly, the sample size is relatively

small. The 46 subjects may not be a sufficient representation of the population (18-to-45-year-old Caucasian females, with a BMI below 30). Nonetheless, the processing of scans, the creation of the contour maps and the spider webs, and the extraction of measurements were all done in Matlab® to ensure reliability and reduce human operation errors. Therefore, the programs developed in this study make it possible to handle large numbers of scans. Currently, there is no national 3D body scan database that includes the scans of nude breasts of Caucasian females. The outcomes can be more compelling if such database is ever available. Secondly, this study did not investigate the position of the breast with respect to the upper torso. Factors such as the thickness of the upper torso may have significant impact on the design of bras, but are not directly assessed by any of the 35 measurements (although those factors might influence the configuration of the contour maps). Thirdly, this study did not include any comparison with results obtained from traditional measurements to validate the effectiveness of the new measurements in shape categorization. Future work can also combine the two ways of extracting measurements to gain a deeper understanding of the shape variations in female breasts.

DISCLOSURE STATEMENT

This chapter is a peer-reviewed journal paper published in 2018. Citation information is listed below. Reuse permission has been acquired from Taylor & Francis.

Pei, J., Fan, J. & Ashdown, S. P. (2018). A Novel Method to Assess Breast Shape and Breast Asymmetry, *The Journal of the Textile Institute, 110*(8), 1229-1240.

REFERENCES

Brown, T. L. H., Ringrose, C., Hyland, R. E., Cole, A. A., & Brotherston, T. M. (1999). A method of assessing female breast morphometry and its clinical application. *British Journal of Plastic Surgery*, *52*(5), 355-359.

Chan, W., Mathur, B., Slade-Sharman, D., & Ramakrishnan, V. (2011). Developmental breast asymmetry. *The breast journal*, *17*(4), 391-398.

Davidson, K. (2005). *U.S. Patent Application No. 11/038,626*.

Denoel, C., Aguirre, M. I., Bianco, G., Mahaudens, P. H., Vanwijck, R., Garson, S., ... & Debrun, A. (2009). Idiopathic scoliosis and breast asymmetry. *Journal of Plastic, Reconstructive & Aesthetic Surgery*, *62*(10), 1303-1308.

Edstrom, L. E., Robson, M. C., & Wright, J. K. (1977). A method for the evaluation of minor degrees of breast asymmetry. *Plastic and reconstructive surgery*, *60*(5), 812-814.

Farinella, G. M., Impoco, G., Gallo, G., Spoto, S., & Catanuto, G. (2006, February). Unambiguous analysis of woman breast shape for plastic surgery outcome evaluation. Paper presented at *Eurographics Italian Chapter Conference* (pp. 255-261).

Grolleau, J. L., Lanfrey, E., Lavigne, B., Chavoin, J. P., & Costagliola, M. (1999). Breast base anomalies: treatment strategy for tuberous breasts, minor deformities, and asymmetry. *Plastic and reconstructive surgery*, *104*(7), 2040-2048.

Hsia, H. C., & Thomson, J. G. (2003). Differences in breast shape preferences between plastic surgeons and patients seeking breast augmentation. *Plastic and Reconstructive Surgery*, *112*(1), 312-320.

Kovacs, L., Eder, M., Hollweck, R., Zimmermann, A., Settles, M., Schneider, A., ... & Biemer, E. (2007). Comparison between breast volume measurement using 3D

surface imaging and classical techniques. *The Breast*, *16*(2), 137-145.

Kim, M. S., Reece, G. P., Beahm, E. K., Miller, M. J., Atkinson, E. N., & Markey, M. K. (2007). Objective assessment of aesthetic outcomes of breast cancer treatment: measuring ptosis from clinical photographs. *Computers in biology and medicine*, *37*(1), 49-59.

Kim, M. S., Sbalchiero, J. C., Reece, G. P., Miller, M. J., Beahm, E. K., & Markey, M. K. (2008). Assessment of breast aesthetics. *Plastic and reconstructive surgery*, *121*(4), 186e.

Kaufman, L., & Rousseeuw, P. J. (2009). Partitioning around medoids (Program PAM). In *Finding groups in data: an introduction to cluster analysis*. New York, NY, United States: John Wiley & Sons.

Isogai, N., Sai, K., Kamiishi, H., Watatani, M., Inui, H., & Shiozaki, H. (2006). Quantitative analysis of the reconstructed breast using a 3-dimensional laser light scanner. *Annals of plastic surgery*, *56*(3), 237-242.

Lee, H. Y., Hong, K., & Kim, E. A. (2004). Measurement protocol of women's nude breasts using a 3D scanning technique. *Applied Ergonomics*, *35*(4), 353-359.

Losken, A., Fishman, I., Denson, D. D., Moyer, H. R., & Carlson, G. W. (2005). An objective evaluation of breast symmetry and shape differences using 3-dimensional images. *Annals of plastic surgery*, *55*(6), 571-575.

Liu, C., Luan, J., Mu, L., & Ji, K. (2010). The role of three-dimensional scanning technique in evaluation of breast asymmetry in breast augmentation: a 100-case study. *Plastic and reconstructive surgery*, *126*(6), 2125-2132.

Lau, W. F. (2014). *Development of seamless knitted bra for optimum fit*. (Doctoral dissertation, Hong Kong Polytechnic University, Hong Kong, China). Retrieved from http://hdl.handle.net/10397/6859

Malata, C. M., Boot, J. C., Bradbury, E. T., Ramli, A. R. B., & Sharpe, D. T. (1994).

Congenital breast asymmetry: subjective and objective assessment. *British journal of plastic surgery*, *47*(2), 95-102.

Møller, A. P., Soler, M., & Thornhill, R. (1995). Breast asymmetry, sexual selection, and human reproductive success. *Ethology and Sociobiology*, *16*(3), 207-219.

Westreich, M. (1997). Anthropomorphic breast measurement: protocol and results in 50 women with aesthetically perfect breasts and clinical application. *Plastic and reconstructive surgery*, *100*(2), 468-479.

Manning, J. T., Scutt, D., Whitehouse, G. H., & Leinster, S. J. (1997). Breast asymmetry and phenotypic quality in women. *Evolution and Human behavior*, *18*(4), 223-236.

Noguchi, M., Saito, Y., Mizukami, Y., Nonomura, A., Ohta, N., Koyasaki, N., ... & Miyazaki, I. (1991). Breast deformity, its correction, and assessment of breast conserving surgery. *Breast cancer research and treatment*, *18*(2), 111-118.

Neto, M. S., Abla, L. E. F., Lemos, A. L., Garcia, É. B., Enout, M. J. R., Cabral, N. C., & Ferreira, L. M. (2012). The impact of surgical treatment on the self-esteem of patients with breast hypertrophy, hypomastia, or breast asymmetry. *Aesthetic plastic surgery*, *36*(1), 223-225.

Oh, S., & Chun, J. (2014). New breast measurement technique and bra sizing system based on 3D body scan data. *Journal of the Ergonomics Society of Korea*, *33*(4), 299–311.

Penn, J. (1954). Breast reduction. *British journal of plastic surgery*, *7*, 357-371.

Park, C. A., David, L. R., & Argenta, L. C. (2006). Breast asymmetry: presentation of a giant fibroadenoma. *The breast journal*, *12*(5), 451-461.

Rencher, A. C. (2003). Classification analysis: allocation of observations to groups. In *Methods of multivariate analysis* (pp. 299-321). New York, NY, United States: John Wiley & Sons.

Sacchini, V., Luini, A., Tana, S., Lozza, L., Galimberti, V., Merson, M., ... & Greco, M. (1991). Quantitative and qualitative cosmetic evaluation after conservative treatment for breast cancer. *European Journal of Cancer and Clinical Oncology*, *27*(11), 1395-1400.

Singh, D. (1995). Female health, attractiveness, and desirability for relationships: Role of breast asymmetry and waist-to-hip ratio. *Ethology and Sociobiology*, *16*(6), 465-481.

Scutt, D., Manning, J. T., Whitehouse, G. H., Leinster, S. J., & Massey, C. P. (1997). The relationship between breast asymmetry, breast size and the occurrence of breast cancer. *The British journal of radiology*, *70*(838), 1017-1021.

Sobah-Wilhelm, M. C. (2008). *U.S. Patent No. 7,413,495*. Washington, DC: U.S. Patent and Trademark Office.

Tsouskas, L. I., & Fentiman, I. S. (1990). Breast compliance: a new method for evaluation of cosmetic outcome after conservative treatment of early breast cancer. *Breast cancer research and treatment*, *15*(3), 185-190.

Waljee, J. F., Hu, E. S., Newman, L. A., & Alderman, A. K. (2008). Predictors of breast asymmetry after breast-conserving operation for breast cancer. *Journal of the American College of Surgeons*, *206*(2), 274-280.

Waljee, J. F., Hu, E. S., Ubel, P. A., Smith, D. M., Newman, L. A., & Alderman, A. K. (2008). Effect of esthetic outcome after breast-conserving surgery on psychosocial functioning and quality of life. *Journal of Clinical Oncology*, *26*(20), 3331-3337.

Yu, W., Fan, J., Li, Y., Gu, H., & Qian, X. (2004). *U.S. Patent Application No. 10/961,660*.

Yu, W., Fan, J., Ng, S. P., & Harlock, S. (2014). *Innovation and technology of women's intimate apparel*. Woodhead *Publishing*.

Zheng, R., Yu, W., & Fan, J. (2007). Development of a new Chinese bra sizing system based on breast anthropometric measurements. *International Journal of Industrial Ergonomics*, *37*(8), 697-705.

CHAPTER 3

DETECTION AND COMPARISON OF BREAST SHAPE VARIATION AMONG DIFFERENT 3D BODY SCAN CONDITIONS: NUDE, WITH A STRUCTURED BRA, AND WITH A SOFT BRA

Abstract

To investigate the effect of structured-bras and soft-bras on the breast shape, 46 female participants (Caucasian, BMI < 30, aged 18-45) were recruited for 3D scanning. Participants were scanned in three conditions: wearing a provided structured-bra, a provided soft-bra, and nude. The impact of the bras on breast asymmetry was quantitatively studied. The change in breast shape and position from the nude condition to the condition when shaped by the bras was also explored. Contour maps that show the topographic shapes of the scans were generated to analyze these comparisons. Thirty-five measurements were extracted from spider web structures which were derived from the contour maps, and were used for statistical analysis. Eight measurements were found to be especially indicative of the shape variations introduced by the bras. Regression models were built to predict the in-bra shape given only the nude breast shape. Lastly, heat maps that visualize the shape variations from the nude-to-bra condition via colors were plotted on the surfaces of the 3D scans of the participants in bras, and were used for qualitative analysis. This study is helpful in understanding how bras interact with the breast tissue, and can provide useful information for the improvement of bra designs for enhanced fitting or desired shaping effects.

1. Introduction

Bras have become an important item of clothing for modern women. A well-designed bra can enhance a woman's body contour, body attractiveness and self-confidence (Luk & Yu, 2016). It has been reported that the support provided by a bra is essential to prevent the elongation of the Cooper's ligaments, which results in breast ptosis (Yu, Fan, Ng & Harlock, 2014). In addition, a well-fitted sports bra can provide constraints on the breasts, thus reducing the embarrassment and the symptom of breast pain caused by excessive breast movement during exercise (Page & Steele, 1999). The importance of bra fit and pressure comfort has been widely acknowledged. On the other hand, the design of a well-fitted, comfortable bra, or a bra with the desired shaping effect, requires knowledge of the 3D shape of the breasts and furthermore, the shape modification that the breasts can experience under the compression of a bra.

Although research has been intensively done to study breast shapes, or to evaluate the fit of bras (Brown et al., 1999; Chan, Yu & Newton, 2001; Lee, Hong & Kim, 2004; Zheng, Yu & Fan, 2007; Wood, Cameron & Fitzgerald, 2008; McGhee & Steele, 2010), limited information was found that objectively assessed the impact of bras on breast shape. Scurr, Loveridge, Brown and Mills measured the nude breasts of 13 participants and studied the measurement changes over time after bra removal (Scurr, Loveridge, Brown & Mills, 2015). An increase in the sternal notch to nipple distance (right: 2.8 mm, left: 3.7 mm) and a decrease in the height of the nipple (right: 4.1 mm, left: 6.6 mm) were found, whereas the nipple-to-nipple distance and the breast projection remained the same over time. The researchers, however, did not report the measurements of the breasts when bras were worn. Ashizawa et al. compared the measurements obtained from the breasts of 11 Japanese participants with and without bras (Ashizawa, Sugane & Gunji, 1990). They found an increase in the bust girth (range: 2-6 cm, mean: 3.4 cm, one outlier removed) and a decrease in the

underbust girth (range: 0-6 cm, mean: 1.9 cm, one outlier removed) after a bra was put on. Four participants were removed due to limitations in measuring the height of the underbust line, but the other seven participants showed an increase in the line height after the bra was worn (range: 0.5-5 cm, mean: 2 cm). They also found that the most prominent point on the left breast moved upward (range: 0.3-3 cm, mean: 2 cm) and forward (range: 0.1-1.6 cm, mean: 0.9 cm), and that the distance between the left and right prominent points became wider with the bra on (range: 0-3 cm, mean: 1.4 cm). However, in another study where researchers investigated how respiration affects the calculated bra size, a mean difference of 1.9 inches (range: 0-6 inches) in bust girth, and a mean difference of 0.75 inches (range: 0-2 inches) in underbust girth between the two respiration states (i.e. inspiration and expiration) were reported (McGhee & Steele, 2006). Since the differences in circumferences between the nude breasts and the in-bra breasts can be very small, and respiration might play a significant role in those minor differences, the circumferential or other types of traditional measurements may not be the best tool to investigate the change in the shape of breasts provided by bras.

In order to fill the research gap, in this study, we endeavor to gain a deeper understanding on how bras interact with the breast tissue. This can provide useful information for the improvement of bra designs. Also, most anthropometric studies conducted with 3D body scanners provided female participants with unstructured bras; however this is not the type of bra worn by most women on a daily basis. Understanding the change in shape to a more commonly worn structured bra style can add value to these scan studies. This paper presents the results of an in-depth study regarding the shape differences between the nude breasts and the same breasts wearing either a structured-bra or a soft-bra. The following are the research questions to be answered:

- What changes does the structured-bra or the soft-bra make in terms of breast asymmetry?
- What kind of measurements can effectively detect the shape differences between the nude-breasts and the breasts with the structured-bra/soft-bra on?
- Are there any patterns in the shape modification of breasts, caused by the structured-bra/soft-bra?
- What is the relationship between the shape modification and the nude-breast shape? Is it possible to predict the in-bra shape given only the nude-breast shape?
- How can the shaping effect of bras be represented visually?

2. Methodology

With approval obtained from Institutional Review Board, 46 Caucasian females (BMI below 30, age range: 18-45) were scanned using a Human Solutions whole body scanner. Their bust circumference ranges from 80.3cm to 125.1cm (median: 92.8cm), and their underbust circumference ranges from 69.5cm to 89.9cm (median: 78.2cm). Each of the participants was scanned wearing a provided structured bra, wearing a provided soft bra, and without wearing any bra (nude breasts), in a standard upright standing posture. A wide range of sizes were provided for the structured bra style (15 sizes) and the soft bra style (four sizes) (see Table 1). Participants were asked to try on multiple sizes to find their best fitting size with the help of a fit expert. However, there were eight participants whose sizes fell out of the provided range. Three of them wore AA cup, four of them wore DD cup and one wore DDD cup. All participants were asked to bring their favorite bra and their most comfortable bra to the study. For those who could not find their sizes from the provided bras, they were scanned either in their favorite bra or in their most comfortable bra, depending on which one fit better and

had similar style with the provided T-shirt bra. We did not remove the eight participants from the data analysis because we aim to capture and understand the variation in breast shape for a wide range of bust sizes, without eliminating any possibly significant sizes, and because we judged that the participant bras were close enough to the bra style provided in the study.

Table 1. The styles of the provided bras

	Structured Bra	Soft Bra
Style		
Description	T-shirt Bra: Molded Contour Cups with Underwire, Unpadded Hook & Eye fastening	Unstructured style: Four-way Stretch Fabric, with no Underwire or Padding Pullover Styling
Available Sizes	32 A/B/C/D 34 A/B/C/D 36 A/B/C/D 38 B/C/D	S, M, L, XL

The 3D scans obtained were processed in Matlab®, with head, limbs, and the section below the underbust line removed. The remaining scan will be referred to as the bust scan. The locations of bust points and underbust level were identified visually.

Because the difference in breast shapes between the nude scan and the in-bra scan may not be big enough to be detected using traditional measurements such as bust girth (in some cases there is very little difference visible), the topographic shapes of the breasts derived from their contour maps were used for analysis (Figure 1a). Scans were processed so that each scan had exactly 18,000 points on 100 horizontal slices (or transverse planes), while each slice contained 180 points, at the angles (with respect to the x-axis) of every 2˚ from -180° to 180°. The points were sorted in the same way for every scan. A total of 35 comparative measurements were then derived from these spider web structures as shown in Figure 1b. Pairwise Hotelling's T^2-tests were performed to see whether the 35 measurements as a whole can detect the differences in shape. Post-hoc tests with Bonferroni correction were conducted to identify the specific measurements that are sensitive to shape modification. In addition, Asymmetry Indices (Pei, Fan & Ashdown, 2019) of the nude breasts and the in-bra breasts were calculated to quantify the impact of the bras on the breast asymmetry. Moreover, the relationships between the nude breast shape and the changes in shape provided by the structured bra and the soft bra, respectively, were investigated. Regression prediction models were then built to predict the in-bra shape given only the nude breast shape.

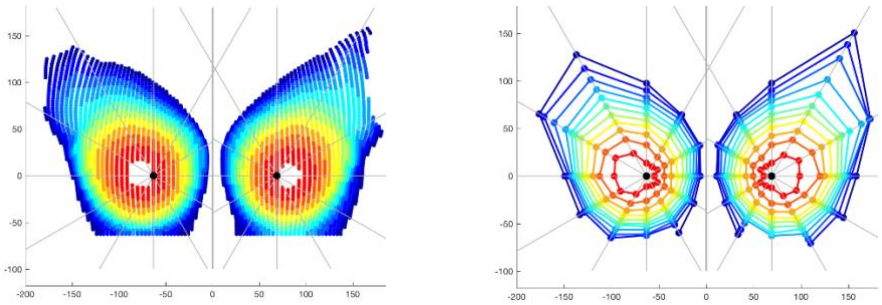

Figure 1. Breast topography shown by a contour map and the corresponding web structure (Note. The black points at y= 0 are the bust points)

To visualize the changes in shape, for each participant, the 3D scan of the nude breasts was first aligned with the in-bra scan (either structured-bra scan or soft-bra scan) and the two scans were merged together. The alignment was based on the central axis (determined by averaging the x-coordinates and y-coordinates respectively of all the points on the bust scan) and the bust plane (defined by the averaged z-coordinates of the right and left bust points). Figure 2a shows the top view of the scans where the nude scan is presented in black while the in-bra scan is in red. Then a heat map was generated and presented on the surface of the in-bra scan (Figure 2b), by comparing and assigning a color for each pair of corresponding points from the two scans. This was done by calculating and recording each point's horizontal distance towards the central axis. The difference in the point-to-axis distances between a point on the in-bra scan and its corresponding point on the nude scan can then be calculated (the nude scan served as the base case). After the calculation, red/orange colors were assigned to points where an increase in the distance, i.e., expansion, was observed. Similarly, blue colors were assigned to points where a decrease in the distance, i.e. compression, was observed (see Figure 2b). Another way of presenting this calculation result is by a 3D colored mesh (Figure 2c), in which case both the colors and surface heights were determined by the calculated difference values. The surface height can be positive,

shown as upward protrusion, or negative, shown as downward indentation. The scan surface heat maps and the contour maps provide the basis for both quantitative analysis and qualitative analysis of the shape changes.

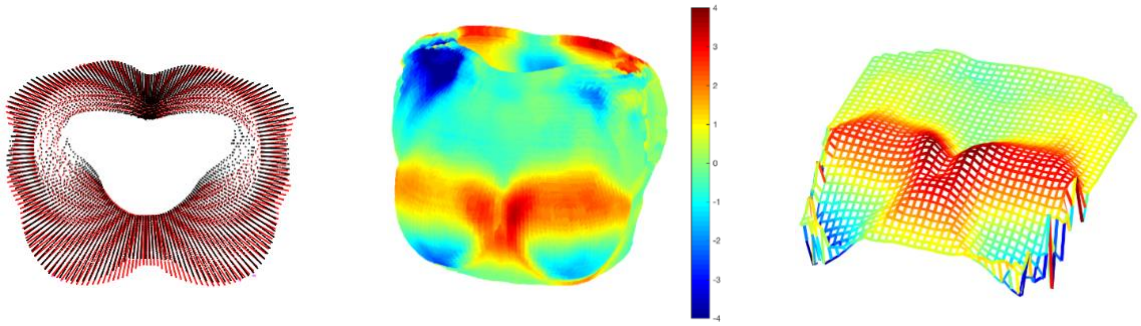

a) Top view of merged scans b) Scan surface heat map c) 3D colored mesh of difference values

Figure 2. Visualization of the shape differences between scans

3. Results and Discussions

3.1. Impact of bra on breast asymmetry

The Asymmetry Index (ASI) values of the nude-breast scans, the structured-bra scans and the soft-bra scans were calculated and the overall distributions were plotted in a boxplot (Figure 3a). The median ASI values are 0.0536, 0.0237, and 0.0232 for the nude scan, the structured-bra scan and the soft-bra scan respectively (larger values indicate increased asymmetry). Both the structured-bra scans and the soft-bra scans have significantly lower ASI values, compared with the nude scans (p-values < 0.0001 for both). This shows that, in general, both structured-bras and soft-bras can help to improve the breast symmetry. In addition, the ranges of the ASI values reduced for both of the in-bra cases. The standard deviation reduced from 0.0167 to 0.0097 (structured-bra) and 0.0077 (soft-bra).

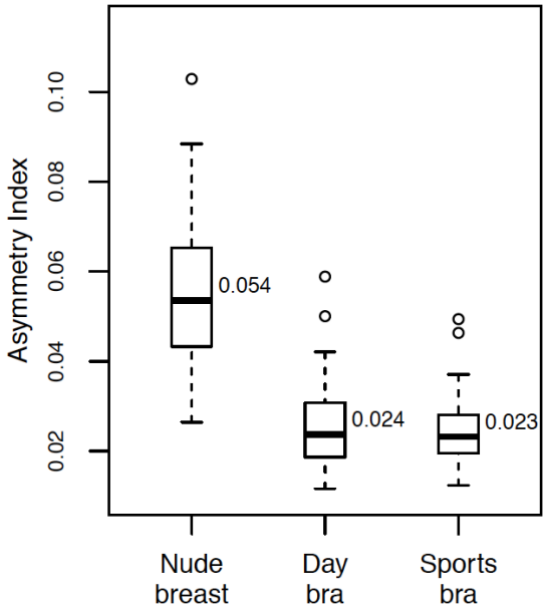

a) Overall distributions

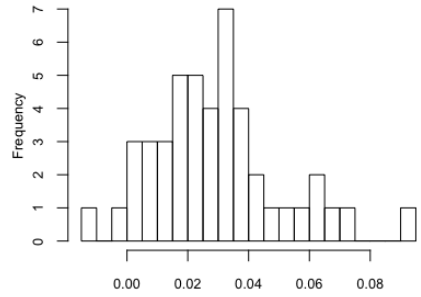

b) Pairwise ASI difference between structured-bra scan & nude scan

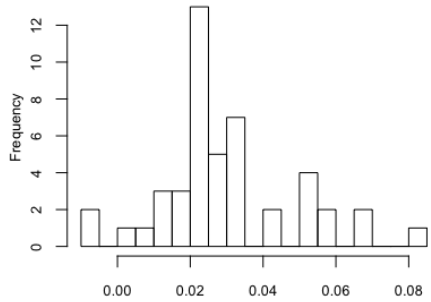

c) Pairwise ASI difference between soft-bra scan & nude scan

Figure 3. Asymmetry index (ASI) comparison

Furthermore, the pairwise analysis (a nude scan paired with one of its in-bra scans) was conducted on the 46 participants individually. Pairwise ASI difference values were calculated by subtracting the ASI value of a nude-breast scan from its corresponding in-bra scan (either structured-bra or soft-bra). The histograms of the pairwise differences can be found in Figure 3b and 3c for the structured-bra scan and the soft-bra scan, respectively. In addition, Table 2 includes two representative cases where significant changes in the breast asymmetry can be observed.

Table 2. Two representative cases to demonstrate the impact of bras on the breast asymmetry

	Nude-breast scan	Structured-bra scan	Soft-bra scan

Case I	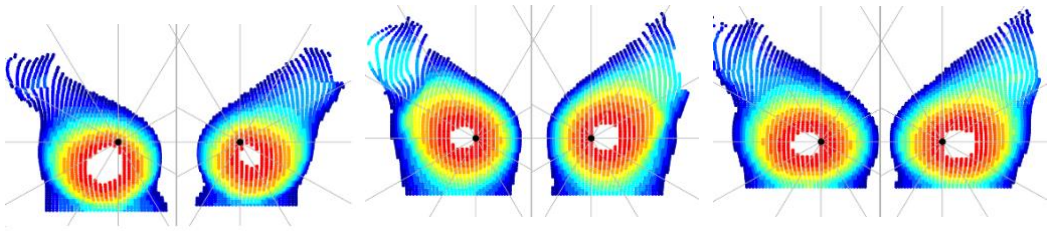		
ASI	0.0674	0.0204	0.0273
	Nude-breast scan	Structured-bra scan	Soft-bra scan
Case II	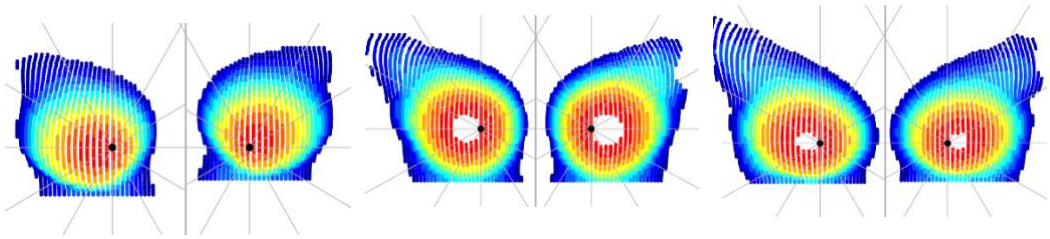		
ASI	0.1029	0.0117	0.0211

Notes. Higher ASI value suggests larger extent of breast asymmetry
The left and right breasts are aligned based on the z-coordinates of their bust points (rather than aligned as they are on the body)

According to Figure 3b, compared with their nude scans, 44 of all the structured-bra scans (95.7%) show a decrease in the ASI value, i.e. an improvement on the breast symmetry, while 2 (4.3%) show an increase in the ASI value, i.e. a decline in the breast symmetry. 7 cases (15.2%) have changes (either increase or decrease) that are less than 0.01, meaning the changes are so trivial that can be ignored. However, the decrease in the ASI value can be as much as 0.0912, and there are 10 participants (21.7%) whose ASI values reduce more than 0.04. According to observation, a significant improvement on the breast symmetry (where the decrease in the ASI value exceeds 0.06) tends to happen to nude breasts that are severely uneven. On the other hand, the increase in the ASI values are always less than 0.011.

For the soft-bra scans (Figure 3c), the distribution looks very similar to Figure 3b. 44 scans (95.7%) show an improvement on the breast symmetry, while 2 (4.3%) show otherwise. 4 cases (8.7%) have a trivial increase or decrease in the ASI value. The

decrease in the ASI value can be as much as 0.0817, and there are 11 participants (23.9%) whose ASI values reduced more than 0.04. Similar conclusions can be drawn as well. A significant improvement on the breast symmetry tends to happen to nude breasts that are severely uneven, while a decrease in the breast symmetry is very rare and is a trivial change (always less than 0.01).

3.2. Analysis of the extracted measurements

Extracted from the web structures (Figure 1b), the 35 measurements include: a) the overall radius (the median value of all radii); b) 12 radii (the median values among layers) at 12 different angles (the included angles between the x-axis and one of the auxiliary lines); c) 12 between-layer radius increments at the 12 angles (one increment value at an angle); d) the median perimeter of all the 11 rings (each layer is essentially a ring); e) the overall perimeter ratio between adjacent layers (the median value of 10 ratios: outer-ring-perimeter to inner-ring-perimeter); f) the median area of all the 11 rings; g) the overall area ratio between adjacent layers (the median value of 10 ratios: outer-ring-area to inner-ring-area) and h) 6 diagonal radius differences (e.g. radius at 30° minus radius at 120°) (Pei, Fan & Ashdown, 2019).

The same set of measurements were extracted from the nude-breast scans, the structured-bra scans and the soft-bra scans, respectively, generating three datasets (46 participants, 35 variables). Then the pairwise Hotelling's T^2-tests were performed to see whether significant differences can be found between any two datasets. As shown in Table 3, the pairs include: 1) the structured-bra data and the nude-breast data; 2) the soft-bra data and the nude-breast data, and 3) the structured-bra data and the soft-bra data. The p-values of the tests are small enough to declare that the differences between any two datasets are statistically significantly different. This means that the 35 measurements, as a whole, can detect the shape modifications. Based on this finding,

further investigation can be done to see which measurements are more efficient in detecting the changes in shape.

Table 3. Hotelling's paired T^2-tests

Datasets	T^2 statistics	Df 1	Df 2	P-value
Structured-bra vs. Nude	17.57	35	11	< 0.001
Soft-bra vs. Nude	23.81	35	11	< 0.001
Structured-bra vs. Soft-bra	24.47	35	11	< 0.001

Therefore, pairwise post-hoc tests with Bonferroni correction were performed on each of the 35 measurements. Bonferroni correction is the most conservative method in adjusting p-values to avoid Type-1 Errors (false positive). The nude-breast data were paired with the structured-bra data and with the soft-bra data, respectively. Table 4 shows the partial results of the tests (Measurements were randomly selected. Measurement names were omitted for conciseness).

Table 4. Pairwise post-hoc tests with Bonferroni correction (partial)

Measurement Number	Adjusted P-values	
	Structured-bra & Nude	Soft-bra & Nude
7	1.0000	0.0008 **
8	0.0049 **	< 0.0001 ***
14	0.0336 *	0.8249
15	1.0000	1.0000
22	< 0.0001 ***	< 0.0001 ***
23	< 0.0001 ***	< 0.0001 ***

30	0.0044 **	< 0.0001 ***
34	0.1106	0.0154

Note. * implies statistically significant at a 0.05 level;
more * suggests significant at a lower level (0.01 or less)

As shown in Table 4, some measurements appear to be insignificant for both dataset pairs (e.g. #15, #34). Some appear to be significant only for one of the dataset pairs (e.g. #7, #14). However, there are a few measurements that are significant for both dataset pairs at an extremely low significance level: #20, #21, #22, #23, #24, #25, #26, #28.

Measurement #20 to #25 are the between-layer radius increments at 30°, 60°, 90°, 120°, 150°, and 180°, divided by the corresponding median radius (i.e. Measurements #2 to #13), respectively (see Figure 4a and Appendix A). Clearly, the shape modification caused by bras mostly happens at the upper section of the breast. Measurement #26 is the overall perimeter ratio between layers (Figure 4b only presents one of the 10 perimeter ratios, the median value of the 10 ratios was used in the analysis), and Measurement #28 is the overall area ratio between layers (Figure 4c only presents one of the 10 area ratios, the median value of the 10 ratios was used in the analysis). Those two overall ratios depend highly on the fullness and the extent of the protrusion of the breast. As demonstrated in Figure 4d, the perimeters and the areas (of cross-sections) drop more dramatically from base to top for a tall cone than for a short cone. They drop more gradually for a hemisphere than for a cone. Therefore, the two ratios will decrease if the breast protrusion reduces but the fullness of the breast increases. This is exactly what can be observed from the majority of the in-bra scans, compared with their corresponding nude-breast scans. Clearly, under compression of a bra, the breast becomes less prominent and less conical.

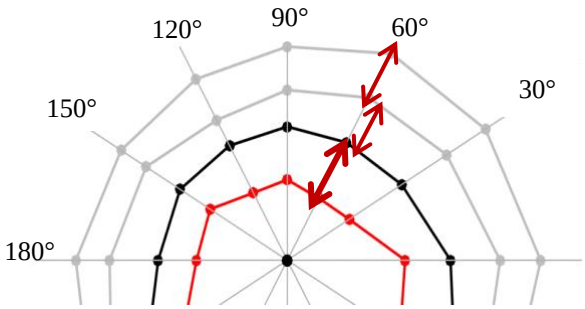

a) Radius increments between adjacent layers at 60°
(Note. This figure only shows 4 layers, and 3 increments. In fact, there are 11 layers and 10 increments. The median value of all the 10 increments was obtained then divided by the median radius at the same angle).

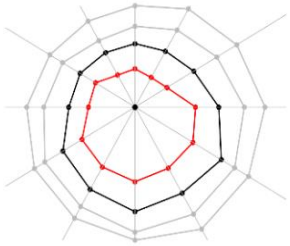

b) Perimeter ratio between layers- Outer ring (black) to Inner ring (red)

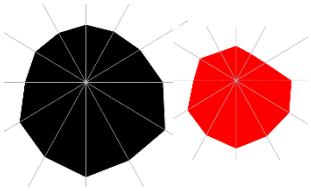

c) Area ratio between layers- Outer ring (black) to Inner ring (red)

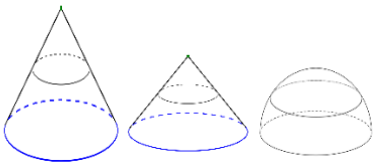

d) The ratios depend on the fullness and the degree of protrusion

Figure 4. Demonstration of significant measurements

3.3. Relationship between the nude shape and the shape modification

The difference values between the in-bra (structured-bra or soft-bra) data and the nude-breast data were calculated for each of the 35 measurements. The difference values will be referred to as the structured-bra/soft-bra shape modification values. The correlations between the shape modification values and the nude-breast data were calculated as well. A substantial portion of measurements show strong negative correlations for the structured-bra modification values: 27 out of the 35 measurements (77.1%) have correlation values (with the nude-breast data) that are less than -0.5 (negatively correlated); 18 measurements (51.4%) have correlation values that are less

than -0.7 (strongly negatively correlated). Fewer measurements show strong correlations with the nude-breast data for the soft-bra modification values: 18 measurements (51.4%) have correlation values that are less than -0.5 (negatively correlated); 9 measurements (25.7%) have correlation values that are less than -0.7 (strongly negatively correlated). In terms of the aforementioned significant measurements (#20, #21, #22, #23, #24, #25, #26, #28), all of them have strong correlation values for both the structured-bra and the soft-bra modification values (median: -0.81, minimum: -0.92, maximum: -0.63).

Furthermore, this study built prediction models to present the in-bra shapes given only the nude breast shape. Each spider web has a maximum of 132 points (12 angles, 11 rings). Regression models were built pointwise. Hence, 132 regression equations were generated to bring association between the nude shape and the in-bra shape (structured-bra shape or soft-bra shape). Both simple linear regression and multiple linear regression had been tried. In the end, multiple linear regression was chosen. The location of a structured-bra/soft-bra point depends on the locations of two points on the nude-breast web: 1) the exact corresponding point, which lies on the same ring at the same angle; and 2) the point that lies on the adjacent outer ring but at the same angle. Moreover, regression models were built based on the data of 45 participants, leaving one participant for testing. The predicted in-bra shapes of that participant, generated through the regression models, were compared with the true in-bra shapes. The predicted in-bra shapes of two randomly selected participants are presented in Table 5, along with their true shapes. Certain degree of similarity can be observed between the predicted shape and the true shape.

Table 5. In-bra shapes predicted by the nude-breast shape based on the regression models

True nude scan		Predicted shape	True shape
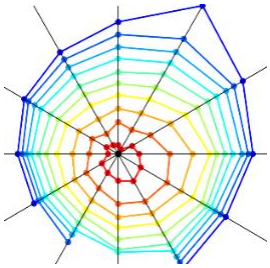	Structured-bra scan:	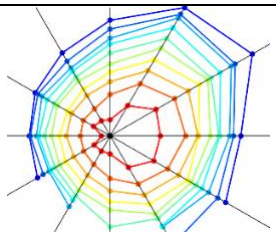	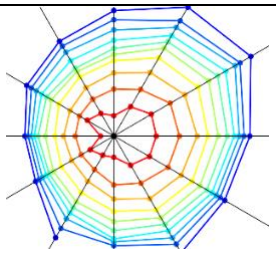
	Soft-bra scan:	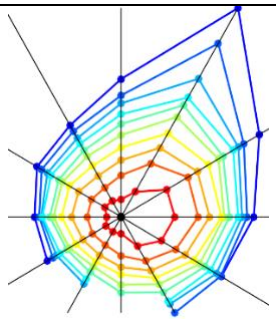	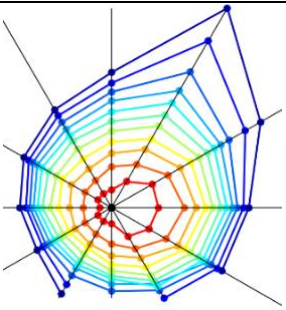

True nude scan		Predicted shape	True shape
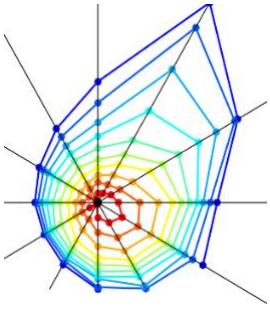	Structured-bra scan:	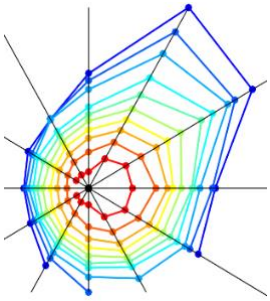	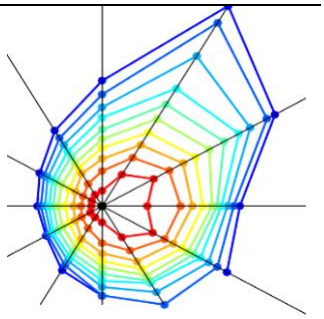
	Soft-bra scan:	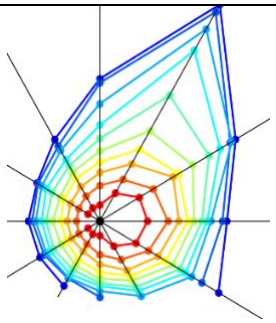	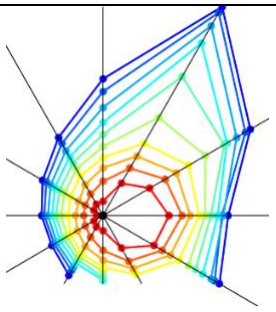

3.4. Qualitative analysis

Table 6 shows the contour maps and the scan surface heat maps of the breasts of two participants. Both participants have symmetric breasts with or without bra.

Obvious distinctions in shapes can be observed among the contour maps.

Table 6. Two representative cases to demonstrate the shaping effect of bras

Case I	Contour map (In-bra)	Scan surface heat map
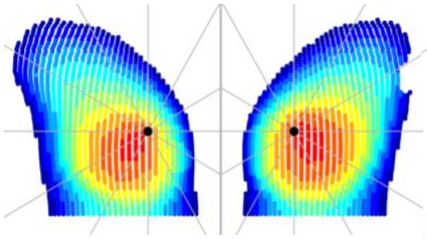 Nude-breast scan	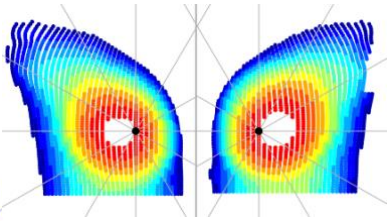 Structured-bra scan	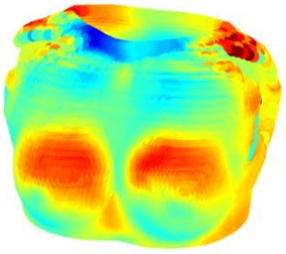 Structured-bra vs. Nude
	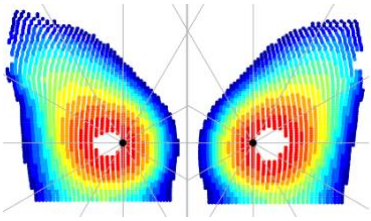 Soft-bra scan	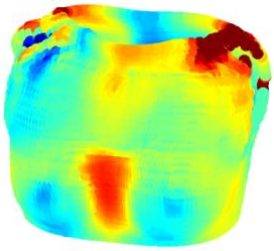 Soft-bra vs. Nude

Case II	Contour map (In-bra)	Scan surface heat map
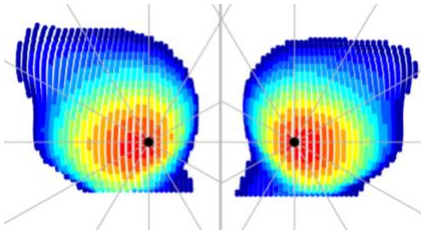 Nude-breast scan	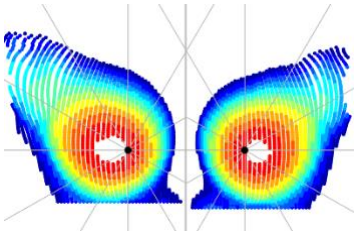 Structured-bra scan	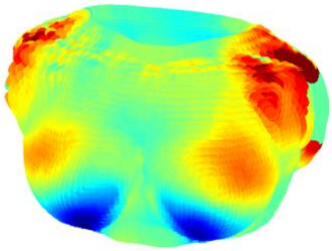 Structured-bra vs. Nude
	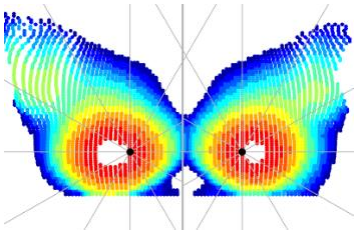	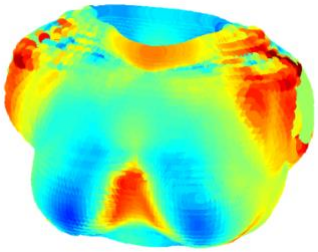

According to the observation of all 46 participants, most of the structured-bra contour maps show certain degree of lift-up effect. Most soft-bra contour maps appear to be flattened to a higher extent vertically than horizontally (see Case II in Table 6). The lift-up effect can be more easily observed in the heat maps. For the structured-bra heat maps, red/orange colors, which implies expansion, can usually be found at the upper section of breasts, while blue/cyan colors, which implies compression, can usually be found at the lower section (Table 6 and Figure 2b). This shows that the whole breasts had been pushed up to a higher level. In addition to push-up, push-in effect can be observed for some participants (Case I in Table 6, and Figure 2b). Their breasts were pushed slightly towards the center (the push-in is not large enough to form cleavage). Although only the same style of bra was used during scanning, many other participants do not show push-in effect at all. Their breasts were pushed upwards but also rotate towards the sides (Case II in Table 6). It appears that the same style of bras can have different shaping effect on different people, but this could also due to how the bras were donned (some people may prefer to move their breasts by hand towards the center intentionally).

The red/orange colors at central bridge area are usually caused by the gap between the bra and the skin surface, rather than by the shape modification of breasts. This pattern in the heat map happens with the soft-bra more often than with the structured-bra, but if the structured-bra is poorly fitted and the bridge is not in contact with the skin, this will appear in the heat map (Figure 2b). Among the soft-bra heat maps, the typical shapes of the red/orange area are triangle (Case II in Table 6) and inverted trapezoid (Case I). Observation shows that if the two breasts are already fairly close together on the torso without the bra, the inverted trapezoidal shape will be more

likely to appear, but since most nude breasts are separated, triangular shape shows up more often. On the other hand, because the soft-bras used in this study were soft and highly stretchable, there are a few instances that do not have the red/orange area. These instances show mild yellow at the bridge area, suggesting the gap between garment and skin is small (some other cases show no gap at all). These are usually the cases where breast size is not as big.

There are three participants who have very flat breasts. They don't have much deformable tissue on their breasts. Therefore, not only their nude breast shapes are quite different from the rest of the participants, the manner in which the bras influence their breast shapes is also very different, and inconclusive. It's hard to tell whether the red/orange areas are caused by expansions in shape or by garment gaps. There is no general trend that can be summarized from the contour maps or the heat maps, due to the limited number of participants with flat breasts and the large differences in bust shapes among them.

Lastly, high asymmetry in the color distribution, which represents shape variations in the breast, can be observed for some cases (e.g. high expansion appears only on one side of the breasts). This is as expected because in general, both the structured-bras and the soft-bras can improve the breast symmetry to some extent (as demonstrated in Section 3.1), and the improvement in symmetry could mean equalization when there was initially more variation on one breast than the other.

4. Conclusions

To investigate the impact of structured-bras and soft-bras on the breast shape, this study recruited 46 female participants (Caucasian, BMI < 30, aged 18-45) for 3D scanning. Participants were asked to wear a structured-bra, a soft-bra, and no bra during scanning. Three scans were obtained for each participant and were processed in

Matlab®. Contour maps that show the topographic shapes of the breasts were generated and studied. Thirty-five measurements were extracted from the spider web structures simplified from the contour maps, and were used for statistical analysis. Scan surface heat maps that represent the shape modification via colors were adopted for qualitative analysis. This study is very useful for researchers to understand how bras interact with the breast tissue, and for bra designers to improve their designs to achieve desired shaping effects.

The impact of bras on breast asymmetry was firstly explored. The breast asymmetry was quantified by calculating the Asymmetry Index (ASI). A higher value in the ASI implies lower degree of symmetry between the left and right breasts. The overall boxplot shows that in general, both structured-bras and soft-bra can help to improve breast symmetry. The ASI differences between a nude-scan and one of the two in-bra scans were also calculated for each individual participant. The individual analysis shows that for both types of bras, a significant improvement on the breast symmetry is more likely to happen to nude breasts that are severely asymmetric.

More quantitative analysis was done on the unconventional measurements. The results of the pairwise Hotelling's T_2-tests show that the 35 measurements are able to detect the shape modifications. The post-hoc tests with Bonferroni correction revealed eight measurements to be especially significant. Among them, six measurements are the radius increments between adjacent layers at certain angles. They all relate to the angles on the upper section of the breast. The other two measurements are the overall perimeter ratio and the overall area ratio between adjacent layers. It was found that under compression of a bra, as the breast becomes less prominent and less conical, both ratios will decrease. Furthermore, to study the relationship between the nude shape and the shape modification introduced by the bras, the correlations between the shape modification values (calculated by subtracting the nude-breast data from the

structured-bra/soft-bra data) and the nude-breast data were obtained for each measurement. A substantial portion of measurements show strong negative correlations, including all of the eight significant measurements. In addition, regression prediction models were built to predict the in-bra shape given only the nude breast shape. Similarities can be observed between the predicted shape and the true shape.

As for the qualitative analysis, according to observations, most of the contour maps of the soft-bra scans indicate that the breasts are flattened to higher extent in the vertical direction. Both the contour maps and the scan surface heat maps show that the breasts had been pushed up by the structured-bras. Some participants' breasts were also slightly pushed in, whereas many other participants do not show push-in effect at all. A gap between the bra and the skin surface can sometimes be observed in the heat maps of the soft-bras. The shape of the gap relates to how separate the breasts are.

In this study, we concentrated on comparisons between the nude breast shape and the structured bra shape, and between the nude breast shape and the soft bra shape. Similar methods could be used to investigate changes in shape between bra styles, by comparing the structured bra to the soft bra. This could result in methodologies to convert scan data from the many body scan studies conducted with soft bras to more useful structured bra shapes.

There are several limitations in this study. Firstly, despite that the scan surface heat map can be a good visual tool to evaluate the shape modifications on the torso, it may not work well for the neck and the shoulders. The generation of the heat map relies highly on the alignment of scans and is very sensitive to displacement and posture changes. Although participants were asked to keep the same posture during scanning, slight posture changes cannot be avoided, especially for the arms. The placement of arms also directly influences the shoulder areas on the scan. Perfect

alignment at shoulder areas and armhole areas is almost unachievable. This is the reason why some abrupt and irregular dark red or dark blue colors appear at the shoulder and armhole areas, as well as neckline area for some participants, on the heat maps. It is also possible that the wearing of different types of bras could be an influencing factor in body posture: the weight distribution of the breasts, and the forces generated by the different straps and bands interacting with the body may have an effect on the position of the shoulders and neck. Secondly, this study was unable to draw informative conclusions for the flat-chest population, partly because of the small sample size (only three participants with flat chests were in the sample). Neither quantitative analysis nor qualitative analysis could reach consensus for these three cases. Although the flat-chested population is a minority among the female population, their need for improved bra designs cannot be overlooked. Future study could be done specifically for this population. In addition, the sample size is relatively small. The 46 participants may not be sufficient in capturing all the breast shape variation in the population (for aged 18 to 45, Caucasian females, with BMI < 30). Moreover, although the prediction regression models predict the in-bra shapes to some extent, there is room for improvement. This is also due to the limited number of participants. Better regression models can be built with increased sample size. In addition, since the shape modification is related to the nude breast shape, a categorization of the nude-breast shape into different groups before regression may improve the accuracy of the prediction. Also, the regression models depend highly on the specific bra style and the fit of the bras; thus cannot be generalized to other designs and styles. Future studies can look into the material properties of the bras and refine the models for an improved generalizability. There also may be variation introduced in the manner in which participants donned the bras; that is, some participants may have manually centered the breast tissue in the bra cup in different ways resulting in different results. A study

in which the bras are donned in a standard manner may result in different outcomes. Lastly, merely comparing breast shape is not sufficient for understanding the relationship of the bust to the torso. Therefore, additional information, for example, the relationship of the bust point to the sternum (a potential measure of how high the bust is lifted by a bra), is needed for bra designers.

DISCLOSURE STATEMENT

This chapter is a peer-reviewed journal paper published in 2019. Citation information is listed below. Reuse permission has been acquired from Sage.

Pei, J., Fan, J. & Ashdown, S. P. (2019). Detection and Comparison of Breast Shape Variation among Different 3D Body Scan Conditions: Nude, with a Structured Bra, and with a Soft Bra, *Textile Research Journal, 89*(21), 4595-4606.

REFERENCES

Ashizawa, K., Sugane, A., & Gunji, T. (1990). Breast form changes resulting from a certain brassiere. *Journal of human ergology*, *19*(1), 53-62.

Brown, T. L. H., Ringrose, C., Hyland, R. E., Cole, A. A., & Brotherston, T. M. (1999). A method of assessing female breast morphometry and its clinical application. *Journal of Plastic, Reconstructive & Aesthetic Surgery*, *52*(5), 355-359.

Chan, C. Y., Yu, W. W., & Newton, E. (2001). Evaluation and analysis of bra design. *The Design Journal*, *4*(3), 33-40.

Lee, H. Y., Hong, K., & Kim, E. A. (2004). Measurement protocol of women's nude breasts using a 3D scanning technique. *Applied Ergonomics*, *35*(4), 353-359.

Luk, N., & Yu, W. (2016). Bra fitting assessment and alteration. In *Advances in Women's Intimate Apparel Technology* (pp. 109-133). Woodhead Publishing.

McGhee, D. E., & Steele, J. R. (2006). How do respiratory state and measurement method affect bra size calculations?. *British journal of sports medicine*, *40*(12), 970-974.

McGhee, D. E., & Steele, J. R. (2010). Optimising breast support in female patients through correct bra fit. A cross-sectional study. *Journal of Science and Medicine in Sport*, *13*(6), 568-572.

Page, K. A., & Steele, J. R. (1999). Breast motion and sports brassiere design. *Sports Medicine*, *27*(4), 205-211.

Pei, J., Fan, J., & Ashdown, S. P. (2019). A novel method to assess breast shape and breast asymmetry. *The Journal of The Textile Institute*, *110*(8), 1229-1240.

Scurr, J., Loveridge, A., Brown, N., & Mills, C. (2015). Acute changes in clinical breast measurements following bra removal: Implications for surgical

practice. *JPRAS Open*, *3*, 22-25.

Wood, K., Cameron, M., & Fitzgerald, K. (2008). Breast size, bra fit and thoracic pain in young women: a correlational study. *Chiropractic & osteopathy*, *16*(1), 1.

Yu, W., Fan, J., Ng, S. P., & Harlock, S. (2014). Innovation and technology of women's intimate apparel. Woodhead Publishing.

Zheng, R., Yu, W., & Fan, J. (2007). Development of a new Chinese bra sizing system based on breast anthropometric measurements. *International Journal of Industrial Ergonomics*, *37*(8), 697-705.

APPENDIX. MEASUREMENT LIST

Note. The illustrations show only four layers for legibility, in fact there are eleven layers/slices.

Measurement Number	Illustration	Description
#1	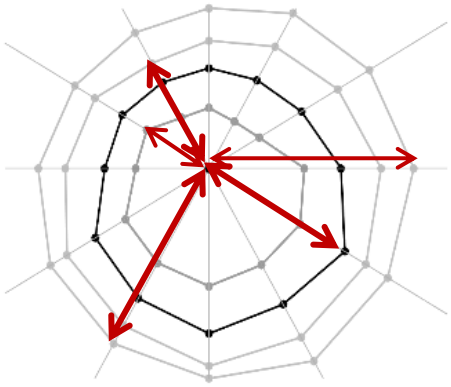	The overall radius (median of all radii at every angle and on every layer)
#2	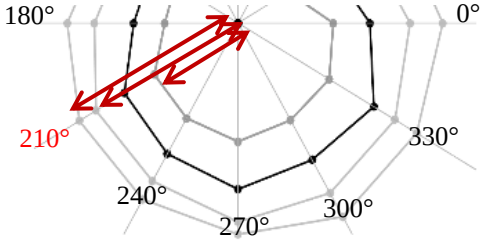	Median radius at 210˚ (-150˚)
#3	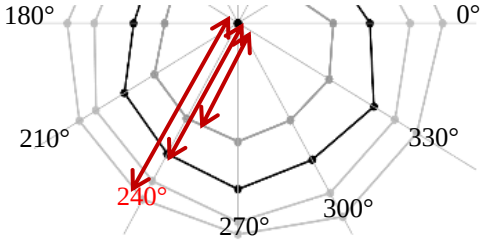	Median radius at 240˚(-120˚)
#4	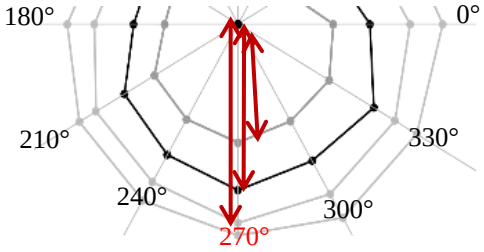	Median radius at 270˚(-90˚)

#5	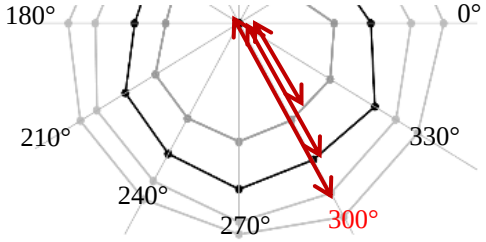	Median radius at 300˚(-60˚)
#6	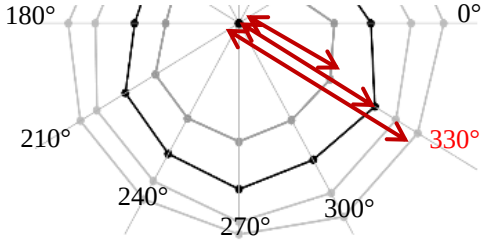	Median radius at 330˚(-30˚)
#7	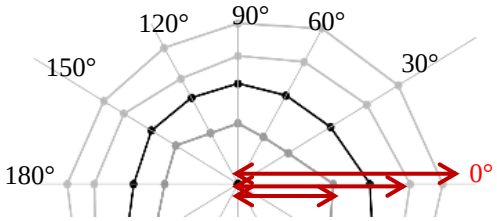	Median radius at 0˚
#8	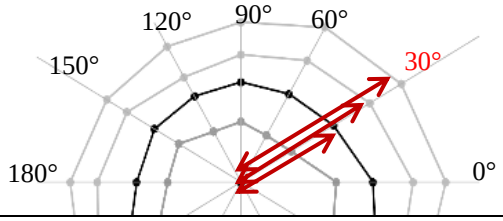	Median radius at 30˚
#9	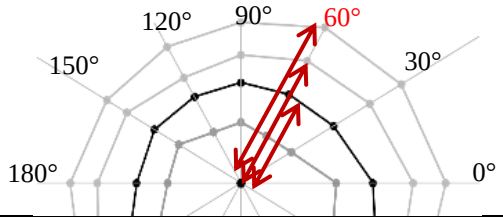	Median radius at 60˚
#10	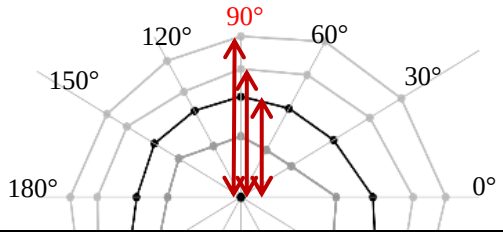	Median radius at 90˚
#11		Median radius at 120˚

	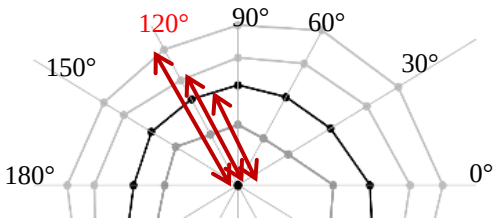	
#12	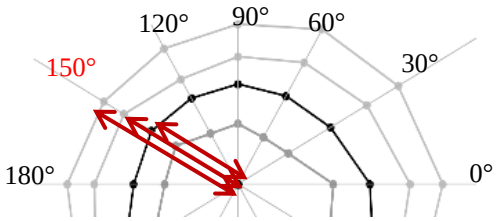	Median radius at 150˚
#13	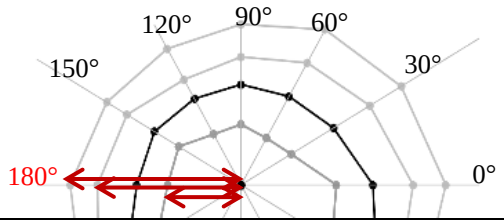	Median radius at 180˚
#14	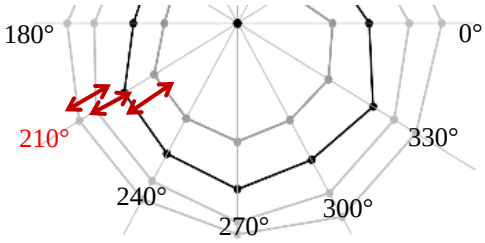	The median of between-layer radius increments at 210° (-150˚), divided by the median radius at 210° (Measurement #2)
#15	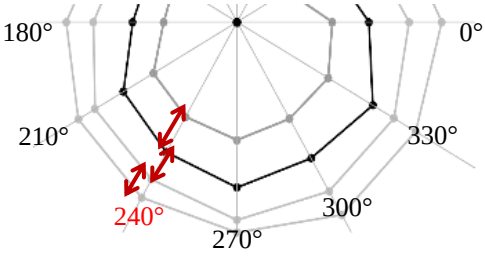	The median of between-layer radius increments at 240° (-120˚), divided by the median radius at 240° (Measurement #3)
#16		The median of between-layer radius increments at 270° (-90˚), divided by the

	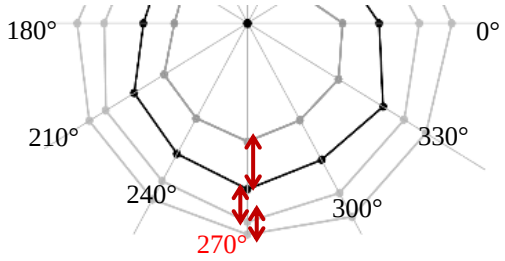	median radius at 270° (Measurement #4)
#17	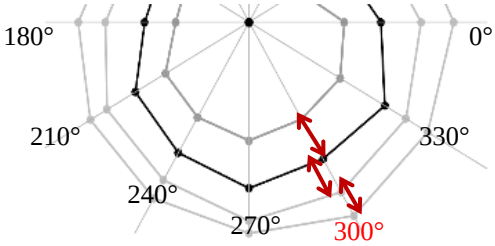	The median of between-layer radius increments at 300° (-60˚), divided by the median radius at 300° (Measurement #5)
#18	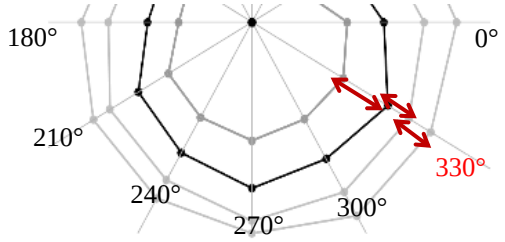	The median of between-layer radius increments at 330° (-30˚), divided by the median radius at 330° (Measurement #6)
#19	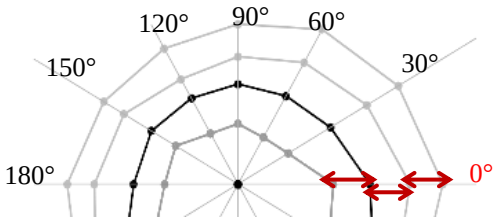	The median of between-layer radius increments at 0°, divided by the median radius at 0° (Measurement #7)
#20	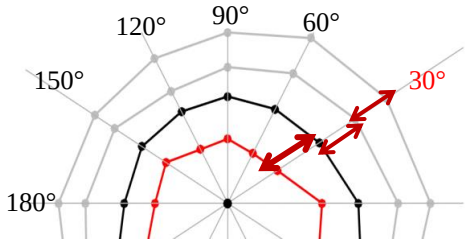	The median of between-layer radius increments at 30°, divided by the median radius at 30° (Measurement #8)

#21	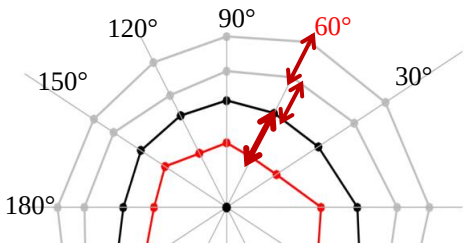	The median of between-layer radius increments at 60°, divided by the median radius at 0° (Measurement #9)
#22	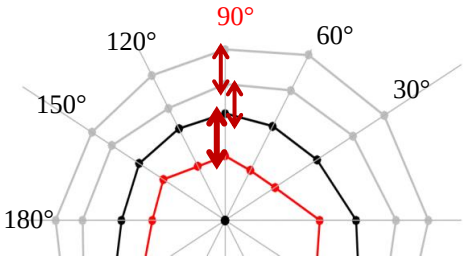	The median of between-layer radius increments at 90°, divided by the median radius at 90° (Measurement #10)
#23	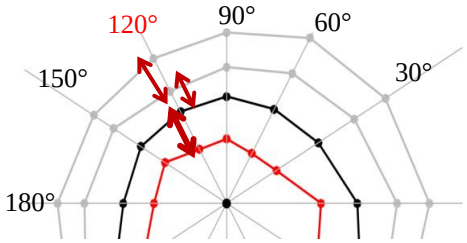	The median of between-layer radius increments at 120°, divided by the median radius at 120° (Measurement #11)
#24	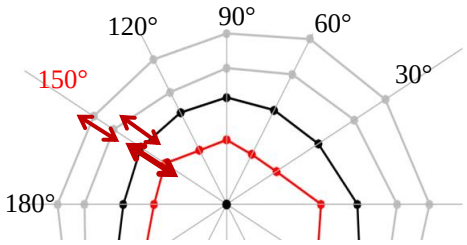	The median of between-layer radius increments at 150°, divided by the median radius at 150° (Measurement #12)
#25	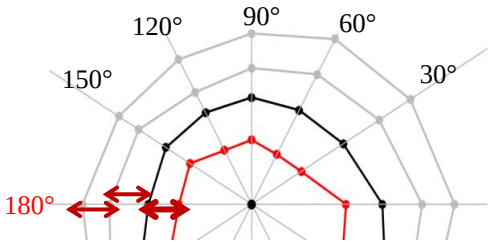	The median of between-layer radius increments at 180°, divided by the median radius at 180° (Measurement #13)

#26	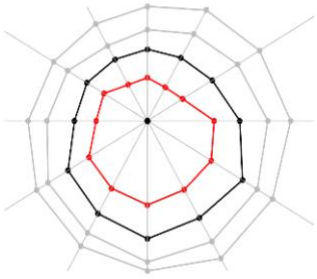	The overall perimeter ratio (the outer ring to the inner ring) between layers, taking the median
#27	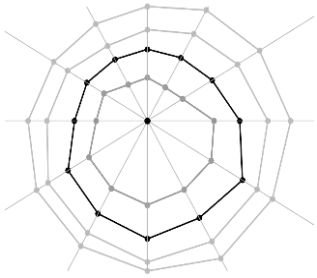	The median perimeter of all layers
#28	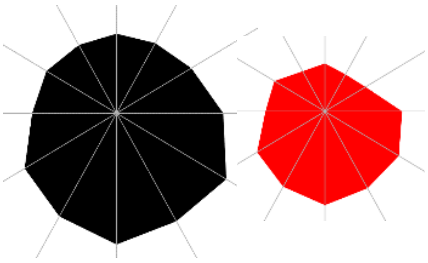	The overall area ratio (the outer ring to the inner ring) between layers, taking the median
#29	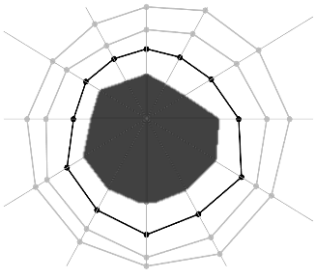	The median area of all layers

#30	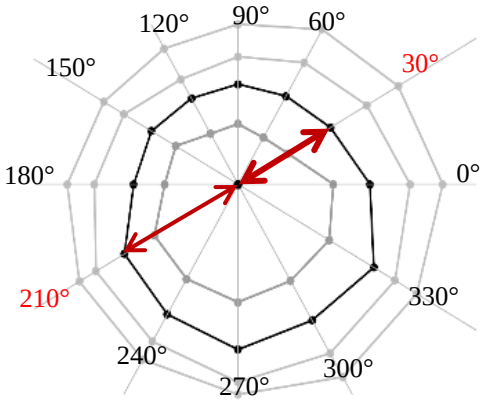	Diagonal radius difference: radius at 30˚minus radius at 210˚ (first compute the difference at each slice, then compute the median among all 11 slices)
#31	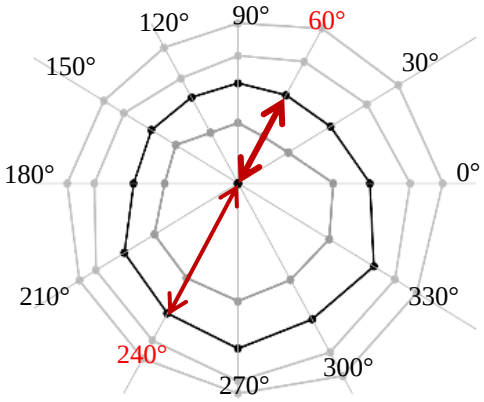	Diagonal radius difference: radius at 60˚minus radius at 240˚ (first compute the difference at each slice, then compute the median among all 11 slices)
#32	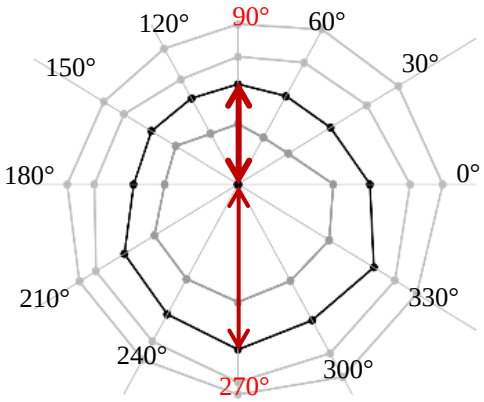	Diagonal radius difference: radius at 90˚minus radius at 270˚ (first compute the difference at each slice, then compute the median among all 11 slices)

#33	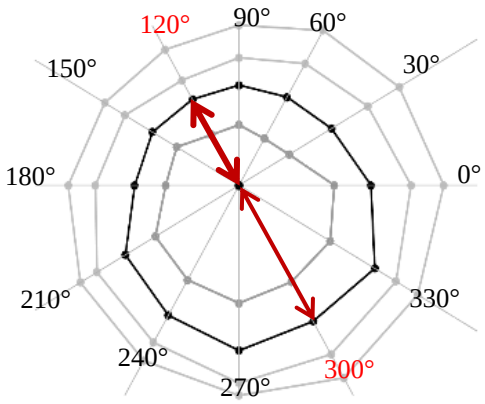	Diagonal radius difference: radius at 120˚minus radius at 300˚ (first compute the difference at each slice, then compute the median among all 11 slices)
#34	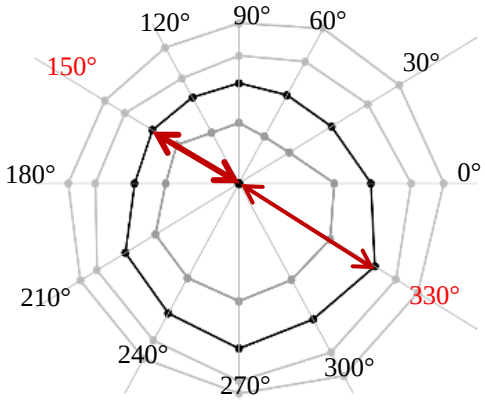	Diagonal radius difference: radius at 150˚minus radius at 330˚ (first compute the difference at each slice, then compute the median among all 11 slices)
#35	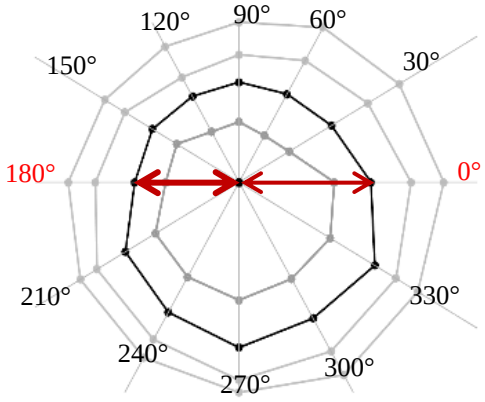	Diagonal radius difference: radius at 180˚minus radius at 0˚ (first compute the difference at each slice, then compute the median among all 11 slices)

CHAPTER 4

STUDY OF BREAST SHAPE DURING RUNNING USING 4D SCANNING TECHNOLOGY

Abstract

Physical activity can lead to the displacement of the female breasts causing psychological and physical discomfort or even breast pain. It is suggested for all exercising females to protect the breasts with additional support and restriction against displacement. For females who are physically active or rely on Personal Protective Equipment (PPE) for work, sports bra, bras in general, and wearable products such as body armors, fall harness systems, etc. that ensure a good fit at the breasts are critical to the wearers' well-being and safety. The purpose of this research was to introduce the use of 4D scanning technology to understand breast shape in motion. Twenty-six female participants who identified themselves as wearing Missy Size 18 were recruited for scanning. Ten breast-related body measurements were tracked in dynamic states and compared with the static state. The results of this study can benefit product development female wearable products that require high degree of fit and mobility at the upper torso. In addition, a protocol to handle and analyze 4D data for application in product design was developed to inform future research. The promises and challenges of the 4D body scanning technology were also discussed.

1. Introduction

It has been well established that physical activities can lead to the displacement of the female breasts causing embarrassment or psychological discomfort and/or physical discomfort for the exercising females (Page & Steele, 1999; Greenbaum, Heslop,

Morris & Dunn, 2003). The displacement may also cause breast pain, shoulder pain and neck pain, thus negatively impact females' willingness and ability to perform in exercise (Lorentzen & Lawson, 1987; Mason, Page & Fallon, 1999; McGhee & Steele, 2011; Coltman, Steele & McGhee, 2019). The extensive vascular supply of the breast stroma makes the breasts vulnerable to internal bleeding resulting from external movement (Page & Steele, 1999). With increased breast size, the chance and severity of musculoskeletal pain is found to be higher (Coltman, Steele & McGhee, 2018). The severe musculoskeletal pain led some females into seeking reduction mammoplasty (Hadi, 2000; Greenbaum, Heslop, Morris & Dunn, 2003). Therefore, it is suggested for all females undergoing physical activities to protect the breasts with additional support and restriction against displacement (Page & Steele, 1999). A sports bra is designed for these purposes and anchors the breasts to the chest wall via strong elastic and/or underwires (Page & Steele, 1999). While providing sufficient restriction over breast displacement is important, excessive pressure of an ill-fitting bra can cause breast pain and may even increase the risk of breast cancer (Singer & Grismaijer, 1995; Chen, LaBat & Bye, 2010). Excessive bra strap compression can cause deep bra furrows and upper limb neural symptoms (Kaye, 1972; Greenbaum, Heslop, Morris & Dunn, 2003). Therefore, achieving a good fit is essential in the design of sports bras or bras in general. Moreover, for females who rely on Personal Protective Equipment (PPE) for work, wearable products, such as body armors, fall harness systems, etc., that ensure a good fit at the breasts are critical to the wearers' well-being and safety (Todd, 2007; Watkins & Dunne, 2015).

1.1. Variation of breast shape and size

Breast shape and breast size vary significantly among females, and the variation causes great difficulty and a lot of challenges in the design of female wearable

products (Hart & Dewsnap, 2001; Pei, Park & Ashdown, 2019). Sigurdson and Kirkland (2006) measured the breasts of 101 females and found a vast range of breast volume, from 330 cc to 2600 cc. McGhee and Steele (2011) also reported vast ranges of volume, i.e. 125-1900 ml for the right breast and 100-1825 ml for the left breast, after measuring 104 females. In addition to breast size, breast shape can be very diverse. It can be descriptively classified based on breasts separation (4 types: touching, separated, splayed and wide-set), upper breast fullness (4 types: full, semi-full, shallow and deflated), position on chest (4 types: self-supported, semi-supported, settled and pendulous), shape (5 types: archetype, uneven, conical, thin and reduced projection) and apex/nipple direction (3 types: forward-pointing, outward-pointing and downward-pointing), according to Herroom.com (n.d.). However, even the full combination of these classification types, a total of 960 types (4×4×4×5×3) may not fully express the variation in breast shape.

Age, body size, ethnicity, and other factors all contribute to the variation in breast size and shape (Lawrence & Lawrence, 2011; Pei, Park & Ashdown, 2019). Even for the same female, her breast shape can be affected by pregnancy, nursing, menopause, and hormone levels, thus goes through changes at various stages of her life (Hussain et al., 1999; Tiggemann, 2004; Lawrence & Lawrence, 2011). Hussain et al. (1999) reported an average of 76 ml of volume variation for a breast during the menstrual cycle equaling to 13.6% of the volume at menses. A breast can increase weight from 200 grams to 400-600 grams during pregnancy, and to 600-800 grams during lactation (Lawrence & Lawrence, 2011). With increased age, a decrease in breast density but an increase in the distance between nipples are reported to be generally seen, additionally, breasts tend to sit lower on the torso (Haars et al., 2005; Ashdown & Na, 2008). Den tonkelaar, Peeters and Van Noord (2004) found that bra size was reported to have increased for 18.6% of their 1130 post-menopause female participants, mostly

due to weight gain. They also claimed that age, age at first childbirth and number of months of breastfeeding had minor impacts for the increase in breast size. Coltman, Steele and McGhee (2017) also found that breast volume can be significantly influenced by Body Mass Index (BMI), but not so very influenced by age. Del Carmen et al. (2007) investigated the breast density of 15292 females and found it to be greater for Asian females and least for African American females, although age and BMI could be the more dominating factors. Shin (2009) compared the breast shapes between 90 Asian females and 90 Caucasian females, and discovered a significant difference.

In this study, 26 female participants, who identified themselves as wearing Size 18 (Missy dress size), were recruited. We did not add additional recruitment criteria such as age range, ethnicity or Body Mass Index (BMI), etc. which are commonly used in anthropometric studies. This is because in real-life applications, bras and other garments are sold to females regardless of their age and ethnicity (BMI is seldomly used as a direct guidance) but only according to sizes. The plus-size population usually has more body shape variations, creating more challenges for garment fit, but is not well studied.

1.2. Previous breast shape studies for product development

Lee, Hong, and Kim (2004) 3D-scanned the nude breasts of 37 Korean females who wore an 80A size bra (Korean size) and suggested that the global average radius for the underbust curve to be a useful design parameter for form-fitting bras. Lee and Hong (2007) further studied the shape of the natural underbust curve and proposed an optimized design for bra underwires that may provide better support for breasts. Zheng, Yu, and Fan (2007) extracted 98 anthropometric measurements from the nude-breast scans of 456 Chinese females (age 20-39) for breast shape classification. They

suggested a breast depth-width ratio in replacement of the traditional measurement of bust-underbust difference for an improved bra sizing system. Chen, LaBat, and Bye (2011) measured the bust prominence of 103 Caucasian female students (age 18-25) using three different methods that determines bra size and found that the lack of support is the most common bra fit problem amongst their participants. Liu, Wang, and Istook (2017) scanned the nude breasts of 275 female college students in China and extracted 108 breast shape-related measurements. They proposed adding the measurement of breast breadth to the current bra sizing system. Coltman, McGhee, and Steele (2015) recruited 23 females who wore a D+ cup to investigate the best bra strap orientations and designs for exercising females with large breasts. They found that bra straps that are vertically orientated, and wide were more desired. Coltman, Steele and McGhee (2018) collected nude-breast scans of 378 Australian women (age 18-over) and classified the breasts based on breast volume, breast surface area, underbust circumference, sternal notch-to-nipple distance and nipple-to-nipple distance. McGhee et al. (2018) obtained the bust and underbust measurements of 111 females (age 21-56) both via manual measure and via 3D scanning. They found that measurements obtained from 3D scans were larger than the manual measurements in females with large breasts for underbust. Pei, Park, and Ashdown (2019) extracted 66 breast measurements from the scans of 478 North American Caucasian females (age 18-45). 41 ratio and angular measurements, calculated from the 66 raw measurements, were used to categorized breast shape. Pei, Fan, and Ashdown (2019) scanned 46 Caucasian females (age 18-45) in three conditions: nude, with a structured bra, and with a soft bra. They discovered that 8 measurements obtained from the topographic plot of breast were more indicative of the shape change introduced by the bras. Pei, Fan and Ashdown (2020) further used the nude scans that they collected and proposed an optimal method to minimize the aggregate-fit-loss for an improved bra sizing

system which can take into account all the 3D information captured in the scan.

Despite the great importance, the difficulty and challenge to improve the fit of products for the breasts continues to plague females on a daily basis (Nethero, 2007; Wood, Cameron & Fitzgerald, 2008; McGhee & Steele, 2011), female PPE are also in great need of improvement for fit at breast area (Page & Steele, 1999; Todd, 2007; Watkins & Dunne, 2015). 3D scanning technology has increased accuracy and insight into the development of design parameters for new wearable products and has enhanced the performance evaluation of garments and related equipment (Istook & Hwang, 2001; Loker, Ashdown, & Schoenfelder, 2005; Luximon, Zhang, Luximon, & Xiao, 2012). However, current research is lacking integrated movement and anthropometric data needed to make wearable product design decisions rooted in quantitative knowledge about the body. Limitations exist in 3D body scanners and motion capture systems' ability to quantify how the body surface changes during motion or provide in-depth data about the interaction of the product and body (Chi & Kennon, 2006). Current technology integration is inadequate and has not been proven successful in showing accurate and precise measurements of body surface change during movement (Sohn & Bye, 2014). When products are developed using static anthropometric data, the range of motion of the product in relation to the wearer can be inaccurate.

Dynamic anthropometric data, on the other hand, can influence innovation at the critical intersection of ergonomics and the sizing and fit of advanced wearable products. The 3dMD Temporal Body System (Temporal 3dMDbody18.t System Model) is one of the first commercial scanning systems that provides 4D data for analysis of the body. The 3dMD 4D full-body system captures and generates a series of 360-degree true anatomical body models over a period of time and combines the

features of the traditional 3D body scanner with a motion capture system. This facilitates the study of dense surface deformations, posture, and pose over prolonged sessions, as well as individual 3D frames. The 4D data from the 3dMD system allow movement to be expressed in terms of dense surface deformation and classification. This new paradigm of body analysis allows researchers to quantify and model the subtleties of human movement and human movement in relation to a worn product. The implications of studying and analyzing these body data will advance how we approach design problems, as well as the design and development of wearable products ranging from sportswear to medical products to spacesuits.

The purpose of this research was to study breast shape in motion using 4D scanning technology. As this is one of the very first studies to use 4D scanning to study breast shape for product design purposes, a protocol to handle and analyze 4D data for application in wearable product design was developed to inform future research. The questions guiding this research are the following:

- How do we process and analyze 4D scans to obtain measurements for product design purposes? (i.e. how do we measure the body in dynamic conditions)
- What are the challenges of 4D scanning technology to be used for facilitating product development?
- To what extent do body measurements change when the subjects are completing dynamic movements compared to static postures?
- How do measurement values of the breast change? Is it possible to see general trends in measurement change across small data sets?

2. Methodology

A specification of the 4D body scanner used in this study can be found in Table 1. The Temporal 3dMD body 18.t System can capture the instant soft-tissue motions

with a linear accuracy of 0.6mm or better. The scanning speed of 10 frames per second is also sufficient to capture all the soft-tissue deformation in detail. The 26 female participants, who identified themselves as wearing Size 18 (Missy dress size), were scanned in their underwear. Approval was obtained from the Institutional Review Board and informed consent was obtained from every participant.

Table 1. 4D body scanner specifications

Name/Model	Temporal 3dMD body 18.t System
Company:	3dMD Inc., Atlanta, GA, USA
Capture:	Single 3D capture or up to 10 color 3dMD frames per second at highest resolution Generates a series of 360-degree body models over a period of time. Freezes actual 3D instances of time
Configuration:	Optics-based system with 18 modular units of 54 machine vision cameras synchronized with a LED lighting system
Technology:	Stereophotography
Output:	One continuous point cloud or textured mesh per frame
Accuracy:	Dense surface with a linear accuracy range of 0.6mm or better. Same level frame-by-frame accuracy as static capture
Precision:	Temporal precision with no 3D jitter on playback
Color/Texture:	High-quality texture maps that exceed full-HD densities

Retrieved from: http://www.humanopia.co.kr/homepage_data/products/3dMD/3dMD%20Product%20Specification_Jan_2017.pdf

The participants were asked to run in place due to the limited space for actual running and the unavailability of a treadmill at the time of the scanning. Most of the

participants wore the bra of their own size but of a consistent style and design (a common T-shirt bra: Molded contour, cups with underwire, unpadded), provided by the researchers (size range: 36C-42G). Note that the bra would impact breast motion to some extent, thus the results would be different from nude breast motion. Several participants could not find their size in the provided bras and therefore wore their own bra during scanning. We did not exclude those participants to preserve the variation of body size and shape within this population. For comparison purposes, a 3D scan of participants in a static pose was captured. Moreover, 17 landmarks were placed onto the participant's body by the researchers before scanning (see Appendix A).

2.1. Selection of critical frames

3D scans of one running cycle were selected from a large number of scans captured by the Temporal 3dMD system. In general, a complete running cycle consists of nine scans or frames. Participants who ran faster could end up with fewer scans within a cycle and vice versa. However, no participant had more than nine frames for a cycle. A running cycle was selected after a few cycles when the running patterns became stable, to allow for a familiarization period. Three keyframes (Figure 1) were identified as the start, the middle and the end frame of the cycle: 1) the frame where the participant's left leg was bent and her left knee was at the highest location; 2) the frame where the participant's right leg was bent and her right knee was at the highest location and 3) the same condition as the first keyframe (the ending of a cycle is the beginning of a new cycle). In order to conduct the analysis in a controlled manner, we kept nine scans for each participant, and sorted the scans so that the first, fifth and ninth scan corresponded to the three keyframes, respectively (Figure 1). For several participants, we duplicated the intermediate scans (which were not associated with the keyframes) to ensure there were nine scans in total.

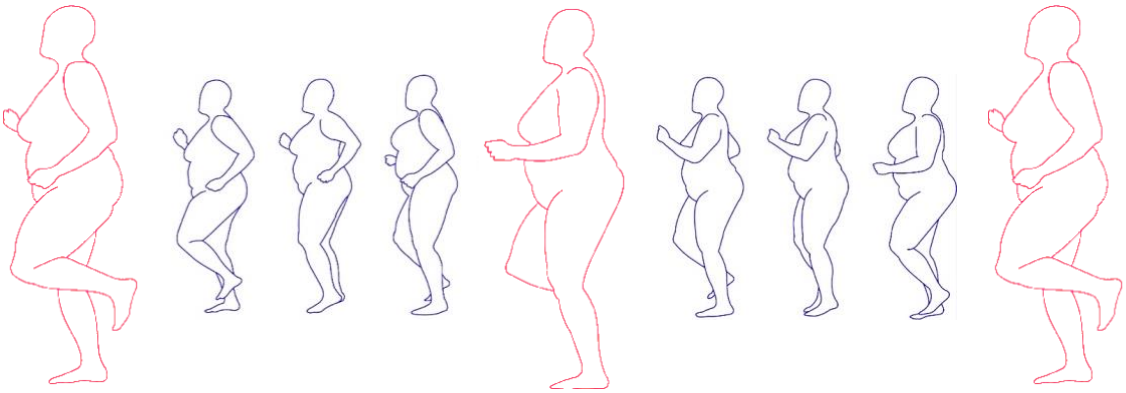

Figure 1. Three keyframes of a complete running cycle

2.2. Scan treatment

The head and the limbs were removed manually for each of the selected scans in MeshLab, an open-source 3D scan processing software. This is a necessary step because the swinging arms may interfere with the extraction of measurements on the torso, especially at the breast area. For some scans, because of the proximal position of the arm, a hole or holes on the scan surface resulted when the arm was removed. (Figure 2a and 2b). The holes were filled while maintaining the curvature of the surrounding area (Figure 2c), using Meshmixer, a 3D scan processing software. The processed scans were exported in .stl format. In addition, the scan-surface color and texture were loaded together with the scans into Meshmixer to make the landmarks identifiable. Then the mesh triangles where the landmarks were located (one triangle at each landmark location) were manually selected and exported in .stl format.

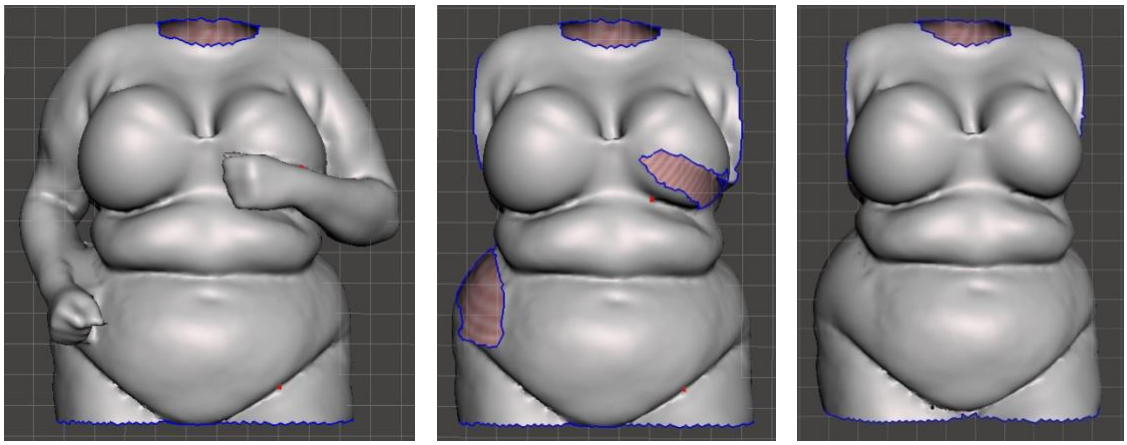

a) Arms too close to the torso

b) Holes resulted from arm removal

c) After filling

Figure 2. Scan preparation: removing limbs and filling holes

Finally, the scans were imported into Matlab®, where the x-y-z coordinates of the vertices of the triangular meshes were obtained and stored in .m format. Similarly, the landmarks were treated just as the scans. As mentioned earlier, there was one triangular mesh (three vertices, thus three sets of x-y-z coordinates) at each landmark location. The geometric center of the triangle was calculated and its x-y-z coordinate was regarded as the exact location of the landmark.

Due to the arm swing and individual habits, the posture of the upper torso varied throughout the running cycle. Scans were reoriented via shifting and rotation. At first, several Matlab® programs were developed to reorient the scans based on landmark pairs (e.g. the left and right bust points, the left and right acromion points). However, we observed some missing landmarks and suspected that several others may have shifted during running. The missing landmarks may have fallen off or been hidden in skin folds. Additionally, the swinging arms may also obstruct the light of the scanner from capturing the landmarks. Moreover, the landmarks placed on the skin surface are prone to slide with respect to the bones underneath, a phenomenon known as soft tissue artefacts (Andersen, et al, 2010). Previous research has also shown that this

phenomenon is more likely to occur for participants with higher body mass index (Shawgi, et al, 2012), the target population of this study. Therefore, instead of aligning based on landmark pairs, all the scans in running postures were shifted and rotated manually such that their upper torso (i.e. the section above the underbust level, which is the immediate cease of the breast swell) could align as much as possible with the upper torso of the scan in standing posture (note that perfect alignment is not possible, even based on landmark pairs). The manual alignment was done in Matlab® as well.

Bust points, the most protruding points on the breasts, are the most important landmarks for breast measurements. However, those landmarks may also shift or fall off during running. To address this issue, we adopted a method to identify bust point locations directly from the body scans (Figure 3). As shown in Figure 3a, the top view of the scan was plotted, where the approximate peak point of each breast was identified visually. Note that only the section above the underbust level was plotted because the abdomen may be more protruding than the breasts, thus interfered with the identification. Figure 3b presents the self-identified bust points (in red), along with the bust points identified through landmarks (in black), for some other scans. In this study, we only adopted the self-identified bust points when the bust point landmarks were missing.

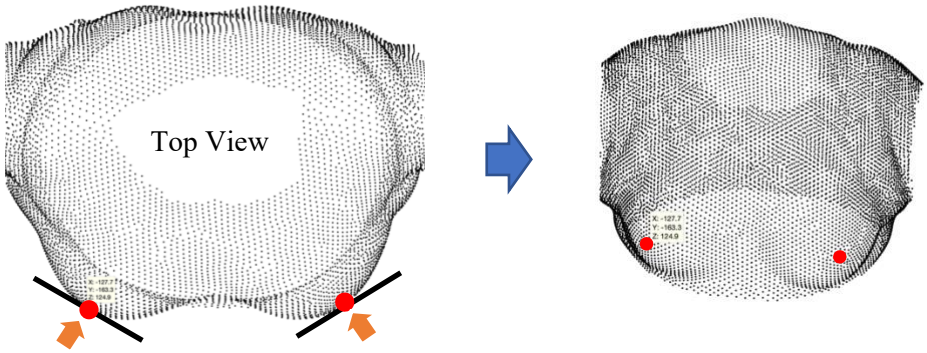

a) Identify the peak points of breasts from the top view of the scan

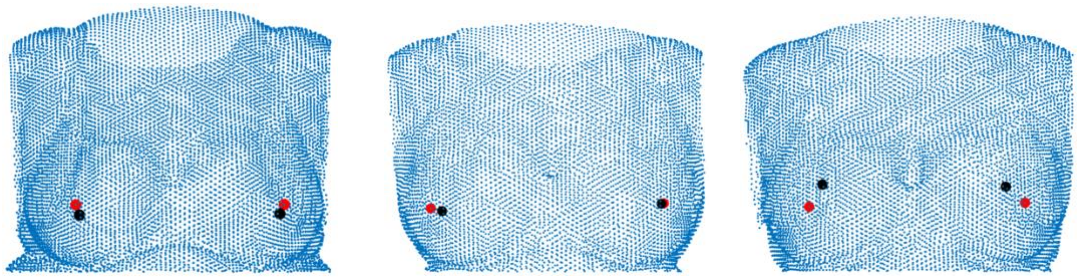

b) Self-identified bust points (in red) and bust points identified through landmarks (in black)

Figure 3. Self-identified bust points for missing landmarks

2.3. Extraction of body measurements

The complete list of the landmarks can be found in the Appendix. Based on the locations of the landmarks, transverse planes at the armpit level, bust level, and underbust level were obtained and plotted together (Figure 4a) and sagittal planes at the right bust point and center front were plotted together (Figure 4b). Note that the underbust level was defined as the most inferior level of the cease of the breast swell that is distinguishable from the chest wall. This is to ensure that the underbust plane does not cut into the breasts.

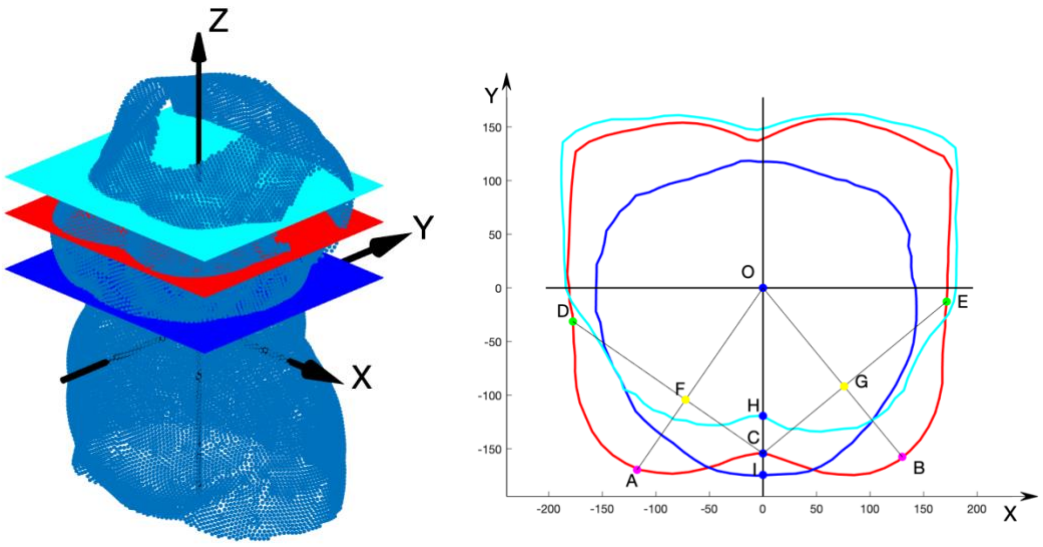

a) Transverse planes at armpit level, bust level and underbust level

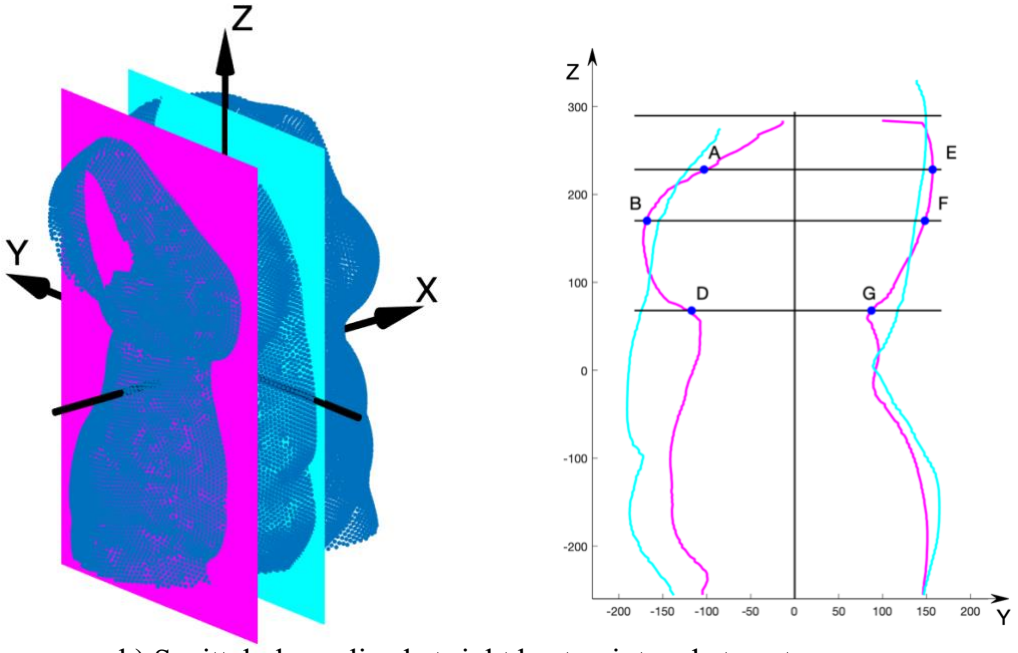

b) Sagittal plane sliced at right bust point and at center

Figure 4. Extraction of planes and breast measurements

A total of 10 breast-related body measurements were extracted from the extracted planes or based on the landmarks (Table 2). The three circumferential measurements were selected because they are commonly used by the apparel industry for product

development and because they are measurements consumers are most familiar with (ISO, 2017). The four linear measurements were selected to ensure there was at least one measured in the exact direction of each of the x, y, and z-axes. The three angular measurements were selected because they were found to be significant by previous researchers (Pei, Park, & Ashdown, 2019). In addition to Table 2, there is one illustration for each measurement presented in the result section.

Table 2. Description of the ten selected breast measurements

	#	Name	Description
Circumferential Measurements	1	Bust	Circumference of the bust-plane
	2	Underbust	Circumference of the underbust-plane
	3	Overbust	A 3D measurement that remains flat at the bust-plane level in posterior body but gradually goes above the swell of the breasts in anterior body
Linear Measurements	4	Width-bust	Width of the body at the bust-plane level Measured along the direction of the x-axis
	5	Width-underbust	Width of the body at the underbust-plane level Measured along the direction of the x-axis
	6	Chest-depth	Depth of the body at the bust-plane level, Measured along the direction of the y-axis
	7	Vertical-acromion	Vertical distance between the right acromion point and the right bust point Measured along the direction of the z-axis
Angular Measurements	8	AngleBPs	The angle between the two bust-points connected respectively to the projection point of the central axis on the bust-plane Measured in the bust-plane
			Point A, B and D are the anterior intersections between the outline of the sagittal plane sliced at right bust-point and the horizontal line at armpit level, bust level and underbust level, respectively
	9	AngleABD	Angle between line segments AB and BD Measured in the sagittal plane sliced at right bust-point

10	AngleBAD	Angle between line segments BA and AD Measured in the sagittal plane sliced at right bust-point

2.4. Statistical analysis

Analysis of variance (ANOVA) test for the nine dynamic frames in running was conducted, to investigate whether the nine frames have significantly different mean values.

To further test whether the mean values differ significantly between static and dynamic measurements, pairwise student t-tests were conducted with the static frame paired with each of the nine dynamic frames. The resulting p-values were adjusted with Bonferroni correction to avoid Type-I Errors.

Moreover, multiple linear regression analysis was conducted for each measurement with their dynamic values as the response (i.e. dependent variable). The corresponding static values were included as the first predictor (i.e. independent variable). Which dynamic frame the response belongs to (variable name: Frame ID) was included as the second predictor, and which human subject the response belongs to (variable name: Subject ID) was the final predictor. The impact of the predictors were examined by ANOVA (Type II) tests, to see whether the static value, Frame ID or the individual variability has a significant impact on the dynamic value.

To further test the impact of Frame ID, mixed effects models were fitted also with the dynamic value as the response. The static value and the Frame ID were treated as fixed effects, whereas Subject ID was regarded as random effect. The fixed effects were examined by Analysis of Deviance (Type II Wald Chi-square) tests due to some deficiencies of the ANOVA F-tests for mixed effects models, however, the p-values of Wald Chi-square tests still need to be interpreted with care. Therefore, instead of solely basing our conclusions on p-values, we examined the estimated coefficients of

the fixed effects which show the average impacts (of the static value, and Frame ID) on the dynamic measurements. The standard deviation of the random effect, which shows the variability between subjects, was also reported.

All statistical analysis was done in RStudio™ using the statistical computing language R (version 3.3.2).

3. Results and Discussion

To present the shape change of breast during running in place, the sagittal planes (at the right bust point) of the same participant were plotted and merged together. Figure 5 shows examples of three participants. The red outline indicates the participant in her standing posture, while the green and blue outlines show the same participant in two running postures. Good alignment can be observed at the upper back area due to the manual alignment process mentioned earlier. The anterior body and the lower posterior body (which includes the hip) have more fat tissue which may undergo more displacement and shape change during movement. In addition, shoulders have relative movement to the ribcage, therefore, the shoulder area is not ideal for scan alignment either. We recommend aligning scans at the upper back area. According to Figure 5, the breasts clearly went through a large amount of shape change during running, and simply studying the breast shape when participants are in a static standing state is not enough.

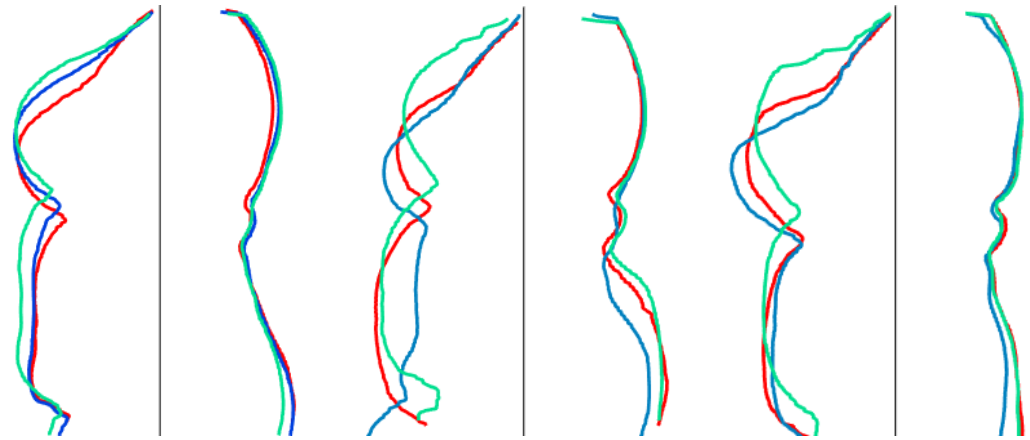

Figure 5. The changes of breast shape during running
(observation of the sagittal plane at right bust point)

Table 3 lists the summary statistics for the ten measurements. The last two columns show the range (i.e. maximum and minimum) for the standard deviation (SD) of each individual participant measured in dynamic (there is only one value for each participant measured in static, therefore individual static SD does not exist).

Table 3. Summary statistics for the ten measurements

Type	Name	Frame	Mean (mm)	Overall SD (mm)	Individual SD-Min (mm)	Individual SD- Max (mm)
Circum-ferential	Bust	Static	1260.7	78.2		
		Dynamic	1263.3	70.4	6.6	24.3
	Underbust	Static	1042.6	75.3		
		Dynamic	1060.1	75.2	5.3	27.5
	Overbust	Static	1164.8	65.4		
		Dynamic	1166.1	60.7	6.2	30.1
Linear	Width-bust	Static	390.8	30.9		
		Dynamic	389.3	26.4	3.3	20.1
	Width-underbust	Static	344.9	26.0		
		Dynamic	352.8	25.9	2.6	15.1
	Chest-depth	Static	310.7	27.5		
		Dynamic	318.3	23.0	2.2	12.0
	Vertical-acromion	Static	183.4	29.3		
		Dynamic	184.8	32.4	6.3	29.0
Angular	AngleBPs	Static	71.3	6.2		
		Dynamic	70.2	5.5	0.7	4.4
	AngleABD	Static	100.8	7.6		

		Dynamic	104.7	9.3	2.5	14.3
	AngleBAD	Static	34.5	6.2		
		Dynamic	33.0	6.7	1.5	8.9

Note. SD: Standard Deviation.

3.1. Circumferential measurements

Figure 6 shows the circumferential measurements of Bust, Underbust, and Overbust, for each participant, where the x-axis is the Subject ID from 1 to 26, and the y-axis shows the measurement values in millimeter (mm). For each participant, the blue dot represents the "static" measurement, which is the measurement obtained in static (i.e. in standing pose), while the range bar in red shows the upper and lower boundaries of the "dynamic" measurements which are obtained from running poses.

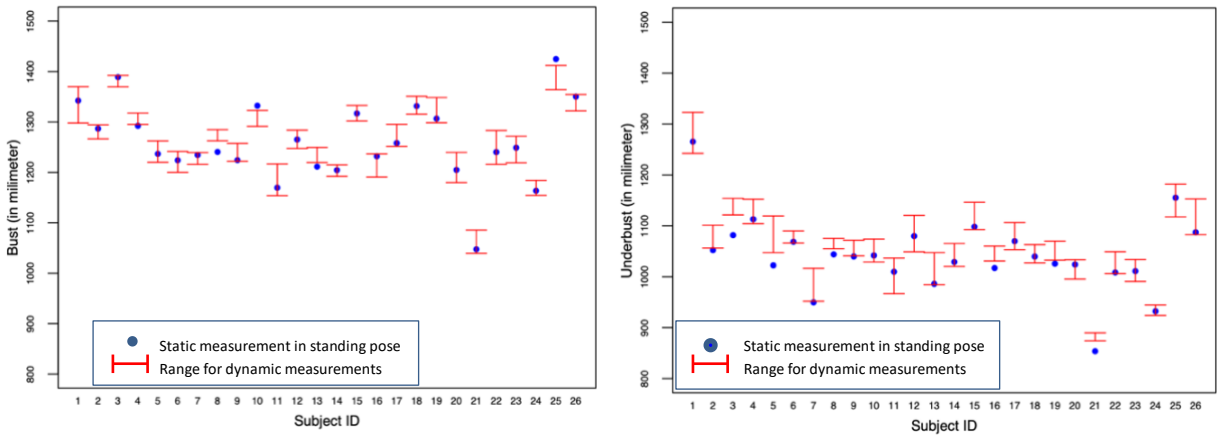

a) Bust b) Underbust

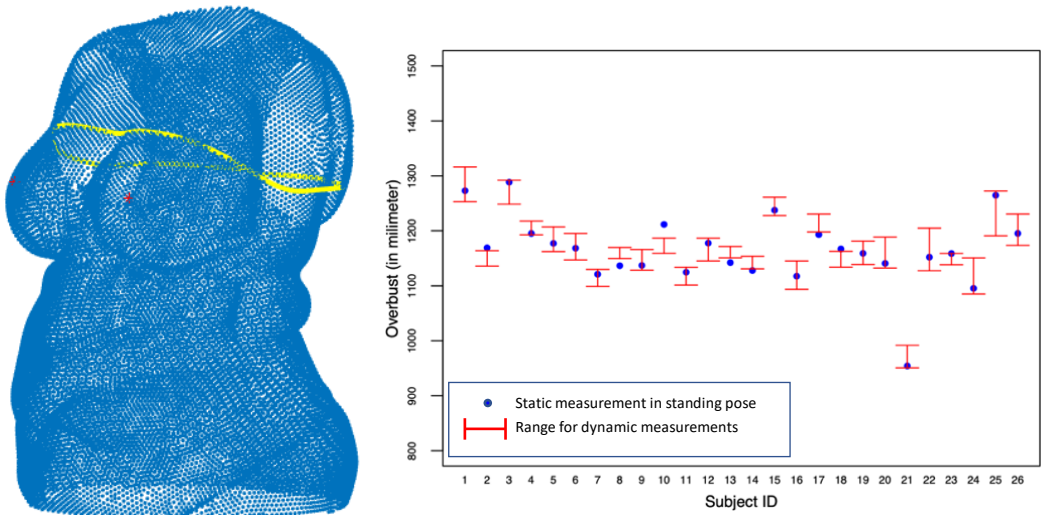

c) Overbust

Figure 6. Circumferential measurements

As shown in Table 3, for Bust, the individual SD ranges from 6.6 mm to 24.3 mm, which is about 9%-35% of the overall dynamic SD across the population (70.4). For Underbust, the individual SD ranges about 7%-37% of the overall dynamic SD. For Overbust, the individual SD ranges about 10%-50% of the overall dynamic SD.

ANOVA test shows that none of the three circumferential measurements show statistically significant differences (p-values are 0.86, 0.69 and 0.96, respectively). This is probably because the variability among individual participants is very large (see the last paragraph) thus more dominating.

Table 4 shows the pairwise student t-test results (the static frame paired with each of the nine dynamic frames). Clearly, for Bust and Overbust, none of the dynamic frames presents a significant difference with the static frame. In other words, their means do not differ much. Nevertheless, it does not mean that the static measurement is a good representation for the dynamic measurements. As shown in Figure 6a, for Bust, 2 participants have a static measurement that is larger than their maximum dynamic measurement (blue dot locates above the range bar), and 3 participants have a

static measurement that is smaller than their minimum dynamic measurement (blue dot locates under the range bar). In other words, 5 static measurements out of 26 (19%) completely fall outside the measurement ranges in running state. Similarly, for Overbust, 7 static measurements (27%) fall outside the dynamic ranges, with 3 above the upper boundary and 4 under the lower boundary (Figure 6c).

Table 4. Pairwise t-test with each of the dynamic frames for the circumferential measurements

	Dynamic frames								
Measurement name	1st (key)	2nd	3rd	4th	5th (key)	6th	7th	8th	9th (key)
Bust	1	1	1	0.35	1	1	0.49	0.19	1
Underbust	0.002**	0.10	0.09	0.003**	<0.001***	0.02*	0.44	0.001**	<0.001***
Overbust	1	1	1	1	1	1	1	1	1

Note. P values were adjusted with Bonferroni correction. The correction may increase p-values to as large as 1.

* Significant at 0.05 level; ** Significant at 0.01 level; *** Significant at 0.001 level.

For Underbust, the key dynamic frames and their immediate frames all present a significant difference with the static frame (Table 4). Figure 6b shows that as many as 9 participants (35%) have a static measurement that falls outside the dynamic range. All of them fall under the lower boundary, which means that Underbust measured in static is likely to underestimate the actual measurement under motion.

Table 5 and 6 include the results from the multiple linear regression and the mixed-effects model. For Bust, the impact of the static value is not as large as the impacts of Frame ID and individual variability: not only is Static value not statistically significant (p-value= 0.6, see Table 5), its estimated coefficient is low (β= 0.9, see Table 6). The 3rd, 4th, 7th, and 8th dynamic frames have much larger coefficients (β= 8.0, 11.4, 10.0 and 11.9, respectively) thus larger impacts on the dynamic

measurements than the other frames have. For Overbust, all three predictors are statistically significant (p-values < 0.05, Table 5), despite of a low coefficient for Static value (β= 0.9, Table 6), the same with that of Bust. In addition, the impact of Frame ID is only slightly different from that of Bust: the 4th, 5th, 7th, and 8th frames have larger coefficients (β= 9.6, 9.0, 7.7 and 8.4, respectively). The 9th frame has a negative coefficient for both Bust and Overbust. In fact, it was found that the correlation between static Bust and static Overbust is 0.91, while the overall correlation between Bust and Overbust is 0.85. Therefore, including Overbust in addition to Bust does not add much to the knowledge for understanding breast shape or for sizing.

Table 5. Multiple linear regression results for the circumferential measurements

	Bust			
	Sum of squares	Df	F value	P value (> F)
Static value	55	1	0.3	0.6
Frame ID	5887	8	4.2	< 0.001***
Subject ID	26245	24	6.3	< 0.001***
Residuals	34787	200		
	Underbust			
	Sum of squares	Df	F value	P value (> F)
Static value	111389	1	484.9	< 0.001***
Frame ID	9763	8	5.3	< 0.001***
Subject ID	63996	24	11.6	< 0.001***
Residuals	45944	200		
	Overbust			
	Sum of squares	Df	F value	P value (> F)
Static value	30132	1	144.3	< 0.001***
Frame ID	3897	8	2.3	0.02*
Subject ID	46194	24	9.2	< 0.001***
Residuals	41750	200		

Note. This table shows results of ANOVA Type II tests. Df: degree of freedom.
* Significant at 0.05 level; ** Significant at 0.01 level; *** Significant at 0.001 level.

Table 6. Mixed effects model results for the circumferential measurements

Bust

		Estimate	Std.Error	t-value	Chi-square	Df	P-value(>Chisq)	SD
Fixed effects	(Intercept)	136.2	35.7	3.8				
	Static value	0.9	0.03	31.6	996	1	< 0.001***	
	Frame ID-2	1.0	3.7	0.3				
	Frame ID-3	8.0	3.7	2.2				
	Frame ID-4	11.4	3.7	3.1				
	Frame ID-5	3.5	3.7	1.0	34	8	< 0.001***	
	Frame ID-6	1.0	3.7	0.3				
	Frame ID-7	10.0	3.7	2.7				
	Frame ID-8	11.9	3.7	3.3				
	Frame ID-9	-1.7	3.7	-0.5				
Random effects	Subject ID							10.1
	Residual							13.2

Underbust

		Estimate	Std.Error	t-value	Chi-square	Df	P-value(>Chisq)	SD
Fixed effects	(Intercept)	52.7	47.9	1.1				
	Static value	1.0	0.05	21.2	449	1	< 0.001***	
	Frame ID-2	-10.8	4.2	-2.6				
	Frame ID-3	-8.5	4.2	-2.0				
	Frame ID-4	3.7	4.2	0.9				
	Frame ID-5	3.4	4.2	0.8	43	8	< 0.001***	
	Frame ID-6	-7.9	4.2	-1.9				
	Frame ID-7	-11.0	4.2	-2.6				
	Frame ID-8	1.8	4.2	0.4				
	Frame ID-9	5.9	4.2	1.4				
Random effects	Subject ID							16.5
	Residual							15.2

Overbust

		Estimate	Std.Error	t-value	Chi-square	Df	P-value(>Chisq)	SD
Fixed effects	(Intercept)	120.6	52.3	2.3				
	Static value	0.9	0.04	20.0	398	1	< 0.001***	
	Frame ID-2	3.4	4.0	0.9				
	Frame ID-3	5.6	4.0	1.4				
	Frame ID-4	9.6	4.0	2.4				
	Frame ID-5	9.0	4.0	2.2	19	8	0.02*	
	Frame ID-6	6.7	4.0	1.7				
	Frame ID-7	7.7	4.0	1.9				
	Frame ID-8	8.4	4.0	2.1				
	Frame ID-9	-3.0	4.0	-0.7				
Random effects	Subject ID							13.8
	Residual							14.4

Note. This table shows results of Analysis of Deviance Type II Wald Chi-square tests.
Std.Error: standard error. Df: degree of freedom. SD: Standard Deviation.
* Significant at 0.05 level; ** Significant at 0.01 level; *** Significant at 0.001 level.

For Underbust, all three predictors are statistically significant (p-values < 0.001, Table 5), while Static value has a low coefficient (β= 1.0, Table 6). The 2nd, 3rd, 6th, and 7th dynamic frames have more impactful but negative coefficients (β= -10.8, -8.5, -7.9 and -11.0, respectively).

3.2. Linear measurements

Figure 7 includes the four linear measurements, namely, Width-bust, Width-underbust, Chest-depth and Vertical-acromion. Table 7 shows the pairwise t-test (the static frame paired with each of the dynamic frames) results, for the four measurements.

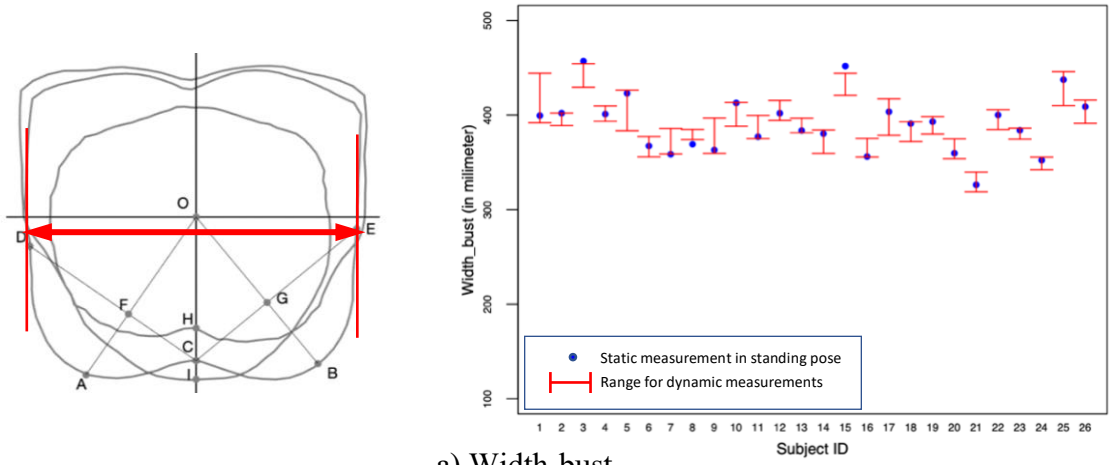

a) Width-bust

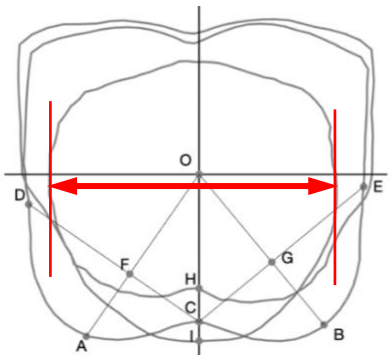

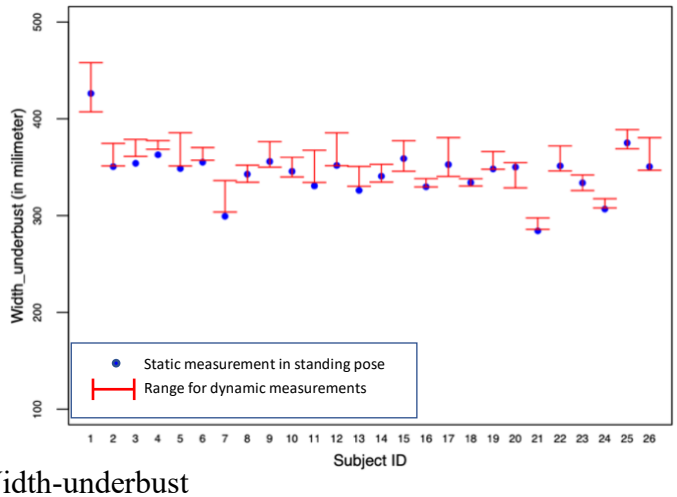

b) Width-underbust

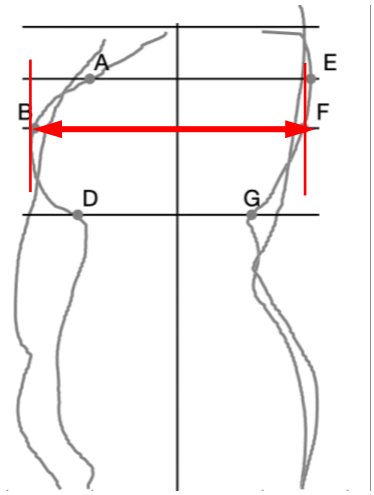

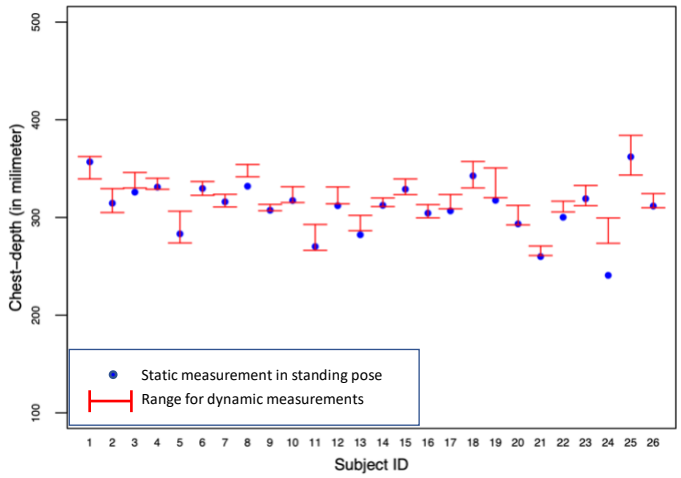

c) Chest-depth

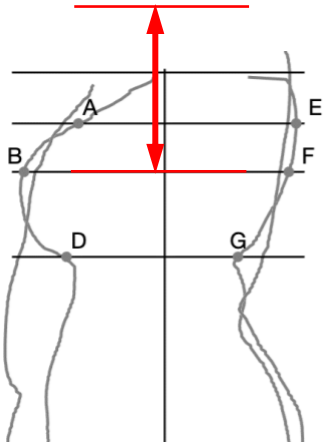

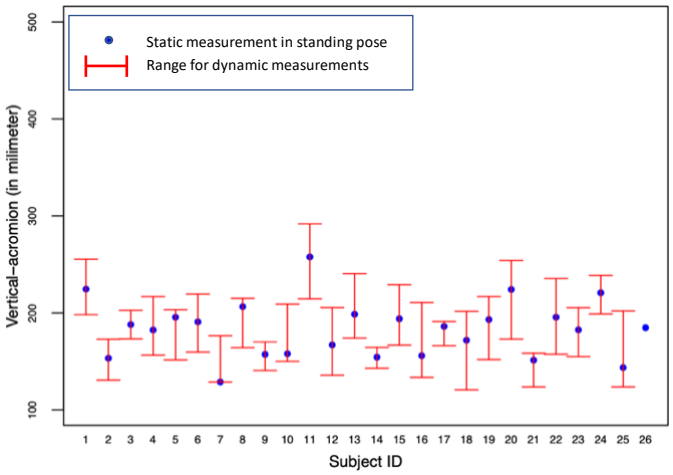

d) Vertical distance between shoulder level and bust level (Vertical-acromion)

Figure 7. Linear measurements

Table 7. Pairwise t-test with each of the dynamic frames for the linear measurements

	Dynamic frames								
Measurement name	1st (key)	2nd	3rd	4th	5th (key)	6th	7th	8th	9th (key)
Width-bust	1	0.85	1	1	1	1	1	1	1
Width-underbust	<0.001***	0.01*	<0.001***	0.02	0.002	0.02*	0.048*	0.08	<0.001***
Chest-depth	0.14	0.15	0.02*	0.09	<0.001***	0.02*	0.002**	0.045*	0.04*
Vertical-acromion	<0.001***	0.41	<0.001***	0.049*	<0.001***	0.10	<0.001***	<0.001***	<0.001***

Note. P values were adjusted with Bonferroni correction. The correction may increase p-values to as large as 1.

* Significant at 0.05 level; ** Significant at 0.01 level; *** Significant at 0.001 level.

ANOVA test shows that none of the four measurements have a significant difference among the nine dynamic frames (p-values are 0.91, 0,76, 0.76 and 0.34, respectively).

For Width-bust, none of the dynamic frames presents significant difference with the static frame (Table 7). The individual dynamic SD ranges from 13%-76% of the overall dynamic SD (Table 3). 4 static measurements (15%) fall outside the dynamic ranges, with 2 above the upper boundary and 2 under the lower boundary (Figure 7a).

For Width-underbust, 6 of the 9 dynamic frames presents a significant difference with the static frame (Table 7). The individual SD ranges from 10%-58% of the overall dynamic SD (Table 3). 10 static measurements (38%) fall outside the dynamic ranges and all of them are under the lower boundary (Figure 7b). This is probably because when the breast tissue moves up, revealing the breast roots on the ribcage originally hidden under the static state, the underbust level (which is defined as the level at the immediate cease of the bust swell) also goes up, causing changes in width (in other words, the ribcage is getting wider above the underbust level in static).

For Chest-depth, 6 dynamic frames presents a significant difference with the static

frame (Table 7). The individual SD ranges from 9%-52% of the overall dynamic (Table 3). 9 static measurements (35%) fall outside the dynamic ranges and all of them are below the lower boundary (Figure 7c). Therefore, in general, the Chest-depth measured in static may also underestimate the actual values under motion (note that the depth also includes the posterior body and the curvature of the spine may have an impact as well).

For Vertical-acromion, 7 dynamic frames presents a significant difference with the static frame (Table 7), and the individual SD ranges from 19%-90% of the overall dynamic SD (Table 3). None of the static measurements falls outside the dynamic ranges.

Table 8. Multiple linear regression results for the linear measurements

Width-bust				
	Sum of squares	Df	F value	P value (> F)
Static value	346	1	4.3	0.04*
Frame ID	638	8	1.0	0.4
Subject ID	9761	24	5.0	< 0.001***
Residuals	16216	200		
Width-underbust				
	Sum of squares	Df	F value	P value (> F)
Static value	18783	1	266.8	< 0.001***
Frame ID	639	8	1.1	0.3
Subject ID	8448	24	5.0	< 0.001***
Residuals	14079	200		
Chest-depth				
	Sum of squares	Df	F value	P value (> F)
Static value	5236	1	119.4	< 0.001***
Frame ID	914	8	2.6	0.0099**
Subject ID	11557	24	11.0	< 0.001***
Residuals	8771	200		
Vertical-acromion				
	Sum of squares	Df	F value	P value (> F)
Static value	5518	1	27.4	< 0.001***
Frame ID	52051	8	32.3	< 0.001***
Subject ID	18533	24	3.8	< 0.001***
Residuals	40044	199		

Note. This table shows results of ANOVA Type II tests. Df: degree of freedom.
* Significant at 0.05 level; ** Significant at 0.01 level; *** Significant at 0.001 level.

Table 9. Mixed effects model results for the linear measurements

		Width-bust						
		Estimate	Std.Error	t-value	Chi-square	Df	P-value(>Chisq)	SD
Fixed effects	(Intercept)	80.8	17.1	4.7				
	Static value	0.8	0.04	18.3	335	1	< 0.001***	
	Frame ID-2	-5.0	2.5	-2.0				
	Frame ID-3	-3.4	2.5	-1.4				
	Frame ID-4	-0.5	2.5	-0.2				
	Frame ID-5	-2.8	2.5	-1.1	8	8	0.5	
	Frame ID-6	-5.1	2.5	-2.0				
	Frame ID-7	-2.7	2.5	-1.1				
	Frame ID-8	-3.2	2.5	-1.3				
	Frame ID-9	-1.8	2.5	-0.7				
Random effects	Subject ID							6.0
	Residual							9.0

		Width-underbust						
		Estimate	Std.Error	t-value	Chi-square	Df	P-value(>Chisq)	SD
Fixed effects	(Intercept)	30.9	16.7	1.9				
	Static value	0.9	0.05	19.4	377	1	< 0.001***	
	Frame ID-2	-1.8	2.3	-0.8				
	Frame ID-3	0.0004	2.3	0.0				
	Frame ID-4	-0.1	2.3	-0.04				
	Frame ID-5	-0.2	2.3	-0.08	9	8	0.34	
	Frame ID-6	-1.7	2.3	-0.7				
	Frame ID-7	-1.9	2.3	-0.8				
	Frame ID-8	-1.2	2.3	-0.5				
	Frame ID-9	3.8	2.3	1.6				
Random effects	Subject ID							5.6
	Residual							8.4

		Chest-depth						
		Estimate	Std.Error	t-value	Chi-square	Df	P-value(>Chisq)	SD
Fixed effects	(Intercept)	75.7	16.6	4.6				
	Static value	0.8	0.05	14.6	212	1	< 0.001***	
	Frame ID-2	-0.4	1.8	-0.2				
	Frame ID-3	3.2	1.8	1.7				
	Frame ID-4	1.2	1.8	0.6				
	Frame ID-5	6.7	1.8	3.6	21	8	0.008**	
	Frame ID-6	1.6	1.8	0.9				
	Frame ID-7	2.5	1.8	1.4				
	Frame ID-8	2.3	1.8	1.2				
	Frame ID-9	0.9	1.8	0.5				

Random effects	Subject ID							7.0
	Residual							6.6
Vertical-acromion								
		Estimate	Std.Error	t-value	Chi-square	Df	P-value(>Chisq)	SD
Fixed effects	(Intercept)	48.3	12.0	4.0				
	Static value	0.8	0.06	13.1	172	1	< 0.001***	
	Frame ID-2	-9.9	3.9	-2.5				
	Frame ID-3	-30.8	3.9	-7.8				
	Frame ID-4	-30,1	3.9	-7.6				
	Frame ID-5	4.9	3.9	1.3	259	8	< 0.001***	
	Frame ID-6	-8.4	3.9	-2.1				
	Frame ID-7	-31.1	3.9	-7.9				
	Frame ID-8	-33.2	3.9	-8.5				
	Frame ID-9	0.6	3.9	0.2				
Random effects	Subject ID							8.0
	Residual							14.2

Note. This table shows results of Analysis of Deviance Type II Wald Chi-square tests.
Std.Error: standard error. Df: degree of freedom. SD: Standard Deviation.
* Significant at 0.05 level; ** Significant at 0.01 level; *** Significant at 0.001 level.

Table 8 and 9 include the results from the multiple linear regression and the mixed-effects model. For Width-bust, the impact of the individual's variability is the largest (p-value < 0.001). The static value is statistically significant only at a 0.05 level (p-value= 0.04), and its estimated coefficient is low (β= 0.8). The 2nd and 6th dynamic frames have slightly more impactful coefficients (β= -5.0 and -5.1, respectively) which are negative.

For Width-underbust, Static value and Subject ID are statistically significant (p values < 0.001), despite of a low coefficient for Static value (β= 0.9). The impact of Frame ID is not significant at all: not only is Frame ID not statistically significant (p-value= 0.3, Table 8) in the linear regression model, none of the dynamic frames has an impactful (large in absolute value) coefficient in the mixed-effects model (Table 9). The impact of the individual variability is more dominating, just as Width-bust.

Significant individual variability can also be observed in Figure 7a and 7b. As in

previous anthropometry research, our study shows that individual variability is as important as the means across populations. Not only do breast shapes vary between individuals, breasts displace and move at different rates between individuals as well.

For Chest-depth, all three predictors are statistically significant (p-values < 0.01, Table 8), while Static value has a low coefficient (β= 0.8, Table 9). The 5th frame is the only dynamic frame that has an impactful positive coefficient (β= 6.7), but the maximum value occurs at the 5th frame for only 9 participants (out of 26).

For Vertical-acromion, all three predictors are statistically significant (p-values < 0.001, Table 8), while Static value has a low coefficient (β= 0.8, Table 9). All of the intermediate frames (the non-keyframes), namely the 2nd, 3rd, 4th, 6th, 7th and 8th frames, have a very impactful (large in absolute value) coefficient that is negative (β= -9.9, -30.8, -30,1, -8.4, -31.1 and -33.2, respectively). While no general trend can be observed across the nine frames for Width-bust, Width-underbust or Chest-depth, a roughly W-shape trend can be observed for Vertical-acromion, with peaks observed at the keyframes and lows at the intermediate frames. In fact, the maximum value occurs at the keyframes (i.e. the 1st, 5th or 9th scan) for 21 out of the 26 participants. Since this measurement is particularly influenced by the running posture at the shoulder area, tracking its changes in dynamic is especially important for sports bra design.

3.3. Angular measurements

Figure 8 shows the three angular measurements for each participant, namely AngleBPs, AngleABD and AngleBAD. Table 10 shows the pairwise t-test results.

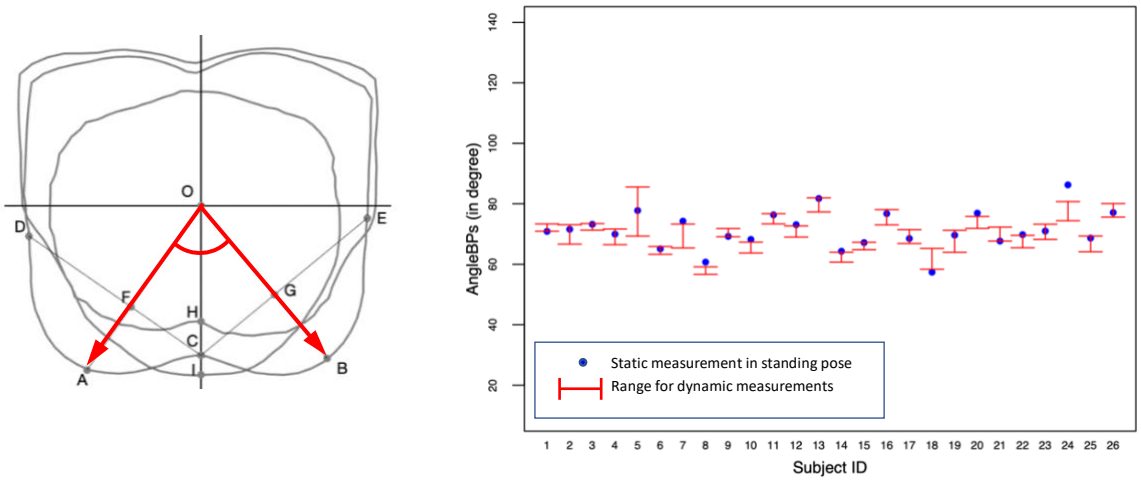

a) AngleBPs

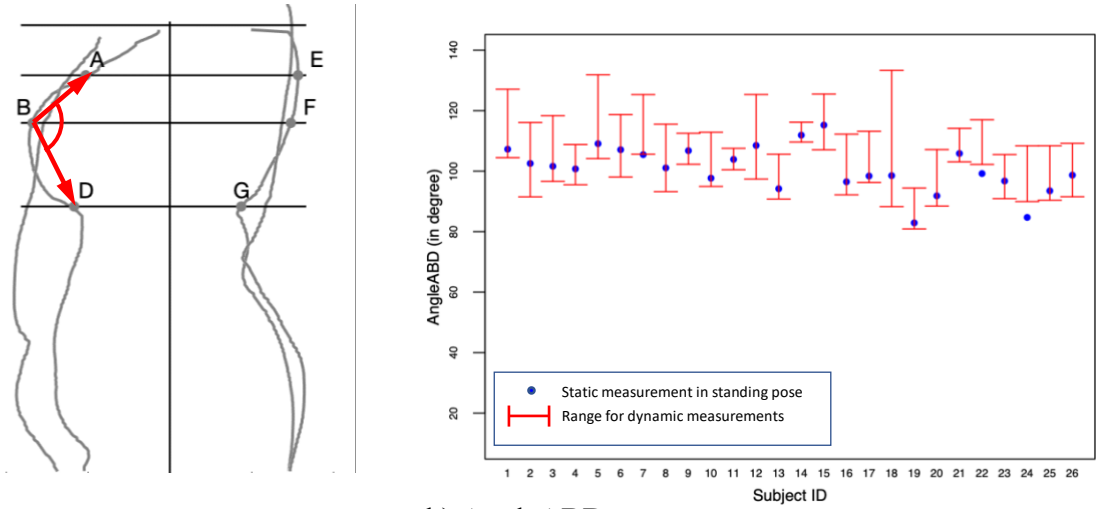

b) AngleABD

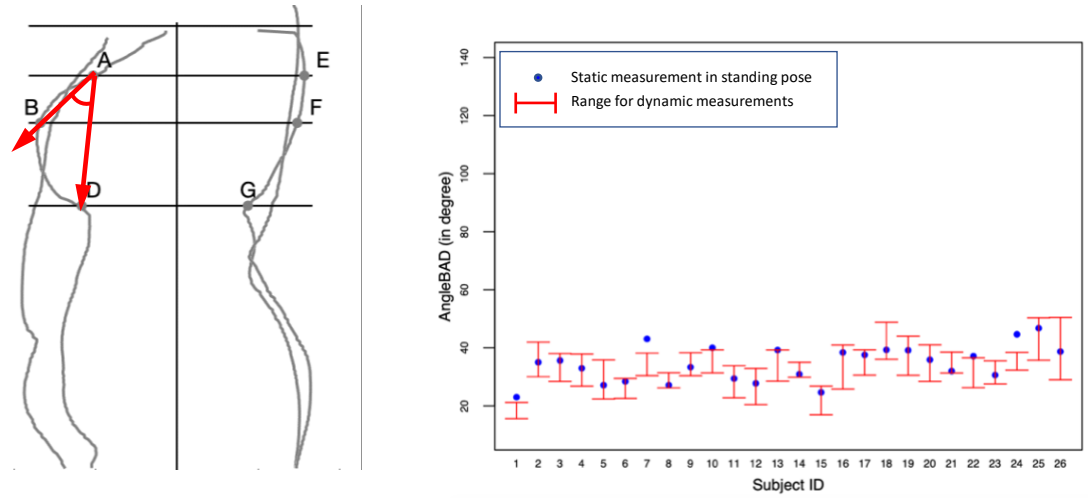

c) AngleBAD

Figure 8. Angular measurements

Table 10. Pairwise t-test with each of the dynamic frames for the angular measurements

	Dynamic frames								
Measurement name	1st (key)	2nd	3rd	4th	5th (key)	6th	7th	8th	9th (key)
AngleBPs	0.49	1	0.16	1	0.02	0.19	0.08	1	0.70
AngleABD	0.86	0.13	<0.001***	<0.001***	1	0.005**	<0.001***	<0.001***	0.19
AngleBAD	0.004**	0.88	1	1	<0.001***	0.18	1	1	0.02

Note. P values were adjusted with Bonferroni correction. The correction may increase p-values to as large as 1.

* Significant at 0.05 level; ** Significant at 0.01 level; *** Significant at 0.001 level.

ANOVA test shows that none of the angular measurements has a significant difference among the nine dynamic frames (p-values are 0.92, 0.58 and 0.64, respectively).

For AngleBPs, none of the dynamic frames presents a significant difference with the static frame (Table 10). The individual SD ranges from 13%-80% of the overall dynamic SD (Table 3). 11 static measurements (42%) fall outside the dynamic ranges, with 8 above the upper boundary and 3 under the lower boundary (Figure 8a).

For AngleABD, almost all the intermediate frames (the 3rd, 4th, 6th, 7th, 8th) appear to have a significant difference with the static frame (Table 10). The individual SD ranges from 27%-154% of the overall dynamic SD (Table 3). Individual SD (e.g. Subject #18) can be higher than the overall SD. Only 3 static measurements fall outside the dynamic measurement ranges but all under the lower boundary (Figure 8b).

For AngleBAD, 2 keyframes (the 1st and 5th frame) appear to have significant difference with the static frame (Table 10). The individual SD ranges from 22%-133% of the overall dynamic SD (Table 3). Note that the individual SD (e.g. Subject #26) can be even higher than the overall SD. 5 static measurements (19%) fall outside the

dynamic ranges and all of them are above the upper boundary (Figure 8c).

Table 11. Multiple linear regression results for the angular measurements

AngleBPs				
	Sum of squares	Df	F value	P value (> F)
Static value	152	1	52.5	< 0.001***
Frame ID	45	8	1.9	0.06
Subject ID	825	24	11.8	< 0.001***
Residuals	581	200		
AngleABD				
	Sum of squares	Df	F value	P value (> F)
Static value	1206	1	43.2	< 0.001***
Frame ID	3928	8	17.6	< 0.001***
Subject ID	1577	24	2.4	< 0.001***
Residuals	5589	200		
AngleBAD				
	Sum of squares	Df	F value	P value (> F)
Static value	2066	1	178.2	< 0.001***
Frame ID	945	8	10.2	< 0.001***
Subject ID	2100	24	7.6	< 0.001***
Residuals	2319	200		

Note. This table shows results of ANOVA Type II tests. Df: degree of freedom.
* Significant at 0.05 level; ** Significant at 0.01 level; *** Significant at 0.001 level.

Table 12. Mixed effects model results for the angular measurements

AngleBPs								
		Estimate	Std.Error	t-value	Chi-square	Df	P-value(>Chisq)	SD
Fixed effects	(Intercept)	13.3	4.5	3.0				
	Static value	0.8	0.06	12.7	162	1	< 0.001***	
	Frame ID-2	0.5	0.5	1.1				
	Frame ID-3	-0.4	0.5	-0.9				
	Frame ID-4	0.3	0.5	0.7				
	Frame ID-5	-0.8	0.5	-1.7	15	8	0.05	
	Frame ID-6	-0.2	0.5	-0.4				
	Frame ID-7	-0.5	0.5	-1.0				
	Frame ID-8	0.5	0.5	1.1				
	Frame ID-9	-0.1	0.5	-0.2				
Random effects	Subject ID							1.9
	Residual							1.7

AngleABD								
		Estimate	Std.Error	t-value	Chi-square	Df	P-value(>Chisq)	SD
Fixed effects	(Intercept)	16.4	7.2	2.3				
	Static value	0.8	0.07	11.6	135	1	< 0.001***	
	Frame ID-2	4.9	1.5	3.3				
	Frame ID-3	8.3	1.5	5.7				
	Frame ID-4	11.3	1.5	7.7				
	Frame ID-5	1.7	1.5	1.2	141	8	< 0.001***	
	Frame ID-6	5.3	1.5	3.6				
	Frame ID-7	7.7	1.5	5.2				
	Frame ID-8	10.4	1.5	7.1				
	Frame ID-9	-0.4	1.5	-0.3				
Random effects	Subject ID							2.1
	Residual							5.3

AngleBAD								
		Estimate	Std.Error	t-value	Chi-square	Df	P-value(>Chisq)	SD
Fixed effects	(Intercept)	5.1	3.6	1.4				
	Static value	0.8	0.1	7.5	57	1	< 0.001***	
	Frame ID-2	1.7	0.9	1.8				
	Frame ID-3	4.2	0.9	4.4				
	Frame ID-4	2.9	0.9	3.1				
	Frame ID-5	-1.9	0.9	-2.0	82	8	< 0.001***	
	Frame ID-6	0.8	0.9	0.8				
	Frame ID-7	4.6	0.9	4.9				
	Frame ID-8	3.2	0.9	3.4				
	Frame ID-9	0.4	0.9	0.4				
Random effects	Subject ID							2.9
	Residual							3.4

Note. This table shows results of Analysis of Deviance Type II Wald Chi-square tests.
Std.Error: standard error. Df: degree of freedom. SD: Standard Deviation.
* Significant at 0.05 level; ** Significant at 0.01 level; *** Significant at 0.001 level.

Table 11 and 12 include the results from the multiple linear regression and the mixed-effects model. For AngleBPs, the impact of Frame ID is not significant at all: not only is Frame ID not statistically significant (p-value= 0.06, Table 11), none of the dynamic frames has an impactful (large in absolute value) coefficient (Table 12). The impact of the individual's variability is more dominating.

For AngleABD, all three predictors are statistically significant (p-values < 0.001,

Table 11), while Static value has a low coefficient (β= 0.8, Table 12). All the intermediate frames, namely the 2nd, 3rd, 4th, 6th, 7th, and 8th frames, have an impactful (large in absolute value) coefficient (β=4.9, 8.3, 11.3, 5.3, 7.7 and 10.4, respectively). The general trend of the nine frames is roughly M-shaped, with lows observed at the keyframes and peaks at the intermediate frames. In fact, the minimum value occurs at the keyframes (i.e. the 1st, 5th or 9th frame) for 23 out of the 26 participants, and the maximum value occurs at one frame before the keyframe (i.e. the 4th and 8th frame, β=11.3 and 10.4) for 19 out of the 26 participants.

For AngleBAD, all three predictors are statistically significant (p-values < 0.001, Table 11), while Static value has a low coefficient (β= 0.8, Table 12). The 3rd, 4th, 7th, 8th dynamic frames (all intermediate frames) have slightly more impactful coefficients (β= 4.2, 2.9, 4.6 and 3.2, respectively). The general trend of the nine frames is also roughly M-shaped. The minimum value occurs at the keyframes (i.e. the 1st, 5th or 9th frame) for 18 out of the 26 participants.

4. Conclusions

This paper proposed a practical way to work with 4D body scan data for the study of breast shape under motion. 26 female participants who identified themselves as wearing Missy Size 18 were recruited for scanning. Nine frames including three keyframes of a complete running cycle (the 9 dynamic frames), as well as one frame of the standard standing posture (the static frame), were selected for analysis.

Landmarks were found not reliable to align scans because: 1) they are easy to fall off or shift under motion (compared with the static standing posture); 2) they can be obstructed by the swinging arms or buried in skin folds; 3) without falling, shifting or obstruction, still they may be inadequate to provide accurate alignment due to soft tissue artifacts. Therefore, the scans in running postures were aligned manually, rather

than based on landmarks, such that their upper torso aligns as much as possible with the corresponding scan in standing posture. It is recommended to align scans at the upper back area, because the upper back area has relatively less fat tissue, compared with the anterior body and the lower posterior body (including the hip).

Three circumferential measurements, four linear measurements, and three angular measurements were selected to examine how the measurement values vary under motion. A few conclusions are listed below:

- ANOVA results show that for all ten measurements, the nine dynamic frames do not have significantly different means. However, testing can be heavily influenced by individual variability. The study of individual variability is as important and can be informative for product design.
- For Underbust, Width-underbust, Chest-depth, Vertical-acromion, and AngleABD, more than half of the dynamic frames (≥ 5) presents a significant difference with the static frame (pairwise t-test with Bonferroni correction).
- Although Bust, Overbust, Width-bust, and AngleBPs present no significant difference between the means of the static frame and the means of any of the dynamic frame, it does not mean that the static measurement is a good representation for the dynamic measurements. These measurements have 5, 7, 4, and 11 instances, respectively, where the static measurement falls completely outside the dynamic range (either above the maximum or below the minimum).
- Overbust (a 3D measurement adopted by a few bra companies) does not bring in much additional information for understanding breast shape or for sizing due to its high correlation with the bust circumference.
- In general, Underbust and Width-underbust measured in static may underestimate the actual values under motion. This is probably because when the breast tissue moves up, revealing the breast roots on the ribcage originally hidden under the

static state, the underbust level (which is defined as the level at the immediate cease of the bust swell identifiable on the scan) also goes up, causing changes in width in accordance with the shape of the ribcage.

- Chest-depth measured in static may also underestimate the actual values under motion.
- For the width measurements (i.e. Width-bust and Width-underbust) and AngleBPs, the impact of individual variability is more dominating than the potential patterns across the nine frames (multiple linear regression analysis).
- Since shoulders have relative movement to the ribcage, the shoulder area is not ideal for scan alignment. However, the measurement of vertical distance between the right acromion point and the right bust point in dynamic is important, especially for sports bra design. This measurement presents a general trend of W-shape across the nine dynamic frames, with peaks observed at the keyframes and lows at the intermediate frames.
- AngleABD and AngleBAD both possess an M-shaped general trend for the nine dynamic frames, with lows observed at the keyframes and peaks at the intermediate frames. For AngleABD, almost all of the intermediate frames (the 3rd, 4th, 6th, 7th, 8th) appear to have a significant difference with the static frame. For AngleBAD, 2 keyframes (the 1st and 5th frame) appear to have significant difference with the static frame.

This study has several limitations. Firstly, the sample size is small, especially for a population that potentially has more body shape variation. Secondly, due to the limited space for actual running and the unavailability of a treadmill at the time of the scanning, the participants were asked to run in place, which may be different from actual running. A treadmill can offer better control over the speed of running as well,

and in return researchers can obtain a consistent number of frames for a running cycle across the population. In our study, we had to duplicate intermediate scans (i.e. the non-key-frame scans) for several participants because of the incapability of controlling running speed (those who ran faster than the majority ended up with fewer than nine frames of scans for a complete cycle). Thirdly, the preparation of the scans requires a great deal of manual process (e.g. manual alignment of scans, manual removal of arms, manual filling the holes, etc.), which is labor intensive and time consuming. Since 4D scanning typically captures hundreds of or thousands of scans within minutes, an automatic process needs to be developed and replace manual work for this technology to be able to effectively benefit human-centered product design. Lastly, the accuracy of the location of the landmarks may have a negative impact on the analysis results (although we did not present measurements associated with suspicious landmarks in this paper). Future researchers need to figure out a way to secure landmarks on participants' bodies and prevent them from shifting, falling off, obstructed by the swinging arms and buried in skin folds.

As technology advances and 4D data become more accessible, apparel researchers and designers need to have the tools to incorporate these data into the design process and product evaluation. 4D technology provides researchers an environment for analyzing, processing, and visualizing body shape and clothing in motion, and allows the collection of dynamic anthropometric data. This is one of the first research studies to use 4D scanning to study female breast shape. We adopted a traditional approach to analyzing breast measurements. This pioneering study introduces 4D scanning technology as a new, but enormously promising, way to conduct anthropometric and ergonomic research. A protocol to handle and analyze 4D data for application in apparel/wearable product design was proposed and future researchers can easily duplicate or revise. In addition, the data and results can facilitate product development,

especially for sports bras and other activewear, as well as for advanced wearable products that require a high degree of a good fit and mobility in order to function (e.g. female body armor, combat suit, PPE, etc.).

Traditional motion capture systems use automated point tracking and sparse meshing techniques to show movement. The 4D data from the 3dMD system allow movement to be expressed in terms of dense surface deformation and classification. This new paradigm of body analysis allows researchers to quantify and model the subtleties of human movement and human movement in relation to a worn product.

The quantitative analysis presented in this paper enables the development and expansion of theory related to the human/product interface. Never before have we had the capability of seeing body surface change during movement in relation to a product. The implications of studying and analyzing this body data will advance how we approach design problems, as well as the design and development of wearable products ranging from sportswear to medical products to spacesuits.

DISCLOSURE STATEMENT

This chapter is a journal paper that is under review by *International Journal of Industrial Ergonomics*, Elsevier.

REFERENCES

Ashdown, S. P., & Na, H. (2008). Comparison of 3-D body scan data to quantify upper-body postural variation in older and younger women. *Clothing and Textiles Research Journal*, *26*(4), 292-307.

Andersen, M. S., Benoit, D. L., Damsgaard, M., Ramsey, D. K., & Rasmussen, J. (2010). Do kinematic models reduce the effects of soft tissue artefacts in skin marker-based motion analysis? An in vivo study of knee kinematics. *Journal of biomechanics*, *43*(2), 268-273.

Chi, L., & Kennon, R. (2006). Body scanning of dynamic posture. *International Journal of Clothing Science and Technology*, *18*(3), 166-178.

Chen, C. M., LaBat, K., & Bye, E. (2010). Physical characteristics related to bra fit. *Ergonomics*, *53*(4), 514-524.

Chen, C. M., LaBat, K., & Bye, E. (2011). Bust prominence related to bra fit problems. *International Journal of Consumer Studies*, *35*(6), 695-701.

Coltman, C. E., McGhee, D. E., & Steele, J. R. (2015). Bra strap orientations and designs to minimise bra strap discomfort and pressure during sport and exercise in women with large breasts. *Sports medicine-open*, *1*(1), 21.

Coltman, C. E., Steele, J. R., & McGhee, D. E. (2017). Breast volume is affected by body mass index but not age. *Ergonomics*, *60*(11), 1576-1585.

Coltman, C. E., Steele, J. R., & McGhee, D. E. (2018). Effects of age and body mass index on breast characteristics: a cluster analysis. *Ergonomics*, *61*(9), 1232-1245.

Coltman, C. E., Steele, J. R., & McGhee, D. E. (2019). Does breast size affect how women participate in physical activity?. *Journal of science and medicine in sport*, *22*(3), 324-329.

Den Tonkelaar, I., Peeters, P. H. M., & Van Noord, P. A. H. (2004). Increase in breast

size after menopause: prevalence and determinants. *Maturitas*, *48*(1), 51-57.

Del Carmen, M. G., Halpern, E. F., Kopans, D. B., Moy, B., Moore, R. H., Goss, P. E., & Hughes, K. S. (2007). Mammographic breast density and race. *American Journal of Roentgenology*, *188*(4), 1147-1150.

Greenbaum, A. R., Heslop, T., Morris, J., & Dunn, K. W. (2003). An investigation of the suitability of bra fit in women referred for reduction mammaplasty. *British journal of plastic surgery*, *56*(3), 230-236.

Hussain, Z., Roberts, N., Whitehouse, G. H., Garcia-Finana, M., & Percy, D. (1999). Estimation of breast volume and its variation during the menstrual cycle using MRI and stereology. *The British journal of radiology*, *72*(855), 236-245.

Hadi, M. S. (2000). Sports brassiere: is it a solution for mastalgia?. *The breast journal*, *6*(6), 407-409.

Hart, C., & Dewsnap, B. (2001). An exploratory study of the consumer decision process for intimate apparel. *Journal of Fashion Marketing and Management: An International Journal*, *5*(2), 108-119.

Haars, G., van Noord, P. A., van Gils, C. H., Grobbee, D. E., & Peeters, P. H. (2005). Measurements of breast density: no ratio for a ratio. *Cancer Epidemiology and Prevention Biomarkers*, *14*(11), 2634-2640.

Herroom.com (n.d.). Classify your breasts. Retrieved Jan 2020 from https://www.herroom.com/breast-separation,333,30.html

Istook, C. L., & Hwang, S. J. (2001). 3D body scanning systems with application to the apparel industry. *Journal of Fashion Marketing and Management: An International Journal*, *5*(2), 120-132.

International Organization for Standardization. (2017). “ISO 7250: Basic Human Body Measurements for Technological Design - Part 1: Body Measurement Definition and Landmarks.” https://www.iso.org/standard/65246.html.

Kaye, B. (1972). Neurologic changes with excessively large breasts. *Southern Medical Journal, 65*(2), 177-180.

Lorentzen, D. & Lawson, L. (1987). Selected Sports Bras: A Biomechanical Analysis of Breast Motion.*Physician and Sports Medicine 15*(5), 128-139.

Lee, H. Y., Hong, K., & Kim, E. A. (2004). Measurement protocol of women's nude breasts using a 3D scanning technique. *Applied Ergonomics*, *35*(4), 353-359.

Loker, S., Ashdown, S., & Schoenfelder, K. (2005). Size-specific analysis of body scan data to improve apparel fit. *Journal of Textile and Apparel, Technology and Management, 4*(3), 1-15.

Lee, H. Y., & Hong, K. (2007). Optimal brassiere wire based on the 3D anthropometric measurements of under breast curve. *Applied Ergonomics*, *38*(3), 377-384.

Lawrence, R. A., & Lawrence, R. M. (2011). *Breastfeeding: a guide for the medical profession*. Elsevier Health Sciences.

Luximon, A., Zhang, Y., Luximon, Y., & Xiao, M. (2012). Sizing and grading for wearable products. *Computer-Aided Design*, *44*(1), 77-84.

Liu, Y., Wang, J., & Istook, C. L. (2017). Study of optimum parameters for Chinese female underwire bra size system by 3D virtual anthropometric measurement. *The Journal of The Textile Institute*, *108*(6), 877-882.

Nethero S. (2007). Method for optimization of bra fit and style for all body sizes and types and for wearing with a variety of clothing styles. Patent 11/829,568, USA.

Mason, B. R., Page, K. A., & Fallon, K. (1999). An analysis of movement and discomfort of the female breast during exercise and the effects of breast support in three cases. *Journal of Science and Medicine in Sport, 2*(2), 134-144.

McGhee, D. E., & Steele, J. R. (2011). Breast volume and bra size. *International Journal of Clothing Science and Technology*, *23*(5), 351-360.

McGhee, D. E., Ramsay, L. G., Coltman, C. E., Gho, S. A., & Steele, J. R. (2018). Bra band size measurements derived from three-dimensional scans are not accurate in women with large, ptotic breasts. *Ergonomics*, *61*(3), 464-472.

Page, K. A., & Steele, J. R. (1999). Breast motion and sports brassiere design. *Sports Medicine*, *27*(4), 205-211.

Pei, J., Park, H., & Ashdown, S. P. (2019). Female breast shape categorization based on analysis of CAESAR 3D body scan data. *Textile Research Journal*, *89*(4), 590-611.

Pei, J., Fan, J. & Ashdown, S. P. (2019). Detection and Comparison of Breast Shape Variation among Different 3D Body Scan Conditions: Nude, with a Structured Bra, and with a Soft Bra, *Textile Research Journal*, *89*(21), 4595-4606.

Pei, J., Fan, J., & Ashdown, S. P. (2019). A novel method to assess breast shape and breast asymmetry. *The Journal of The Textile Institute*, *110*(8), 1229-1240.

Pei, J., Fan, J. & Ashdown, S. P. (2020). A Novel Optimization Approach to Minimize Aggregate-Fit-loss for Improved Breast Sizing, *Textile Research Journal*, accepted.

Singer, S. R., & Grismaijer, S. (1995). Dressed to Kill. The Link Between Breast Cancer & Bras. *Journal of Applied Nutrition*, *47*(3), 90-92.

Sigurdson, L. J., & Kirkland, S. A. (2006). Breast volume determination in breast hypertrophy: an accurate method using two anthropomorphic measurements. *Plastic and reconstructive surgery*, *118*(2), 313-320.

Shin, W. K. (2009). *The origins and evolution of the bra* (Doctoral dissertation, Northumbria University).

Shawgi, M., Tonge, C. M., Lawson, R. S., Muthu, S., James, J., & Arumugam, P. (2012). Attenuation correction of myocardial perfusion SPET in patients of normal body mass index. *Hellenic journal of nuclear medicine*, *15*(3), 215-219.

Sohn, M., & Bye, E. (2014). Exploratory study on developing a body measurement method using motion capture. *Clothing and Textiles Research Journal*, *32*(3), 170-185.

Tiggemann, M. (2004). Body image across the adult life span: Stability and change. *Body image*, *1*(1), 29-41.

Todd, W. L. (2007). Sizing for the military. In Sizing in Clothing (pp. 277-308). Woodhead Publishing.

Wood, K., Cameron, M., & Fitzgerald, K. (2008). Breast size, bra fit and thoracic pain in young women: a correlational study. *Chiropractic & osteopathy*, *16*(1), 1.

Watkins, S. M., & Dunne, L. (2015). *Functional clothing design: From sportswear to spacesuits*. Bloomsbury Publishing USA.

Zheng, R., Yu, W., & Fan, J. (2007). Development of a new Chinese bra sizing system based on breast anthropometric measurements. *International Journal of Industrial Ergonomics*, *37*(8), 697-705.

APPENDIX. LANDMARKS

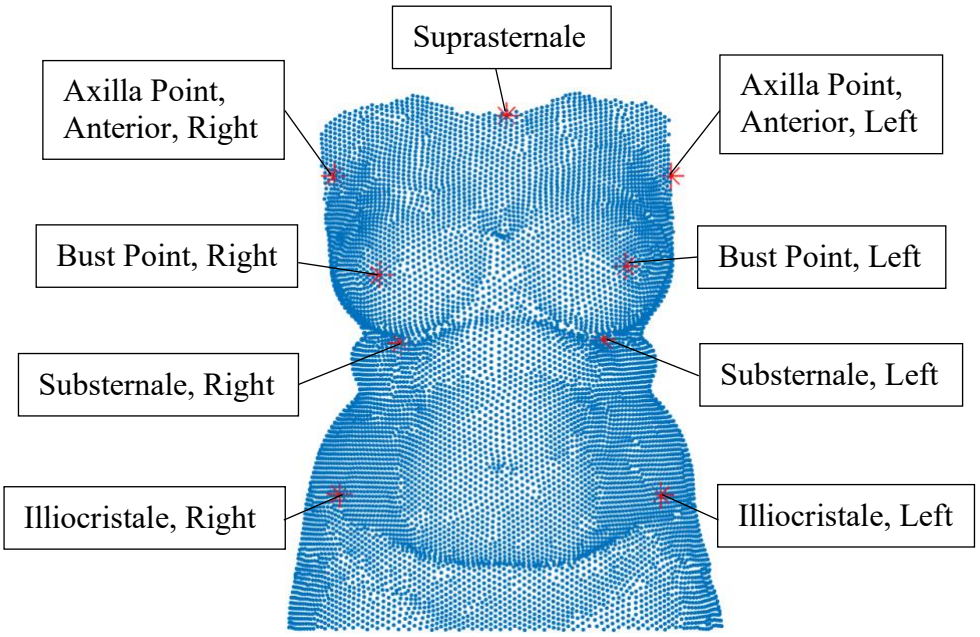

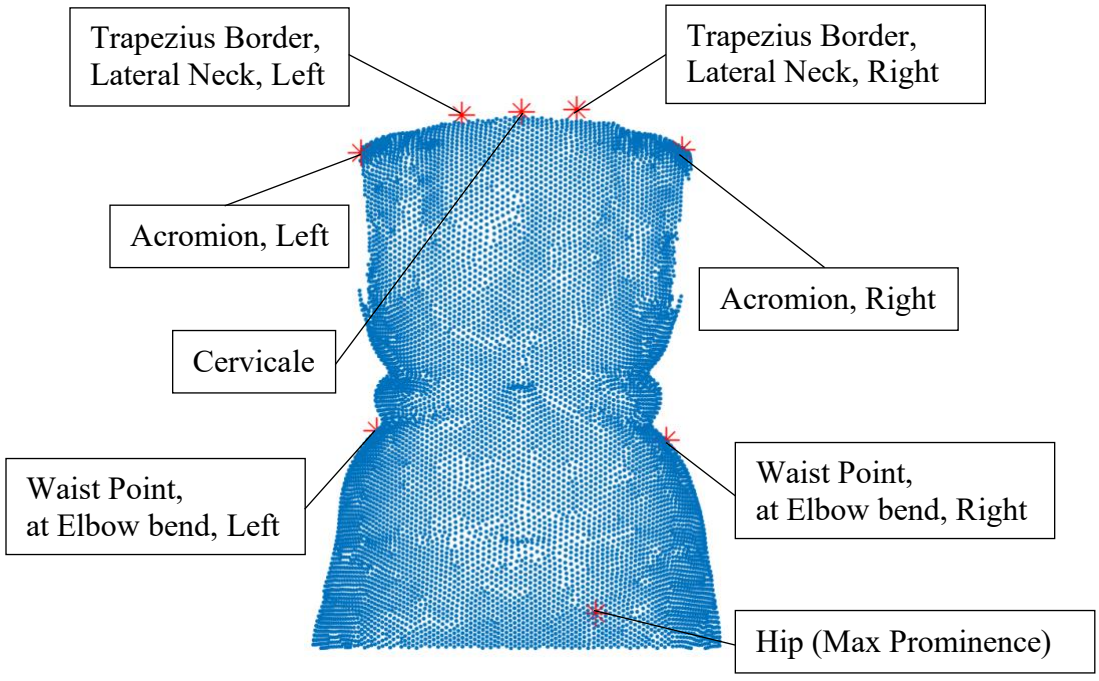

CHAPTER 5

THE DETECTION OF THE UPPER BOUNDARY OF BREASTS USING 4D SCANNING TECHNOLOGY

Abstract

Defining the boundary of breasts is necessary step for calculating the volume or surface area of the breast. Anthropometric measurements such as volume and surface area are critical to the understanding of breast shape and size, and directly contribute to the product development of bras, activewear, female body armor and other types of personal protective equipment (PPE) for women of which bad fit could potentially put the wearer's safety at risk. However, a non-contact method that accurately detects the boundary between breasts and the chest wall, for breasts evaluated in the upright body position, has not been reported before. In this study we 4D-scanned 26 female participants using the Temporal 3dMD system, and took advantage of the time delay in the vertical displacement between the breasts and the chest wall during physical activity to propose a method of visualizing variability of the relative displacement in the vertical direction to facilitate the definition of the upper boundary of breasts. This is also one of the first comprehensive studies that investigates the vertical displacement and the shape deformation of breasts during running using 4D scanning technology. Ultimately, the method and results can increase the understanding of breast kinematics, and benefit the product design of bras, especially for sports bras, and other products for women that require a close-to-body fit on the torso.

1. Introduction

Studies have shown that up to 85% of women have issues with bra fit (McGhee &

Steele, 2010). According to a survey conducted on 1500 U.S. women, 65% of them had experienced discomfort from wearing bras (Nethero, 2008). Insufficient support, underwire pain, bra straps sliding off or digging into the shoulders, etc., are the common reasons causing discomfort (Nethero, 2008). In addition, an ill-fitted bra can bring health concerns to the wearer. It may cause her back pain, shoulder pain and neck pain (Greenbaum, Heslop, Morris & Dunn, 2003) and may eventually hinder her ability and willingness to participate in physical activity (McGhee & Steele 2010; Coltman, Steele & McGhee 2019). Some women even had to seek mammoplasty because of the severe musculoskeletal pain due to lack of appropriate bra fit and functionality (Greenbaum, Heslop, Morris & Dunn, 2003). For female body armor and personal protective equipment (PPE), fall harness systems, turnout gear, etc., bad fit in the bust area may result in the failure of the entire wearable system in providing sufficient protection (Todd, 2007). Bad fit may also reduce the wearer's mobility, also putting the wearer's safety at risk (Todd, 2007). Therefore, understanding breast shape is extremely critical for product designers. Moreover, for plastic surgeons, having accurate measurements of breasts is of great importance to achieve optimal surgical outcome and to protect the patient's well-being (Kim et al., 2007; Kovacs et al., 2007). For healthcare providers, accurate and up-to-date measurements of breasts for the population are critical information to establish breast care guidelines that benefit the vast female population (Kim et al., 2007).

Defining the boundary of breasts is a necessary and essential step for estimating the volume or surface area of the breast (Smith, Palin, Katch & Bennett, 1986; Edsander-Nord, Wickman & Jurell, 1996; Bulstrode, Bellamy & Shrotria, 2001; Kovacs et al., 2007; Xi et al., 2014; Coltman, Steele & McGhee, 2018). Anthropometric measurements such as these are critical to the understanding of breast shape and the development of wearable products for women (Lee, Hong & Kim, 2004;

McGhee, Steele, Zealey & Takacs, 2013; Coltman, McGhee & Steele, 2017). Multiple methods have been proposed to find the boundary of breasts for mammograms or for breast MR images (Ojala, Näppi & Nevalainen, 2001; Ferrari et al, 2004; Giannini et al, 2010; Wang & et al, 2012; Kus & Karagoz, 2012), however, their focus is to separate breasts from the background (the ambient environment) rather than from the chest wall. Coltman, Steele and McGhee (2018) scanned their participants while they were laying in prone position, letting the breasts naturally suspend in a gap between two tables (similar to the standard posture for breast MRI). They defined the boundary of the breasts on the 3D scans in Geomagic® based on visual judgment. Determining the breast boundary for participants in the upright position is more useful for designers, but also more challenging, especially for small chested females. Lee, Hong and Kim (2004) proposed a folding line method to find breast boundary for participants in the upright position. Their method requires pushing the entire breast upward and inward by hand to reveal the skin folds, where the natural boundary locates. The method itself can be efficient, but it involves hand contact and manipulation of a sensitive body area, which may cause psychological discomfort for some participants. To the best of our knowledge, a non-contact method that facilitates the accurate detection of the boundary between breasts and chest wall, for breasts evaluated in the upright body position, has not been reported before.

The development of 4D scanning technology introduces the fourth dimension, i.e. time, and provides a method to acquire the boundary information. This is because when in movement the breasts exhibit a time delay in displacement compared to the chest wall. This relative displacement in vertical direction causes the bouncing of breasts when women participate in activities such as jogging (Haake & Scurr, 2010; McGhee, Steele, Zealey & Takacs, 2013). Understanding the vertical displacement of breasts is very critical as many studies have shown that the vertical displacement

during physical activities is closely related to breast discomfort (Lorentzen & Lawson, 1987; Page & Steele, 1999; Mason, Page & Fallon, 1999; Starr et al., 2005). In addition, understanding the kinematics and kinetics of breasts is a necessity to ensure that bras are designed to provide efficient control over breast motion during physical activity (Page & Steele, 1999). Although the displacement of breasts has been intensively investigated (Lorentzen & Lawson, 1987; Mason, Page & Fallon, 1999; Starr et al., 2005; Scurr, White & Hedger, 2009 & 2011; Haake & Scurr, 2010; McGhee, Steele, Zealey & Takacs, 2013), the previous studies only involved the tracking of the nipple points and/or a few other marked points. 4D scanning, however, makes it possible to track the whole breast under motion, therefore, it can offer more information regarding the shape change of breasts during physical activity. To our knowledge, this is the first paper that uses 4D scanning on breast kinematics.

In this study, we 4D scanned 26 female participants in motion using the Temporal 3dMD system and we propose a method to visualize the amount of variability for relative displacement in the vertical direction to facilitate the definition of the upper boundary of breasts. We also studied the overall shape change of breasts during running. Ultimately, the method and results presented in this paper can increase the understanding of breast kinematics, and benefit the product design of bras (sports bras in particular), other female activewear and apparel products, PPE and additional types of functional wearable products for women.

2. Methodology

With approval obtained from IRB (Institutional Review Board), 26 female participants, who self-identified as wearing Missy Size 18 dress size, were recruited for 4D body scanning, using a Temporal 3dMD full body scanner (18.t System Model). We did not put other constraints such as age, BMI and ethnicity for the

recruitment. Consents were obtained from all of the participants. Participants were scanned wearing the bra of their own size but of a consistent style and design (a common T-shirt bra), provided by the researchers (size range: 36C-42G). A 4D scan is essentially a series of 3D scans captured in time while the participant is in motion. For each participant, we selected nine frames (or nine 3D body scans) which form a complete running cycle while the participant was running-in-place. We also obtained a static scan captured while the participant was in a standing position, with the arms slightly abducted from the torso, as this is the standard scanning posture for 3D body scanning. The selected scans were processed in MeshLab and Meshmixer to remove the head and the limbs, leaving only the torso, and to fill holes in the scan (see Pei, Griffin, Ashdown & Fan, 2019 for details).

After also removing the area below the most inferior point of the breasts, each scan was processed in Matlab® to have exactly same number of points on the scan surface sorted in an organized fashion. One way of re-organizing points is to create 50 horizontal slices, and to define points on each slice using angles with respect to the origin point where the central axis passes through the slice. The shape of the slices is quasi-circular, facilitating this process. The central axis is defined by averaging the x and y coordinates of all points on the torso (Pei, Fan & Ashdown, 2019). In other words, on each slice one point is identified at each degree from -180° to 180°. Figure 1a shows the anterior portion of a processed scan (-180° to 0°, 181 points on each slice). The total number of points is 9050 (181×50) for the 50 slices. This method of processing scans provides useful data for analyzing the change in shape but is not as effective for studying vertical displacements of the breasts. Therefore, the scans were also processed by creating vertical slices. One breast was processed at a time to allow each breast to be processed along its own axis, which is determined by the location of the corresponding bust point. Nipple points were regarded as bust points and were

identified on the scans through body landmarks placed on the bras. As the position of the nipple could not be seen through the bra, participants were asked to self-identify their nipples by pointing to their location on the bra. We assume that the shape of breast is quasi-hemispherical or quasi-conical (slicing horizontally assumes that the torso is quasi-cylindrical). Based on this assumption, when each vertical slice throughout the height of the breast is quasi-circular, we can control the number of points on each slice (as we did for slicing horizontally). Let the coordinates of a bust point (right or left) of a scan be (X_{bust}, Y_{bust}, Z_{bust}), then the axis for the breast (on the corresponding side) is Line $x = X_{bust}$ and $z = Z_{bust}$ ($y \in (-\infty, \infty)$). Note that the height of the breast can be measured along this axis. After shifting the scan of the breast to make $X_{bust} = 0$, and $Z_{bust} = 0$, the final axis essentially coincides with the y-axis, and Point (0, 0) on each of the frontal planes (i.e. the 2D vertical slices sliced at various y's) becomes the origin for the quasi-circles. As shown in Figure 1b, there are 40 vertical slices (sliced by equally spaced frontal planes) and 180 points on each slice (locating points at every 2 degrees from -180° to 180°, note that -180° and 180° are essentially the same angle, corresponding to the same point, i.e. the beginning and the end of a circle). Therefore, the total number of points is 7200 (180×40).

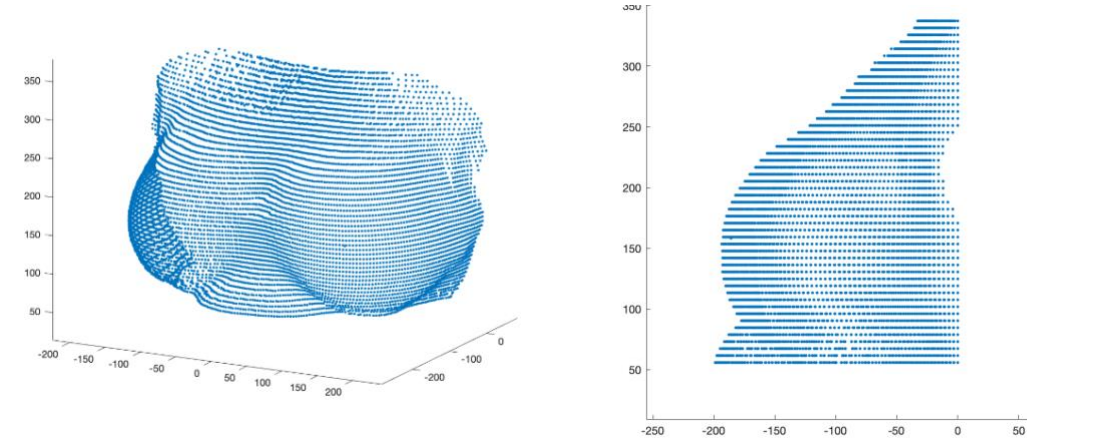

b) The right breast processed to identify exactly 40 vertical slices and 180 points on each slice

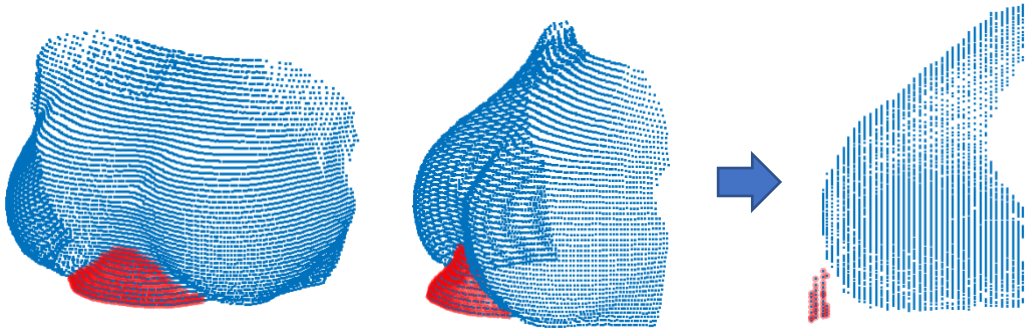

c) The protrusion of the upper abdomen is removed from the scan

Figure 1. The processing of the scans in Matlab®

Moreover, it is necessary to remove the points locate at the bridge area (i.e. the

lower and central area between the two breasts, highlighted in red in Figure 1c), because the protrusion of the upper abdomen may interfere with the processing and may invalidate the quasi-hemispherical assumption for breast shape, see Figure 1c. Since the participants in this study belonged to the Size-18 population, the protrusion of the upper abdomen can be observed for most of them.

The nine scans from a participant captured during motion were then plotted against the scan captured in static state, one at a time, and each of them was shifted and rotated manually to align with the static scan in the upper back area. Perfect alignment cannot be achieved, but the upper back area has relatively less change in shape, and therefore it is more ideal to be the benchmark for alignment (note that body landmarks are not ideal for various reasons, see Pei, Griffin, Ashdown & Fan, 2019).

Now that every scan is processed to have the same number of points and is aligned, we were able to compare the z-coordinates of the corresponding points. The point-wise relative displacement in vertical direction between a scan captured during motion, and its corresponding scan captured in static state, can be estimated via Eq.1. To estimate the amount of variability of the relative displacements, we further calculated the standard deviation of those z-coordinate differences via Eq. 2.

$$d_j = z_{ij} - z_{i0} \tag{1}$$

where d_j is an array containing the vertical displacements of all the 7200 points for one of the nine scans captured during motion, i.e. the *j*-th scan ($1 \leq j \leq 9$), z_{ij} is the z-coordinate of the *i*-th point of that scan ($1 \leq i \leq 7200$), while z_{i0} is the z-coordinate of the *i*-th point of the static scan (of the same participant) ($1 \leq i \leq 7200$).

$$SD = \sqrt{\frac{\sum(d_j - d_{avg})^2}{n-1}} \tag{2}$$

where SD represents the standard deviation of d_j, d_{avg} is the mean value of d_j, and n = 9 is the total number of scans captured in motion state.

Heat maps were then created with the SD values mapped onto the 3D surface of the static scan (i.e. the base scan) and presented by gradient colors. The dark blue color corresponds to minimal variability in vertical displacement, whereas the dark red color corresponds to maximal variability in vertical displacement. The SD values were calculated for the right breast and the left breast separately, then both breasts were plotted together (see Figure 2).

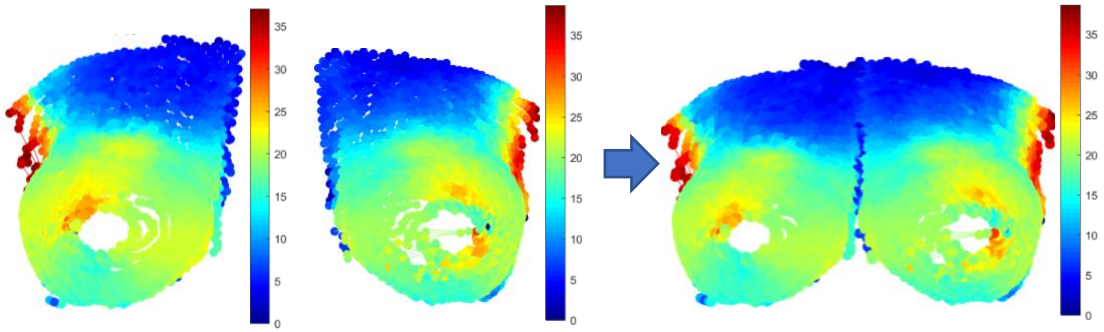

a) Right breast b) Left breast c) Both breasts plotted together

Figure 2. The creation of heat maps to visualize the variability in vertical displacements

3. Results and Discussion

3.1. Deformation of breasts during running

As mentioned before, slicing the scan horizontally assumes that the torso is quasi-cylindrical. We also assumed that the height of this "cylinder" remained the same during running, which usually does not involve intense flexion and extension of the torso. In this way, the horizontal slices are always defined at fixed heights, and on each slice, the distance of each point from the origin (the central axis) determines the overall shape of the breasts. Therefore, for the same participant, we were able to

quantify the relative shape change (with respect to the static scan) at point level through the calculation of the changes of how far the points are from the central axis (see Eq. 3).

$$d'_j = \sqrt{x_{ij}^2 + y_{ij}^2} - \sqrt{x_{i0}^2 + y_{i0}^2} \quad (3)$$

where d'_j is an array containing the horizontal distances from the central axis for each of the 9050 points for the *j*-th scan ($1 \leq j \leq 9$) captured during running x_{ij} and y_{ij} is the x-coordinate and y-coordinate, respectively, of the *i*-th point of that scan ($1 \leq i \leq 9050$), while x_{i0} and y_{i0} is the x-coordinate and y-coordinate, respectively, of the *i*-th point of the static scan (of the same participant) ($1 \leq i \leq 9050$).

Furthermore, we used Eq.2 to estimate the amount of variability of the shape changes at point level. Heat maps were created with each SD value mapped onto the 3D surface of the static scan (i.e. the base scan). Figure 3 shows the heat maps for six randomly selected participants. The dark blue color corresponds to minimal changes, whereas the dark red color corresponds to maximal changes in shape.

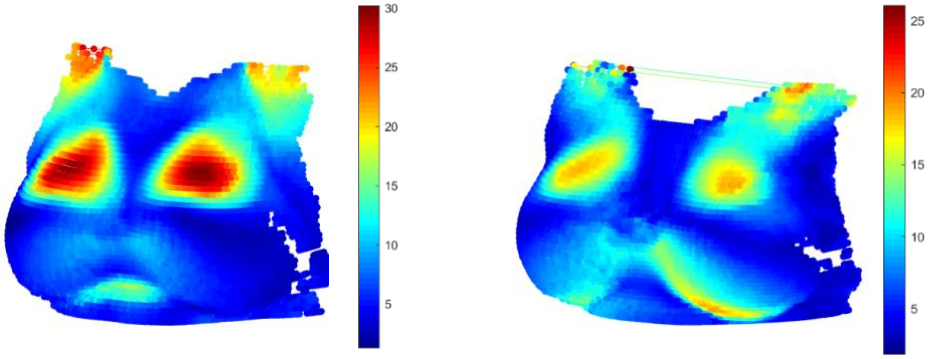

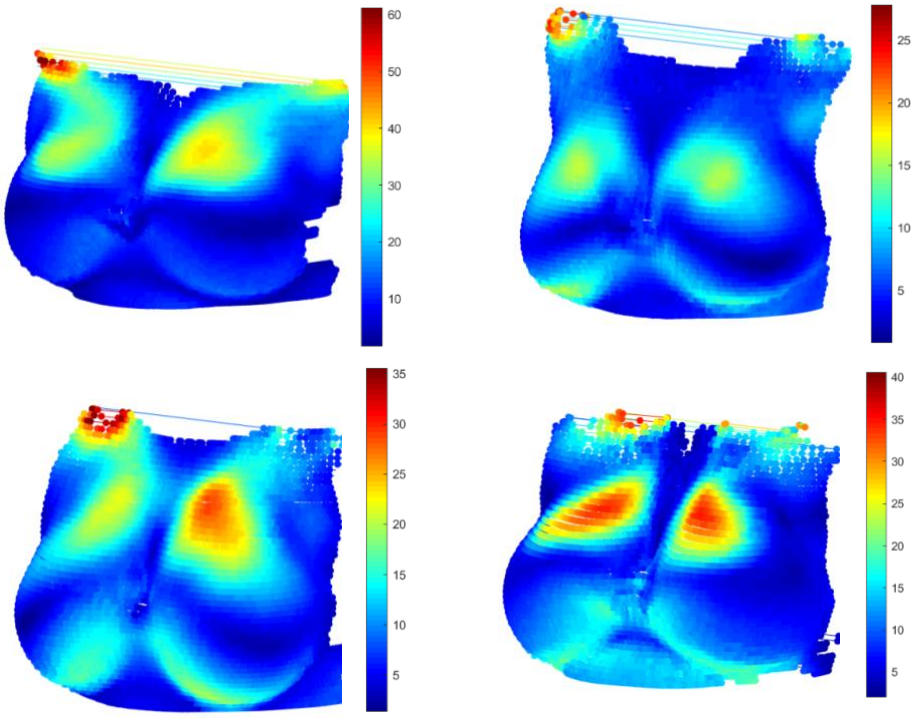

Figure 3. Heat maps showing the amount of variability of shape changes

As shown in Figure 3, it can be observed that the upper breasts have the most variability in shape deformation for all participants. Variability at the lower hemispheres of the breasts can also be observed for most participants, however, due to the restraint and support provided by the bra, the variability is not as high as the upper breast area. For some participants, the degrees of variability are not the same for the right breast and the left breast, which may be caused by the asymmetry of the breasts, the running postures, and/or the interaction between the bra and the breasts. To further investigate this, we calculated the Asymmetry Index (Pei, Fan & Ashdown, 2018) for each of the participants scanned in static state. It turns out that breast symmetricity may have little to do with the asymmetric color patterns shown in the heat maps. Since all participants were wearing a bra of a similar style, their Asymmetry Index values were low (suggesting high symmetric level, see Pei, Fan & Ashdown, 2019) and

similar (Mean± SD.: 0.0284 ± 0.008, min: 0.0179, max: 0.0532). The six participants involved in Figure 3 have a mean Asymmetry Index value of 0.0247 with a 0.004 standard deviation. Although the fifth participant has a very distinguishable difference in the color patterns between the left and right breasts she has the lowest Asymmetry Index value among the six. Therefore, the asymmetry in the color patterns between both breasts is more likely impacted by running postures, i.e. the rotation and sway of the torso during running, and/or the interaction between the bra and the breasts.

3.2. Vertical displacement of breast during running

Figure 4 shows the heat maps for the relative vertical displacements, of the same participants presented in Figure 3. The points at the edges of the right breast and the left breast as independently processed (Figure 2a and 2b) often exhibited noise. Therefore, when plotting the two breasts together the overlapping of these noisy points often creates a noticeable crease line with abrupt and irregular color patterns (Figure 2c and Figure 4). This crease line can be ignored. For some participants, high SD (standard deviation) values can be observed at the armpit area and/or the shoulder area (note that higher SD in shape change area can also be observed at the shoulder area, see Figure 3). This is most likely due to the arm swing rather than the breast tissue extending all the way to the armpit.

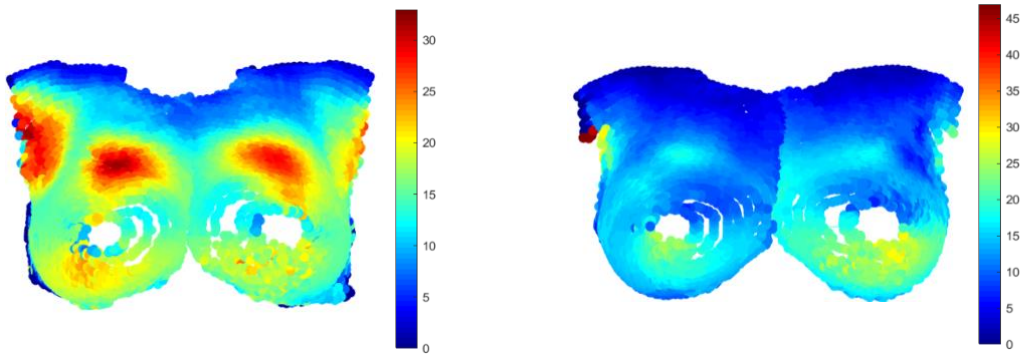

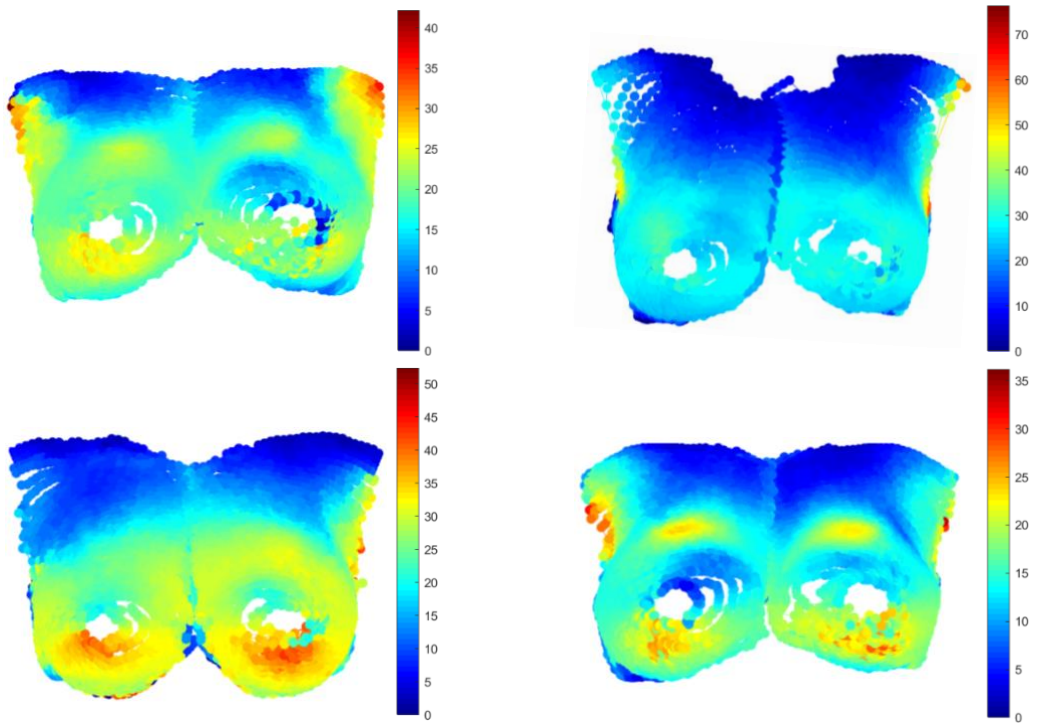

Figure 4. Heat maps showing the amount of variability of the relative vertical displacements

The heat maps can provide helpful information to facilitate the definition of the boundary of breasts. The next step in the analysis was to isolate the breasts from the chest wall. Based on the calculated SD value of the relative vertical displacements, a threshold value was defined for each participant with the reference of the color patterns in her heat map. Points with SD values smaller than the threshold value (indicating less variability in the relative displacements) were identified and mapped back to the original scan (where points are not sorted by slices and angles). Those points on the original scan and their neighboring points were highlighted in red, and the combination of them forms the area of the chest wall; these points could then be deleted leaving the breast only (see the first column in Table 1). Furthermore, we manually modified the area slightly to remove points at the armpit area with higher SD values, as these points are not an extension of the breast (as explained earlier), but are

caused by arm movement (Section 3.1). We also modified an area impacted by the bra strap (which will be discussed later), and smoothed the boundary curves (see the second column in Table 1). In the end, we obtained the 3D model of the breasts separated from the chest wall (the last column in Table 1).

Table 1. Separation of the breasts from the chest wall for the participants from Figures 3 and 4

#	Area to be removed (in red) according to the SD values	Modified area of deletion (in red)	Final outcomes
1	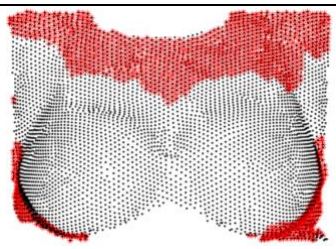	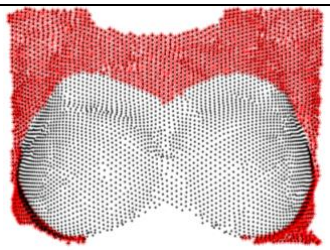	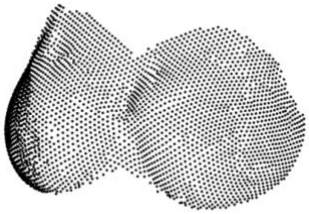
2	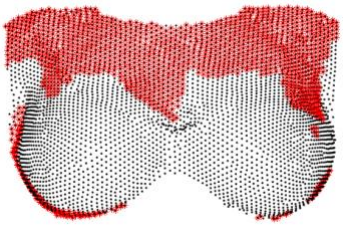	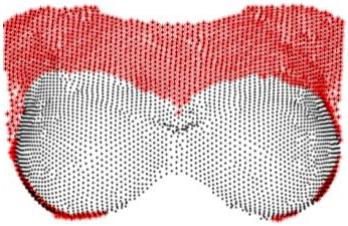	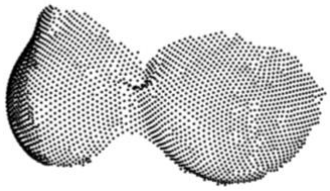
3	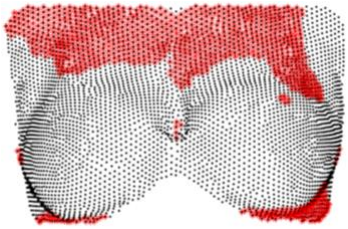	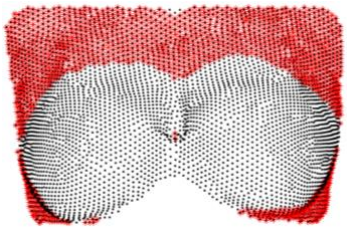	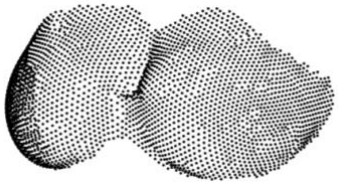
4	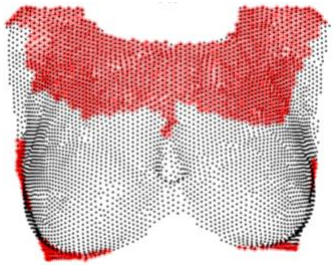	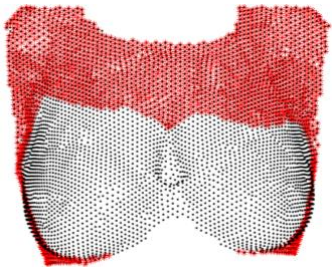	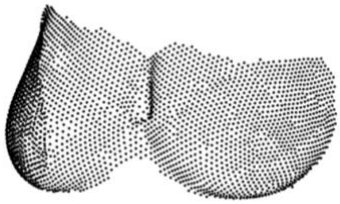

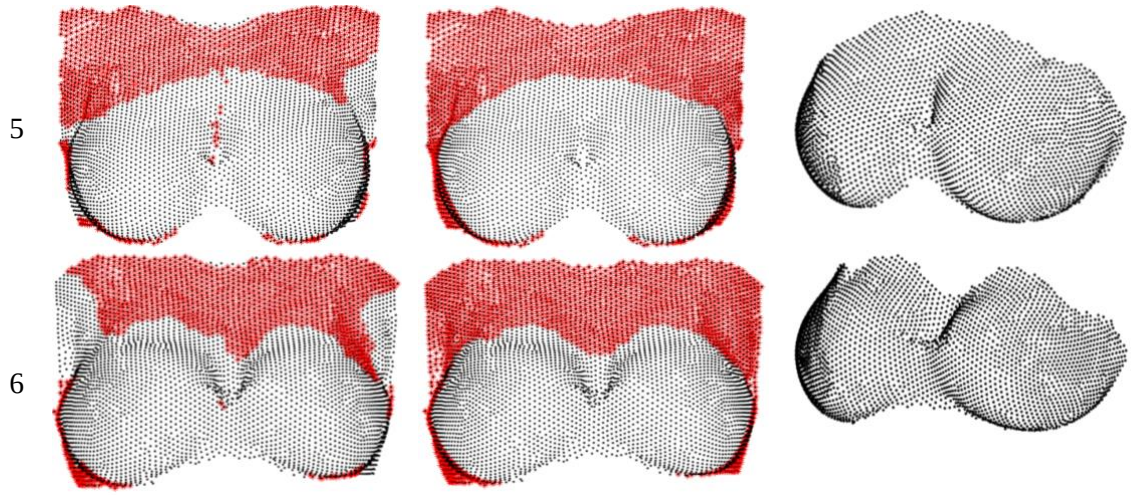

Figure 5 comprises the same three participants (namely, Participant #2, #3, and #6) as presented in Figure 4 and Table 1, to show the most visible impact of the bra on the vertical displacement of breasts. The lower part of the bra cups provide extra support to the breasts (as explained in Section 3.1) and thus impact the lower limit of the vertical displacements (i.e. how low the breasts can reach in the downward movement), but upper boundary of the breasts is not contained by the bra. However, the connecting area between the bra cup and the shoulder strap (as circled in Figure 5) can contain the upward movement of the breast, resulting in a lower SD value for the relative vertical displacement in that area. It is more visible if we increase the threshold value to enlarge the area for deletion (Figure 5c). This impact was observed for about 65% of the participants, and it should be taken into consideration when the boundary curve is being modified and smoothened.

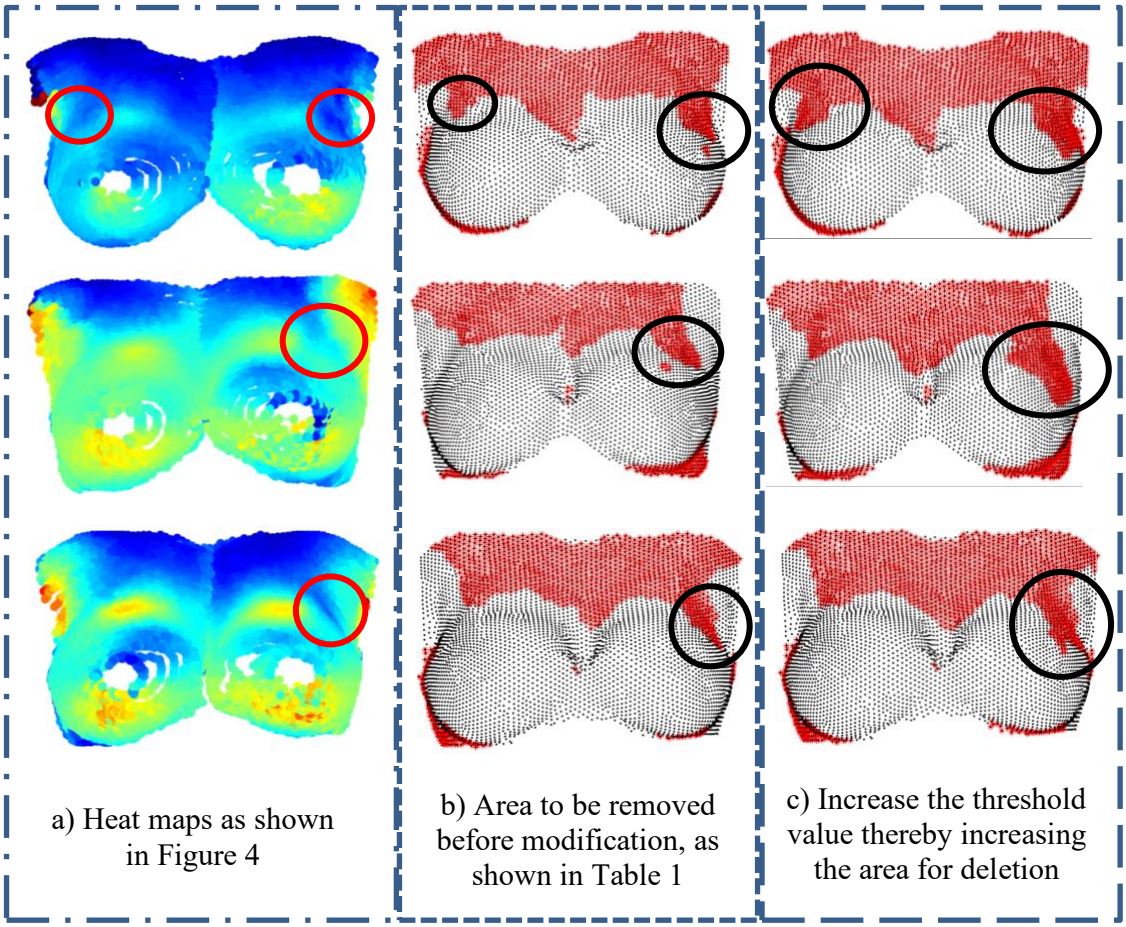

Figure 5. The impact of bra on the vertical displacement of breasts

Lastly, we investigate how the number of frames (i.e. scans captured during motion) included impacts the results. The method is computationally intense, and though some aspects can be made more automatic, reducing the number of scans to be

processed would be an advantage. The heat maps generated based on three (the 2nd, 5th, and 8th frames of the original nine frames) or two frames (the 1st and 5th frames of the nine) are presented in Table 2. Clearly, if we include fewer frames, it is less likely that we will obtain a heat map with clear boundary curves and enough data to separate the breasts from the chest wall. In addition, the minimum number of frames required for an informative heat map varies by individuals. As shown in Table 2, three frames may be considered sufficient for Participant #4 and #5, but not for the other participants. In fact, the three frames (the 2nd, 5th, and 8th frames) provided enough data for 35% (9 out of 26) of the participants, but the two frames (the 1st and 5th frames) were not sufficient for any of the 26 participants. Which frames to include also impacts the results, for example, if we switch to another two frames, i.e. the 3rd and 6th frames of the original nine frames these provided enough data for 2 participants (of all the 26 participants). One strategy might be to start with fewer frames and then to keep adding frames until enough data are accumulated. In this way we can reduce the amount of work needed to prepare the scans (e.g. removing head and limbs, fill holes, alignment, etc.).

Table 2. The importance of including enough frames

#	Heat maps as presented in Figure 4 (nine frames)	Heat maps based on three frames	Heat maps based on two frames
1	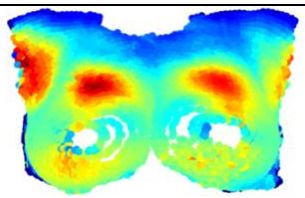	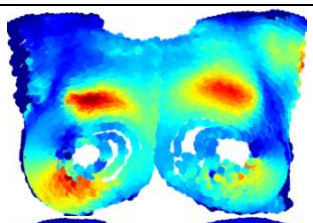	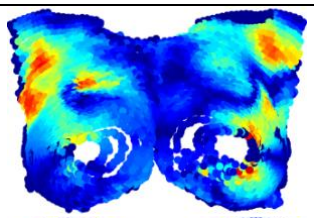
2	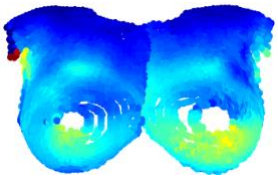	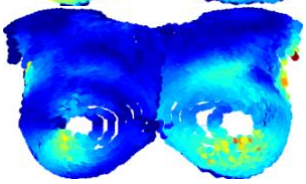	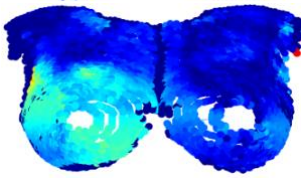

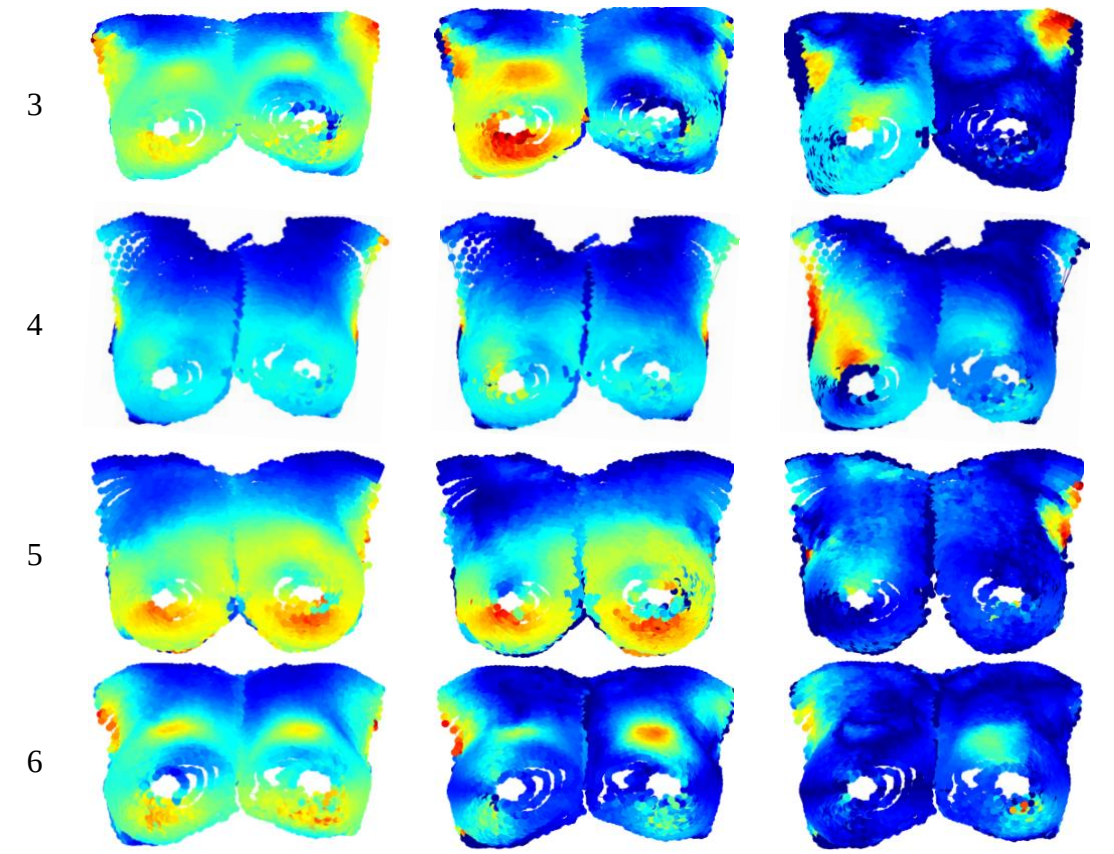

4. Conclusions

In this study, we 4D scanned 26 size 18 female participants wearing a provided bra using Temporal 3dMD system. Nine frames from participants running-in-place, and one frame while the participant was in a standing posture were included in the analysis. For each scan, the head, the limbs and the section below the swell of the breasts were removed. The remaining scan was processed in Matlab® to have exactly same number of points sorted in an organized fashion: 1) by assuming the shape of the torso as quasi-cylinder and slicing it with horizontal planes, we were able to study the shape deformation of breasts during running; 2) by assuming the shape of each breast as quasi-hemispherical or quasi-conical and slicing it with vertical planes, we were able to quantify the vertical displacement of each breast.

The study of shape deformation shows that the upper breasts have the most

variability in shape change. The variability in shape change of the lower hemispheres of the breasts is reduced due to the support of the bra, as the bra contains the downward movement of the breasts. Lastly, the extent of variability may not be the same for the right breast and the left breast, possibly due to the impact of the running posture (i.e. the rotation and sway of the torso during running) and/or the interaction between the bra and the breasts. The asymmetry of the breasts was measured in the static scan, and was not a factor in the asymmetry observed in analysis of the active scans.

The main goal of this paper is to define the upper boundary of breasts. To achieve this goal, we first aligned each scan by computing the differences in z-coordinates between a scan captured during motion, and its corresponding static scan. We then computed the standard deviation (SD) of those z-coordinate differences which represents the amount of variability of the relative vertical displacements. The breast tissue has more variability in vertical displacement, compared with the none-breast-tissue area. Heat maps were created with the SD values mapped onto the 3D surface of the static scan (i.e. the base scan) and used as a reference to determine the threshold value for the separation of the breasts from the chest wall (in other words, to determine the boundary of the breasts). Furthermore, the boundary curves defined solely based on the SD values were modified slightly to: 1) remove points at the armpit area, for its high variability is more likely due to the impact of arm swing rather than the breast tissue extending all the way to the armpit, 2) to compensate for the asymmetry caused by running posture, and 3) to compensate for the impact of the bra strap. We observed that the connecting area between the bra cup and the shoulder strap can restrict the upward movement of the breast in this area, resulting in a lower SD value for the relative vertical displacement in that area. Future studies can test our method on nude breasts.

There are several limitations in this study. Firstly, the participants were scanned while performing running-in-place, which may be different from other physical movements or postures. However, our method to detect breast boundaries used a simple action performed in an upright position that effectively induced a rapid up-and-down movement of the torso and could be easily captured in the 4D scanner. The participant group was limited in number and was limited to women self-identified as wearing a size 18 dress size. Testing of the method on more women with a wider variety of body sizes and breast sizes may yield different results. Fewer frames could be included to generate the heat maps to reduce the amount of work for preparing the scans; though some experimentation with fewer frames resulted in loss of data further testing could identify ways of selecting fewer frames that would not affect the results. In addition, the way we processed scans does not guarantee the tracking of the same points on the skin surface across the various scans captured during motion; such tracking could improve results. Lastly, our method requires a manual modification on the boundary curves based on subjective judgements, for example, we tried to compensate the impact of the bra via this modification but the interaction between the breasts and the bra is not quantified nor thoroughly investigated. Future studies can 4D scan participants with and without wearing a bra to study the impact of bras on the shape change of breasts during motion.

As 4D scanning makes it possible to track the whole breast in dynamic conditions, it can offer more information regarding the shape change of breasts during physical activity. This study is one of the first reports using 4D scanning on breast kinematics. By providing a solution to increase the understanding of breast kinematics and breast shape, similar studies can impact the product design for bras, PPE, and other types of wearable products for women, for which good fit is essential to the function of the product. Finally, with iteration to rid our method from the need for subjective manual

processes, a rapid, accurate and automatic program to obtain individual breast volume can be achieved. Automation of the data will allow for rapid creation of customized product prototypes and enable data collection of large populations to create meaningful size charts or improve existing ones.

DISCLOSURE STATEMENT

This chapter is a journal paper that is under review by Sports Medicine – Open. Permission to include the content of this paper in this dissertation has been acquired from SpringerOpen.

REFERENCES

Bulstrode, N., Bellamy, E., & Shrotria, S. (2001). Breast volume assessment: comparing five different techniques. *The Breast*, *10*(2), 117-123.

Coltman, C. E., McGhee, D. E., & Steele, J. R. (2017). Three-dimensional scanning in women with large, ptotic breasts: implications for bra cup sizing and design. *Ergonomics*, *60*(3), 439-445.

Coltman, C. E., Steele, J. R., & McGhee, D. E. (2018). Effects of age and body mass index on breast characteristics: a cluster analysis. *Ergonomics*, *61*(9), 1232-1245.

Coltman, C. E., Steele, J. R., & McGhee, D. E. (2019). Does breast size affect how women participate in physical activity?. *Journal of science and medicine in sport*, *22*(3), 324-329.

Edsander-Nord, Å., Wickman, M., & Jurell, G. (1996). Measurement of breast volume with thermoplastic casts. *Scandinavian journal of plastic and reconstructive surgery and hand surgery*, *30*(2), 129-132.

Ferrari, R. J., Frere, A. F., Rangayyan, R. M., Desautels, J. E. L., & Borges, R. A. (2004). Identification of the breast boundary in mammograms using active contour models. *Medical and Biological Engineering and Computing*, *42*(2), 201-208.

Greenbaum, A. R., Heslop, T., Morris, J., & Dunn, K. W. (2003). An investigation of the suitability of bra fit in women referred for reduction mammaplasty. *British journal of plastic surgery*, *56*(3), 230-236.

Giannini, V., Vignati, A., Morra, L., Persano, D., Brizzi, D., Carbonaro, L., ... & Regge, D. (2010, August). A fully automatic algorithm for segmentation of the breasts in DCE-MR images. In *2010 Annual International Conference of the*

IEEE Engineering in Medicine and Biology (pp. 3146-3149). IEEE.

Haake, S., & Scurr, J. (2010). A dynamic model of the breast during exercise. *Sports engineering*, *12*(4), 189-197.

Kim, M. S., Reece, G. P., Beahm, E. K., Miller, M. J., Atkinson, E. N., & Markey, M. K. (2007). Objective assessment of aesthetic outcomes of breast cancer treatment: measuring ptosis from clinical photographs. *Computers in Biology and Medicine*, *37*(1), 49-59.

Kovacs, L., Eder, M., Hollweck, R., Zimmermann, A., Settles, M., Schneider, A., ... & Biemer, E. (2007). Comparison between breast volume measurement using 3D surface imaging and classical techniques. *The Breast*, *16*(2), 137-145.

Kus, P., & Karagoz, I. (2012). Fully automated gradient based breast boundary detection for digitized X-ray mammograms. *Computers in biology and medicine*, *42*(1), 75-82.

Lorentzen, D., & Lawson, L. (1987). Selected sports bras: a biomechanical analysis of breast motion while jogging. *The Physician and Sportsmedicine*, *15*(5), 128-139.

Lee, H. Y., Hong, K., & Kim, E. A. (2004). Measurement protocol of women's nude breasts using a 3D scanning technique. *Applied Ergonomics*, *35*(4), 353-359.

Mason, B. R., Page, K. A., & Fallon, K. (1999). An analysis of movement and discomfort of the female breast during exercise and the effects of breast support in three cases. *Journal of Science and Medicine in Sport*, *2*(2), 134-144.

McGhee, D. E., & Steele, J. R. (2010). Optimising breast support in female patients through correct bra fit. A cross-sectional study. *Journal of Science and Medicine in Sport*, *13*(6), 568-572.

McGhee, D. E., Steele, J. R., Zealey, W. J., & Takacs, G. J. (2013). Bra–breast

forces generated in women with large breasts while standing and during treadmill running: Implications for sports bra design. *Applied ergonomics*, *44*(1), 112-118.

Nethero, S. (2008). *U.S. Patent Application No. 11/829,568*.

Ojala, T., Näppi, J., & Nevalainen, O. (2001). Accurate segmentation of the breast region from digitized mammograms. *Computerized Medical Imaging and Graphics*, *25*(1), 47-59.

Page, K. A., & Steele, J. R. (1999). Breast motion and sports brassiere design. *Sports Medicine*, *27*(4), 205-211.

Pei, J., Fan, J. & Ashdown, S. P. (2018). A Novel Method to Assess Breast Shape and Breast Asymmetry, *The Journal of the Textile Institute*, *110*(8), 1229-1240.

Pei, J., Fan, J. & Ashdown, S. P. (2019). Detection and Comparison of Breast Shape Variation among Different 3D Body Scan Conditions: Nude, with a Structured Bra, and with a Soft Bra, *Textile Research Journal*, *89*(21), 4595-4606.

Pei, J., Griffin, L., Ashdown, S. P. & Fan, J. (2019). The Study of Breast Shape During Running Using 4D Scanning Technology, *Ergonomics*, under review.

Smith, J. D., Palin, J. W., Katch, V. L., & Bennett, J. E. (1986). Breast volume and anthropomorphic measurements: normal values. *Plastic and reconstructive surgery*, *78*(3), 331-335.

Starr, C., Branson, D., Shehab, R., Farr, C., Ownbey, S., & Swinney, J. (2005). Biomechanical analysis of a prototype sports bra. *Journal of Textile and Apparel, Technology and management*, *4*(3), 1-14.

Scurr, J., White, J., & Hedger, W. (2009). Breast displacement in three dimensions during the walking and running gait cycles. *Journal of Applied Biomechanics*, *25*(4), 322-329.

Scurr, J. C., White, J. L., & Hedger, W. (2011). Supported and unsupported breast

displacement in three dimensions across treadmill activity levels. *Journal of sports sciences*, *29*(1), 55-61.

Todd, W. L. (2007). Sizing for the military. In *Sizing in Clothing* (pp. 277-308). Woodhead Publishing.

Xi, W., Perdanasari, A. T., Ong, Y., Han, S., Min, P., Su, W., ... & Lazzeri, D. (2014). Objective breast volume, shape and surface area assessment: a systematic review of breast measurement methods. *Aesthetic plastic surgery*, *38*(6), 1116-1130.

CHAPTER 6

A NOVEL OPTIMIZATION APPROACH TO MINIMIZE AGGREGATE-FIT-LOSS FOR IMPROVED BREAST SIZING

Abstract

Ready-to-wear is typically based on the body-shape of human fit models that an apparel company hires. The body-shape difference between a consumer and the fit model of their size results in a fit-loss of certain degree. Aggregate-fit-loss is a concept attempting to quantify and estimate the accumulative fit-loss that a population may encounter. This paper reports on a novel method that minimizes the aggregate-fit-loss of a sizing system for bras, through shape categorization and optimized selection of prototypes (which can be regarded as the most appropriate fit models, or standard dress forms) for the categorized groups. A fit-loss function was introduced that calculates the dissimilarity between any two 3D body-scans, via pointwise comparisons of the point-to-origin distances of 9,000 points on scan surface. The within-group aggregate-fit-loss is minimized by an algorithm that returns the optimal prototype for the group. The overall aggregate-fit-loss is reduced by breast shape categorization based on the dissimilarities between the scans. Finally, the constraint of band sizes was brought into the categorization to provide a more feasible solution for improved bra sizing. The findings of this study can also contribute to the optimization of sizing systems for other apparel products.

1. Introduction

Clothing fit is directly associated with the human body anatomy (Cain, 1950). A well fitted garment creates a smooth appearance on the wearer's body and provides

optimal comfort and mobility (Shen & Huck, 1993). It also affects the wearer's confidence and psychological well-being (Smathers & Horridge, 1979). Fit problems often have a strong negative impact on consumer purchases and return rates, which are directly related to the financial profits of manufacturers (Alexander, Connell & Presley, 2005). Sizing, on the other hand, is the foundation for mass-produced ready-to-wear clothing. Successful sizing strategies can improve consumer's satisfaction of fit and comfort, improve production planning and material control, increase sales and reduce inventory (Pei, Park, Ashdown & Vuruskan, 2017). Sizing and fit are closely correlated (Gribbin, 2014). The ultimate goal of sizing is to use the fewest sizes possible to provide the best fit possible for as large a percentage of a population as possible (McCulloch, Paal & Ashdown, 1998; Gribbin, 2014).

1.1. Traditional bra sizing systems

Traditionally, a band size and a cup size are used to define the size of a bra (Tadisina, Frojo, Plikaitis & Bernstein, 2016). The underbust circumference, which is measured at the level of the inframammary fold, is more relevant to chest size (size of the ribcage) and determines the band size indicated by numbers, such as 32, 34, 36 etc. in USA/UK sizes (McGhee & et al., 2018). The bust circumference is measured at the fullest, most anteriorly projecting aspect of the breast (Tadisina, Frojo, Plikaitis & Bernstein, 2016). The bust circumference or the difference between the bust and underbust circumferences determines the cup size, which is typically indicated by one or more letters, such as A, B, C, D, DD=E, etc. (Tadisina, Frojo, Plikaitis & Bernstein, 2016; McGhee et al., 2018). However, the accuracy and reliability of these measurements are often questioned (Han, Nam & Choi, 2010; Tadisina, Frojo, Plikaitis & Bernstein, 2016; McGhee et al, 2018; Peterson & Suh, 2019). Han, Nam and Choi (2010) reported the underbust circumference measured from three-

dimensional (3D) body scans to be significantly larger than the measurement obtained through manual tape measure, for the overweight and obese population. McGhee and et al. (2018) found underbust circumference measured from 3D body scans to be inaccurate for women with large and ptotic breasts, due to scanners' incapability of capturing the lower aspect of the breasts that are in contact with the upper abdomen. More importantly, these one dimensional (1D) measurements are not sufficient in describing the complicated shape of the breasts in 3D, and merely using the two measurements can end up with inaccurate cup size and inconsistent intervals between cup sizes (Chen, LaBat & Bye, 2011; Pandarum, Yu & Hunter, 2011; Peterson & Suh, 2019).

As a result of falling to incorporate breast shape information (Pei, Park & Ashdown, 2019), the current bra sizing systems are far from efficient: while a large number of women at both ends of the size range (i.e. the flat-chest and large breast populations) find their sizes excluded from many of the size charts (Filipe, Carvalho, Montagna & Freire, 2015), the existence of "sister sizes", where a woman who wears 34C can potentially also fit into a 36B or even a 32D bra, brings confusion to women whose breast size is at the center of the size range (Bengtson & Glicksman, 2015, Peterson & Suh, 2016). It was reported that up to 85% of women wear the wrong size bra (McGhee & Steele, 2010; McGhee et al., 2018). In addition, there is a lack of standardization in the sizing systems of bras, leaving the sizes of bras to vary greatly by designs and companies (Bengtson & Glicksman, 2015, Tadisina, Frojo, Plikaitis & Bernstein, 2016), bringing frustrations to consumers who try to find consistent sizes (Kennedy, 2009). Each company has their own rules of converting the bust-underbust difference into letter graded cup sizes, and the offset can range from 0 to 6 inches (Wang & Suh, 2019). Practices of vanity sizing, where companies deliberately alter size labels to flatter smaller-busted consumers by indicating that bigger than actual

sizes are the right fit, exacerbate the inconsistency (Ketron & Naletelich, 2017). Moreover, the current bra sizing systems also receive criticisms for their ambiguity in measurement definition and inadequacy in approximating breast volume (Pei, Park & Ashdown, 2019).

Researchers commonly agree that existing bra sizing systems cannot satisfy both the manufacturers and the consumers (McCulloch, Paal & Ashdown, 1998; Zheng, Yu & Fan, 2007; Peterson & Suh, 2019; Pei, Park & Ashdown, 2019). However, despite of all this, and the increased diversity in women breast shapes and sizes, bra sizing systems have not changed fundamentally since 1935 (Zheng, Yu & Fan, 2007; Peterson & Suh, 2019). No major development of a scientific and practical method that improve bra sizing fundamentally has been found in recent years (Yu, Fan, Ng & Harlock, 2014; Peterson & Suh, 2019). Many attempts to categorize female breasts based on shape have been proposed (Zheng, Yu & Fan, 2007; Liu, Wang & Istook, 2017; Coltman, Steele & McGhee, 2018; Pei, Park & Ashdown, 2019). Zheng, Yu and Fan (2007) categorized the nude breasts of 456 Chinese women (aged 20 to 39) based on 98 anthropometric measurements, and suggested that underbust circumference and a breast depth-width ratio to be adopted for an improved bra sizing system. Liu, Wang and Istook (2017) obtained 108 breast measurements from the topless scans of 275 female college students in China, and proposed that the breadth of the breast should be included to categorize breasts for sizing systems. Coltman, Steele and McGhee (2018) categorized the nude breasts of 378 Australian women (aged 18 and over) based on breast volume, breast surface area, underbust circumference, sternal notch-to-nipple distance and nipple-to-nipple distance. Pei, Park and Ashdown (2019) categorized the breast shapes of 478 North American Caucasian women (age 18 to 45) based on 41 ratio and angular measurements, constructed from 66 body measurements. However, the categorization methods and results can be difficult to put into practice without a

solution for consumers to quickly and easily identify their own shape and size (Chun-Yoon & Jasper, 1996; Kinley, 2003; Petrova, 2007; Chun, 2007).

1.2. Aggregate fit loss

Aggregate-fit-loss is a concept developed to evaluate individual fit provided by a sizing system (Paal, 1997). A fit-loss function quantifies the goodness of fit of a garment for an individual who belongs to a particular size according to the sizing system (McCulloch, Paal & Ashdown, 1998). A small fit-loss measure implies a small discrepancy, in terms of body size and body shape, between the individual and the prototype (viz. standard dress form or fit model) that fits perfectly in that garment, and vice versa (McCulloch, Paal & Ashdown, 1998). By summing or calculating the average fit-loss of all individuals of all sizes, the aggregate-fit-loss can be obtained (McCulloch, Paal & Ashdown, 1998). Lowering aggregate-fit-loss is a logical strategy to improve sizing and fit (Zakaria & Gupta, 2014).

Traditionally, aggregate-fit-loss is assessed based on some combinations of body measurements (McCulloch, Paal & Ashdown, 1998; Gupta & Gangadhar, 2004; Chung, Lin & Wang, 2007; Hsu, 2009; Doustaneh, Gorji & Varsei, 2010; Salehi & Shahrabi, 2012). Tryfos (1986) proposed the measure of aggregate discomfort, a similar concept to the aggregate-fit-loss, using body height and body weight as control dimensions. McCulloch, Paal and Ashdown (1998) regarded four body measurements, namely, hip circumference, waist circumference, crotch height, and crotch length, as critical parameters, and used them in the calculation of discrepancies when constructing an optimized sizing system for pants that minimizes aggregate-fit-loss. To validate their proposed size charts, Gupta and Gangadhar (2004) calculated the aggregate-fit-loss for the following body dimensions: bust, natural waist, hip, cervical to natural waist, center front to natural waist, shoulder width, neck girth at midway,

neck girth at neck base, outer and inner leg seams. Salehi and Shahrabi (2012) evaluated their final size chart through the aggregate-fit-loss of chest, waist and hip circumferences. In calculating the aggregate-fit-loss, Doustaneh, Gorji and Varsei (2010) adopted bust girth and body height; Hsu (2009) adopted hip and waist circumferences; Chung, Lin and Wang (2007) adopted chest girth, waist girth, front waist length and shoulder width for the upper garment, and waist girth, hip girth, waist-to-ankle length and crotch height for the lower garment.

However, as noted by previous researchers and explained above, linear body measurements are not sufficient in describing the complicated body shapes in three dimensions (Robinette, Daanen & Paquet, 1999; Bye, Labat & Delong, 2006; Chen, LaBat & Bye, 2011; Ashdown, 2014; Peterson & Suh, 2019). Therefore, the use of 1D measurements may not be optimal for apparel sizing, especially for form-fitting garments such as bras and shapewear. Moreover, even if the 1D measurements are correctly chosen and proven to be efficient, it can be difficult to find the fit models who satisfy all the constraints on body dimensions (Ashdown & Loker, 2010). This also becomes the limitation to effectively implement the results of previous studies, as human fit models are still generally used by apparel companies and play a significant role in product development (Vinué, León, Alemany & Ayala, 2014; Gribbin, 2014). Vinué, León, Alemany and Ayala (2014) proposed two clustering algorithms to select human fit models based on anthropometric data. However, no literature has been found which proposed solutions for finding proper fit models based on 3D shape instead of a combination of body measurements.

The aim of the paper is to present a scientific and practical method to improve bra sizing, by taking full advantage of the 3D body scanning technology, which is gaining acceptance and accessibility to consumers (Arbutina, Dragan, Mihic & Anisic, 2017; Haleem & Javaid, 2019). Also with the development of the technology of body

scanning using personal cellphones (Zhu, Mok & Kwok, 2013; Zhu & Mok, 2015; Arbutina, Dragan, Mihic & Anisic, 2017; Xia, West, Istook & Li, 2018), expecting consumers to upload their body scans to online stores or to step into the 3D scanners in physical stores is no longer implausible.

Based on the research gap identified through the literature review, we propose a novel method for minimizing the aggregate-fit-loss of a bra sizing system, through categorization and optimized selection of prototypes (which can be regarded as the most appropriate fit models, or standard dress forms) for the categorized groups. Instead of using traditional body measurements, our fit-loss function calculates the discrepancy between two scans, via pointwise comparisons of the point-to-origin distances of 9,000 points on scan surface, making this the first true 3D system ever developed for categorizing shape in 3D. In addition, by replacing traditional measurements with new parameters, we avoid the concerns of inaccurate body measurements such as the underbust circumference taken from the 3D body scans (Han, Nam & Choi, 2010; McGhee & et al., 2018), while taking full advantage of the 3D scanning technology, which is able to collect consistent data without bias introduced by human measurer, in a relatively fast, efficient and non-intrusive manner (Kim et al., 2015). Our solution facilitates selection of fit models based on 3D breast shape, and our method allows the fit models to be closely associated with individual consumers while maintaining its practicability to the industry. Furthermore, we provide consumers a technological and helpful solution for finding their shape-based selection of products that may best fit them.

Although our method can be applied to other apparel products as well, we focused on the optimization of bra sizing, which has more fit challenges and higher requirements on understanding the human anatomy, specifically, the female breast shape (Zheng, Yu & Fan, 2007; Pei, Fan & Ashdown, 2019; Pei, Park & Ashdown,

2019). Nude breasts, instead of dressed ones, are the focus of this study because female breasts are soft, deformable and on many occasions, even able to conform to bras that do not provide good fit or comfort. While studying the shape modification caused by a bra is important, the shape of the breast in its natural state is equally important, and the acquired knowledge can inform bra companies to modify their patterns and designs.

2. Methodology

A total of 46 female participants were recruited for 3D body scanning. Participants were all Caucasian, non-obese (BMI below 30), 18 to 45 years of age. They were scanned in the standard standing posture with their upper body nude. A Human Solutions VITUS/XXL 3D Body Scanner (Technology: Laser triangulation; Output formats: ASCII, DXF, OBJ, STL; Average girth error < 1 mm) was used. The approval from Institutional Review Board and consents from participants were obtained before scanning.

2.1. The Preparation of Scans

Figure 1 shows part of the initial scan processing procedure. Small holes on the scans were filled based on surrounding curvatures beforehand. Figure 1a shows how the bust and underbust planes were defined in this study: the transverse plane at the averaged z-coordinate of the right and left nipple points was defined as the bust plane; the transverse plane at the immediate cease of the swell of the breast was defined as the underbust plane. They were defined in this way (and not according to traditional definitions) to ensure that the whole breasts were included and did not get truncated in the middle, and to ensure consistency in measurement extraction in case of an absence of a clear fullest projecting aspect for ptotic breasts. The scans were processed in

Matlab® (Version R2018b), with the limbs, neck, head, and the portion below the underbust plane removed.

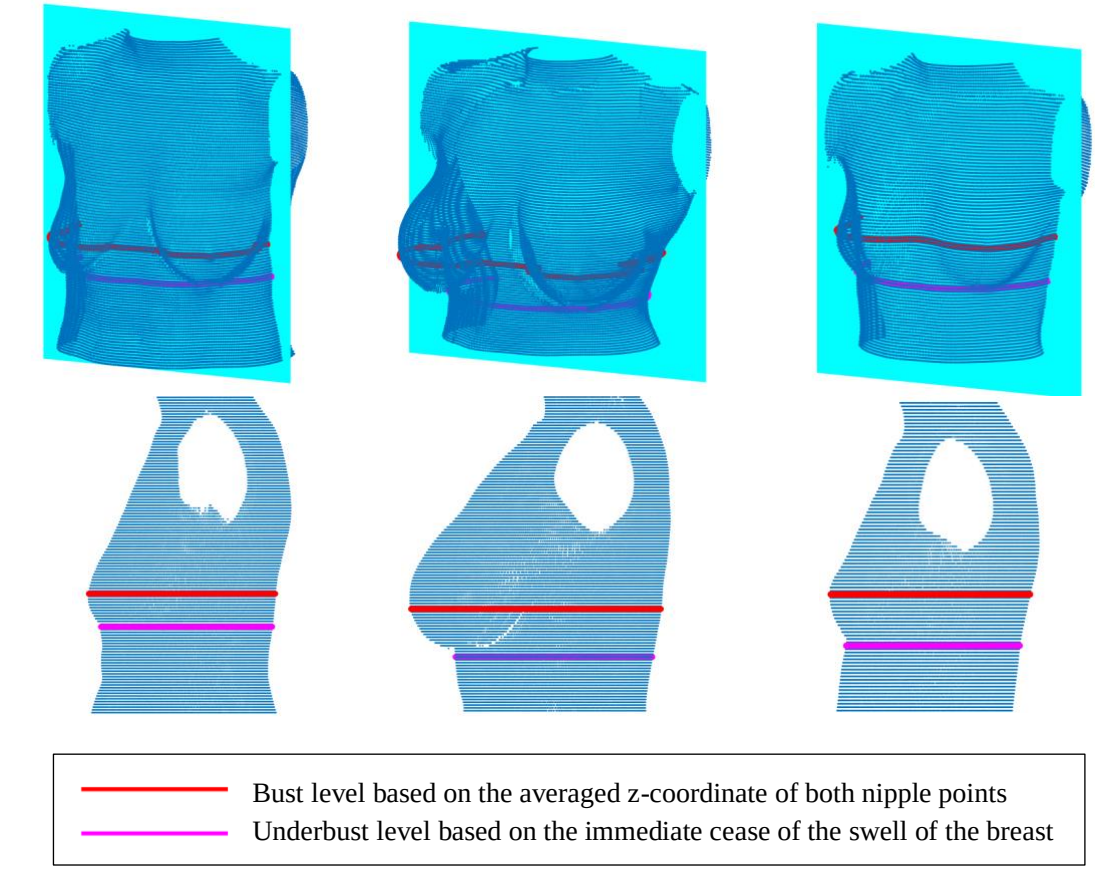

a) Self-defined bust and underbust planes

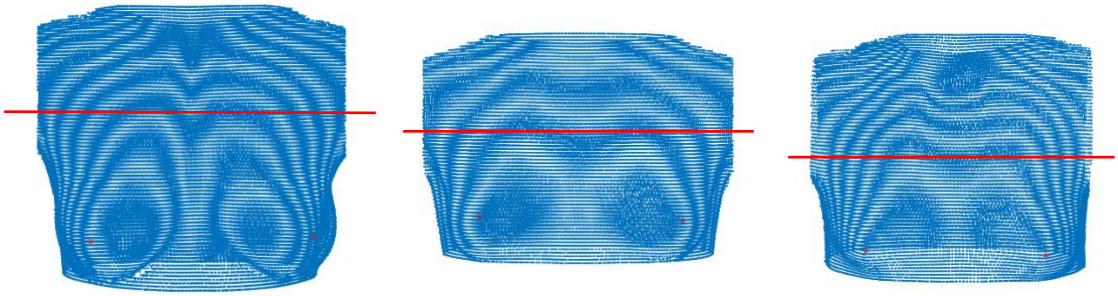

b) Moiré patterns as a reference to determine the upper boundary of breasts

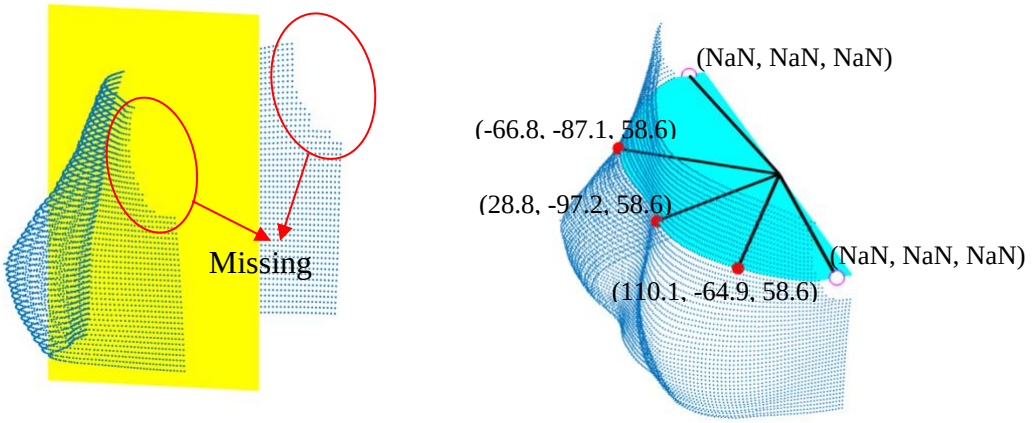

c) The coordinates of the missing points were replaced by NaN's

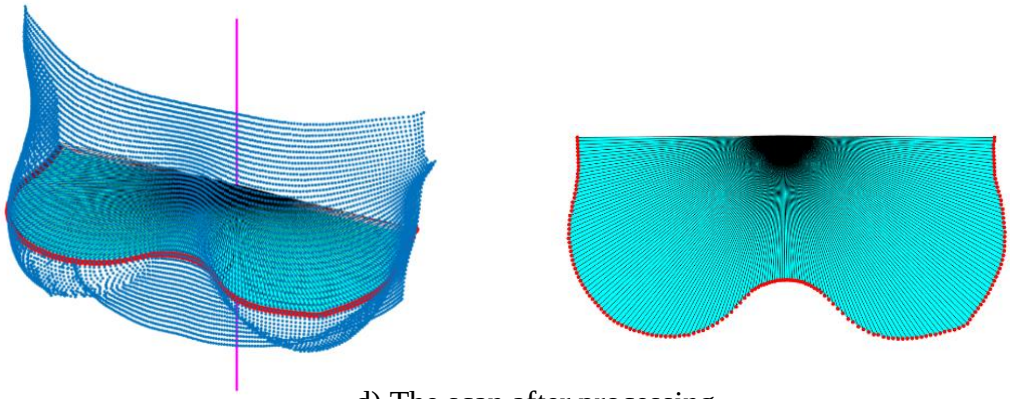

d) The scan after processing
(Points on the bust plane at z=0 were highlighted in red)

Figure 1. The preparation of scans

The upper boundary of breasts is difficult to define visually (Lee, Hong & Kim, 2004). Therefore, the 3D scans of breasts were examined three times to ensure the total inclusion of breasts while excluding the shoulder area to the largest extent. Moiré patterns are interference patterns that were created by two closely placed patterns of regular geometry, such as spaced lines and dots (Miao et al., 2016). It has been used to reveal the contour lines on the 3D surface of a human body since 1970 (Takasaki, 1970). In our study, the scans were rotated and viewed at multiple perspectives for inspection. Figure 1b shows the Moiré pattern which appear on scan surface during

rotation. They were used as a reference to determine a separation height, above which the portion of the scan is also removed (Figure 1b).

Then shifting was done horizontally to make the central axis, defined by the averaged x-coordinates and y-coordinates of all points on the remaining scan, coincided with Line x= 0, y= 0. Shifting was also done vertically to make the bust plane coincided with Plane z= 0. After shifting, the posterior portion of the remaining scan (i.e. $y < 0$) was removed. Every scan was processed in the same way so that they were aligned at the central axis and at the bust plane if plotted together.

Lastly, the scans were processed such that each of them has exactly 9,000 points, which were arranged in the exact same order without distorting the scan. Specifically, each scan contains 50 equally-spaced horizontal slices (or transverse planes), arranged by their z-coordinates. Each slice has 180 points. The angle increment is 1 degree, which means that starting from -180° to 0° there is one point at every degree (see Figure 1c). For example, the 10th point is the point that locates on the bottom slice, at the angle of -170° (-180° + 10 × 1°). The number of slices and the number of points on each slice can both be altered as long as they are consistent across all the scans. Figure 1c shows how we handled the missing points at the armhole. If a point is missing, its coordinates are replaced by NaN's (representing undefined values) to hold the space for the point, and more importantly, to maintain the sequence and indexing of other points (Figure 1c). The scan after processing will be referred to as the breast scan. Figure 1d shows an example of a scan after processing, with all the points that are on the bust plane (i.e. Plane z=0) highlighted in red.

2.2. Estimation of the Aggregate-Fit-Loss

As mentioned earlier, traditionally, fit loss is calculated using body measurements such as circumferences, lengths, etc. However, due to the complexity of the breast

shape, the traditional breast measurements cannot fully describe the concavity, convexity and subtle fluctuations on the breast surface, all of which may significantly influence the morphology of breast. In addition, the extraction of body measurements depends on the actuate placement of body landmarks, but the definition and identification of landmarks can be a real challenge on the soft breast tissue (nipple is an exception). Therefore, instead of using traditional breast measurements, we propose the direct usage of the locations of points on scan surface, with respect to the origin, i.e. Point (0, 0, 0) (see Eq.1). The points had been sorted into the same order (see Section 2.1), eliminating the need for traditional anatomical landmarks.

$$d_i = \sqrt{{x_i}^2 + {y_i}^2 + {z_i}^2} \quad \text{(Eq. 1)}$$

where, $(x_i,\ y_i,\ z_i)$ is the coordinates of the i-th point on scan surface (i ranges from 1 to 9,000), and d_i is the distance of that point from the origin, Point (0, 0, 0). Based on the calculated distances, the fit-loss function between any two breast scans is given by the following equation (Eq.2).

$$L(d1, d2) = \frac{1}{m}\sum_{i=1}^{n}(d1_i - d2_i)^2 \quad \text{(Eq. 2)}$$

where, d1, d2 represent two different breast scans, $d1_i$ refers to the i-th point on the first scan, while $d2_i$ refers to the corresponding point, i.e. the i-th point, on the second scan (i ranges from 1 to 9,000). n is the total number of points and equals 9,000 (note that any value subtracting or being subtracted by an NaN value will result in an NaN value, but all the NaN values were removed before the addition). m is the total number of pairs of points that are both none-null (i.e. when $d1_i$ and $d2_i$ is neither NaN). This is essentially a dissimilarity function that quantifies the shape difference between two scans. If one of the two scans is chosen to be the prototype

breast shape (regarded as the fit model or the standard dress form), the equation calculates the amount of fit-loss of the other scan.

One breast scan was randomly selected from the 46 scans and was reserved for later demonstration. The rest of the 45 scans were involved in the calculation of the pairwise fit-loss. A 45-by-45 dissimilarity matrix was generated, containing the values calculated from the fit-loss function for all pairs of scans. The matrix is symmetric about its diagonal (i.e. L(d1, d2)= L(d2, d1)), and values on the diagonal are uniformly zero, because the fit loss of a scan to itself is zero (i.e. L(d1, d1)= 0). Then the aggregate fit-loss can be calculated from the dissimilarity matrix. For example, if Scan #1, #2, #3 and #4 are in the same shape group and Scan #1 is regarded as the prototype shape of this group, then the aggregate-fit-loss can be obtained by adding the values in Row #2, #3 and #4 of Column #1 from the dissimilarity matrix.

2.3. Reducing the Aggregate-Fit-Loss

The overall aggregate fit loss can be reduced by categorizing the breasts into appropriate groups. The within-group aggregate fit loss can be minimized by selecting the right prototype breast shape. We approached the two tasks using different methods.

To find the optimal prototype breast shape for a given group, we let every scan in the group be the prototype shape and calculate the corresponding aggregate-fit-loss. Our algorithm searches for and returns the lowest aggregate-fit-loss value and the prototype shape.

Cluster analysis aims at grouping objects so that objects within the same group are similar, whereas dissimilar objects are categorized to different groups (Kaufman & Rousseeuw, 2009). To categorize breast shapes, more than one clustering methods

were tried. However, instead of including 9,000 variables (by regarding every point-to-origin distance as a variable) in the cluster analysis, we selected a few clustering algorithms which directly use the dissimilarity matrix as their grouping standard. K-medoid clustering and Hierarchical clustering were considered. K-medoid clustering seeks to find k representative objects (also known as medoids) from the data and a corresponding data partition solution that minimizes the distance between each individual objects and the medoids (Kaufman & Rousseeuw, 2009). Hierarchical clustering seeks to construct a hierarchy of clusters based on dissimilarity or similarity among objects, where the "top-down" approach starts with one cluster and has it split recursively until reaching the bottom of the hierarchy, whereas the "bottom-up" approach starts with each object having its own cluster and has them merged recursively until reaching the top of the hierarchy (Wit & McClure, 2004). There are many methods to conduct Hierarchical clustering, and Ward's method, Complete-linkage clustering, and Centroid-linkage clustering were selected. The three Hierarchical clustering methods and the K-medoid clustering method were used for the categorization and the results were compared. The one that ends up with the lowest aggregate fit loss is finally chosen.

3. Results and Discussions

3.1. Aggregate-Fit-Loss Minimization Results

The overall aggregate-fit-loss was calculated by summing up the within-group aggregate-fit-loss of all the groups. Figure 2 shows the clustering results, where the x-axis is the number of groups, and the y-axis is the overall aggregate-fit-loss. The number of groups (k) ranges from 1 to 45. k= 1 is the case when no categorization is done, and it is when the overall aggregate-fit-loss is the largest. k= 45 is the case when each subject has its own group, and when the overall aggregate-fit-loss equals zero.

Clearly, among the four clustering methods, K-medoids clustering results in the lowest overall aggregate-fit-loss for the majority of k's. Therefore, K-medoids clustering is finally chosen. We called this finalized method the complete AFL method (AFL stands for aggregate-fit-loss).

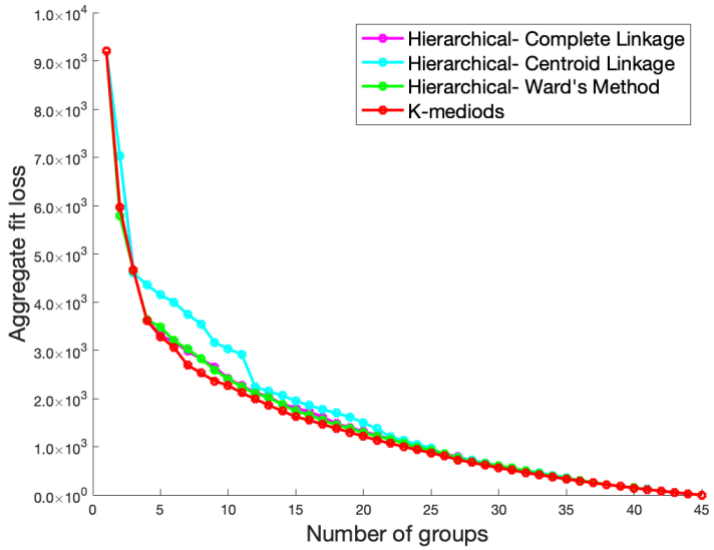

Figure 2. Comparing the results from different clustering methods

Categorizations were also done based on the traditional measurements. We measured the bust and underbust circumferences on the bust and underbust planes of the scan, respectively (Figure 1a). The difference between the bust and underbust circumferences, which is generally used to determine cup sizes, will be referred to as DeltaB. Evenly spaced intervals were created for the full range of underbust circumference within the data, and the number of intervals is also k ($1 \leq k \leq 45$). Figure 3 shows four examples when k= 2, 4, 5 and 6, respectively, assuming the full range of underbust circumference is from 28 to 40 inches (assumed integer values rather than actual values were used for better legibility). In addition, the prototype shape of a group (of an interval) was set to be whosever the underbust circumference

was closest to the mid interval value (Figure 3). Same thing was done for DeltaB. This way of categorization will be referred to as the traditional method. Furthermore, if we create groups based on either underbust circumference or DeltaB, but use our algorithm to select the best prototypes that come with the lowest within-group aggregate-fit-loss, we will have an improved version of the traditional method, which we will call the partial AFL method.

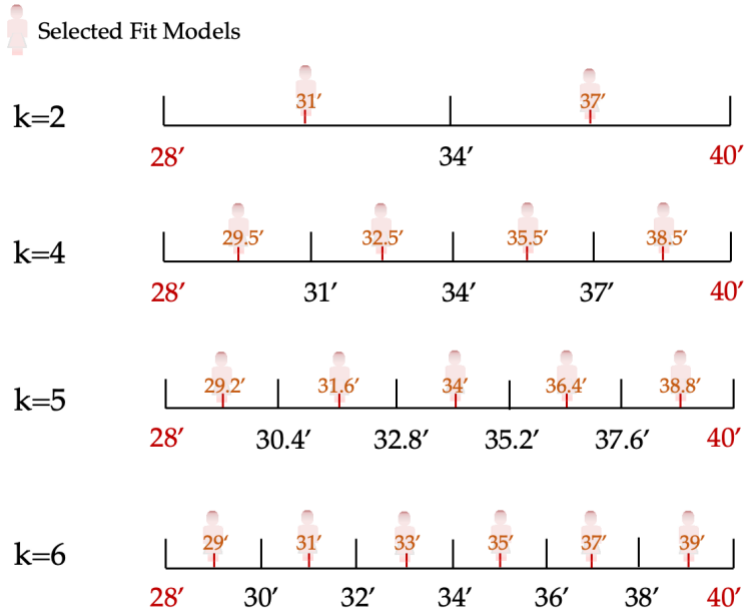

Figure 3. Demonstration of how size groups were created based on underbust measurement

Figure 4 shows the comparison among the traditional method, the partial AFL method and the complete AFL method using K-medoids clustering, represented by a black curve, a blue curve and a red curve, respectively. In both cases (categorized by underbust circumference or by DeltaB), a significant reduction in the overall aggregate-fit-loss can be observed in the blue curve from the black curve. A much more significant reduction can be observed in the red curve.

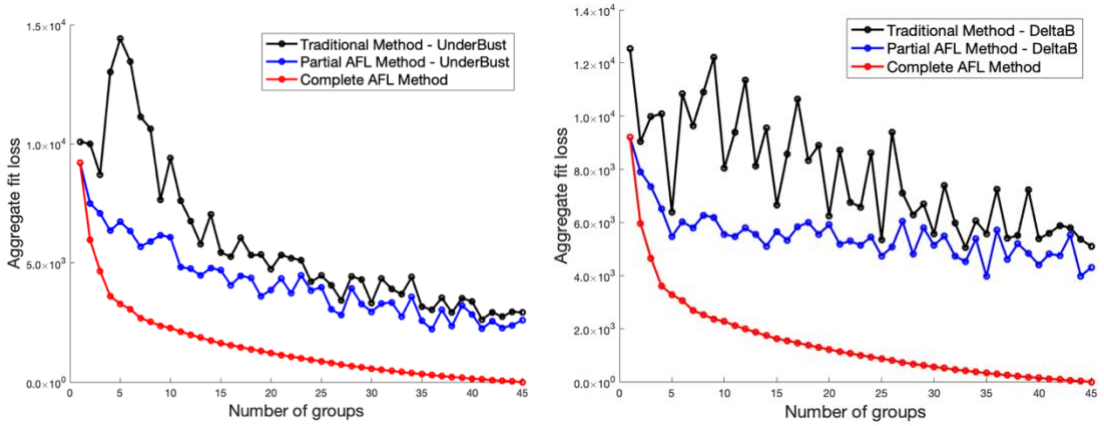

a) Traditional categorization based on Underbust circumference

b) Traditional categorization based on DeltaB (difference between bust and underbust)

Figure 4. The complete AFL method compared with the traditional sizing method and the partial AFL method

3.2. Prototype breast shapes

The selection of the number of sizes is always a challenging task for the development of sizing systems. On the one hand, fewer number of sizes is preferred for cost-effectiveness and out of the concerns of the limited retail sale space. On the other hand, larger number of sizes can accommodate a higher percentage of the population and provide better fit. As shown in Figure 2 and Figure 4, the overall aggregate-fit-loss reduces accordingly as the subjects are categorized into a larger number of groups. The curve of the complete AFL method (i.e. the red curve), however, has a gradual change in its slope. The overall aggregate-fit-loss drops more dramatically at the beginning (the slope is much steeper when $k \leq 4$), whereas it drops less significantly thereafter. This means that increasing the number of groups is more efficient when the number of groups is small. When k= 4, the accumulative reduction in the overall aggregate-fit-loss reaches 60% of the initial aggregate-fit-loss value (when k= 1). It requires $k \geq 13$ for the accumulative reduction to reach 80% of the

initial value, and k ≥ 24 to reach 90%. Therefore, we selected k= 4 to be the appropriate number of groups. The four prototype breasts are shown in Figure 5. The four women who own the prototype breasts shown in Figure 5a, b, c and d will be referred to as Subject a, b, c and d, respectively. They have the most representative breast shapes for this small group of females. For this target population, we suggest bra companies to recruit the four women back as fit models or at least develop products based on their dress forms.

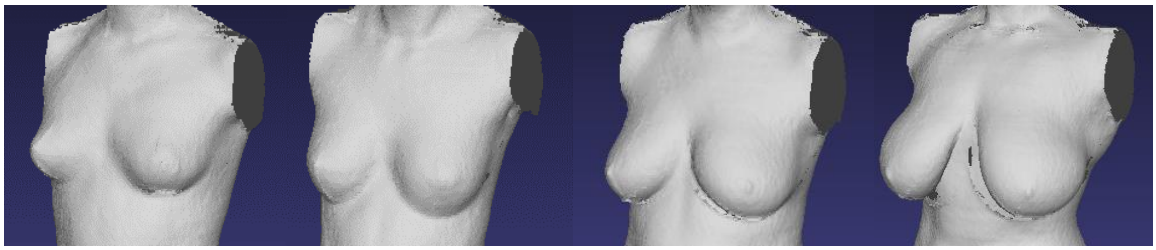

a) Bust: 94.1 cm Underbust: 82.5 cm DeltaB: 11.6 cm

b) Bust: 86.0 cm Underbust: 72.3 cm DeltaB: 13.7 cm

c) Bust: 100.5 cm Underbust: 83.0 cm DeltaB: 17.5 cm

d) Bust: 125.1 cm Underbust: 88.0 cm DeltaB: 37.1 cm

Figure 5. The prototype breast forms when k= 4

3.3. Application of the clustering results

Now that the categorization of the 45 scans has been finalized, the clustering results can be considered as the basis of a sizing system. As mentioned in Section 2.2, one breast scan was randomly selected and reserved for demonstration purpose. This reserved subject can be considered as a new case (or a new consumer) waiting to be assigned to one of the existing groups. An appropriate way to locate the right group for a new case is essential, because it can help a new consumer to find her correct (or best fitting) apparel product from the sizing system provided.

The fit models or dress forms, i.e. the prototype breasts obtained through the clustering and optimization, is the basis for product development. Maintaining the prototypes can ensure the consistency in the products in terms of fit. It is also the

fastest and most calculation-efficient way for the allocation of a new case. It contains two steps: 1) calculate the fit-loss between the new case and each of the prototypes; 2) designate the new case to the group of which the prototype has the lowest fit-loss value associated. Moreover, because the prototypes remain the same, all the other cases are impact free, thus the increase in the overall aggregate-fit-loss is the same as the fit-loss between the new case and the prototype of a group.

Table 1 includes the fit-loss of the reserved case from each of the prototypes (see the fourth column), among which the fit-loss from Subject c is the lowest. Therefore, the reserved case should be designated to Group 3. The increase in the overall aggregate-fit-loss by including this new case can be as low as 104.7. Moreover, before the reserved case was included, the averaged fit-loss values between a prototype and each of its group members are 75.2, 68.4, 108.3 and 0, respectively, for the four groups (the third column of Table 1). 104.7 is a value smaller than the original averaged fit-loss value of 108.3, which also confirms that designating the reserved case to Group 3 is a good choice. Even though the fit-loss between the reserved case and Subject c is only 130.3, designating the case to Group 1 will cause an increase in the averaged fit-loss value for Group 1, as 130.3 is much larger than 75.2.

Table 1. The impact of the new case on the overall aggregate-fit-loss

Group #	Prototypes	The original averaged fit-loss between a prototype and each group members	The fit-loss of the new case from the prototype	The aggregate-fit-loss increase when the new case becomes the prototype of the group
1	Subject a	75.2	130.3	3533.1
2	Subject b	68.4	202.9	4336.6
3	Subject c	108.3	104.7	2001.7
4	Subject d	0	1578.0	1578.0

The scan of the reserved subject


Furthermore, in the rare case scenario where the breast shape of a new subject has the same amount of fit-loss with more than one prototypes, then the scan of the subject can be classified into any of the corresponding groups, and the subject herself can try on all of the corresponding sizes and make judgment based on her subjective preference.

Meanwhile, if a considerable number of new cases have been added into the database, it may be preferable to change the prototypes. The reserved case was also used to demonstrate how to allocate a new case while allowing for the new case itself to be the new prototype of a group. The new case may or may not be suitable as the new prototype, depending on the amount of the within-group aggregate-fit-loss that it brings in. Again, the other groups remain impact free, thus the change in the within-group aggregate-fit-loss of one group, to which the new case got assigned, is the same as the change in the overall aggregate-fit-loss.

The increase in the overall aggregate-fit-loss was calculated when the reserved case was made the prototype of that group temporarily (see Table 1, the last column). As shown in Table 1, for most of the cases, the increase in the aggregate-fit-loss is very large, much larger than when the new case was not made to be the prototype. Therefore, for this particular subject, it is more appropriate to just make it an ordinary group member. However, for another subject, it is possible that making it the prototype of a certain group will result in a smaller increase in the aggregate-fit-loss.

In addition, the two values associated with Subject d of Group 4 in Table 1 are exactly the same (1578.0). It is because originally Group 4 only contained one subject (i.e. Subject d). Whether the new case becomes the prototype or not, the increase in the aggregate-fit-loss is always the fit-loss value between the two. The group with only one or very few number of subjects can be removed to further reduce the total number of groups, sacrificing the accommodation rate of the population.

In this section, the randomly-selected reserved scan was presented as a demonstration. The subject to which the scan belongs was regarded as a new consumer, looking for her size. Any new scans of female breasts can be handled in the exact same way as described above.

3.4. Optimization results constrained by band sizes

Thus far, we have demonstrated how to apply our method to a population unconstrained by preconditions such as breast size. To further investigate the relationship between breast size and shape, and to provide a more feasible solution for the improvement of bra sizing using our method, we brought in the constraint of band sizes into the categorization and proposed a hybrid AFL method. The 45 subjects were firstly sorted into band size groups based on their underbust measurements, then the optimization of aggregate-fit-loss was done within each size group. A total of five band sizes were involved, namely Size 28, Size 30, Size 32, Size 34 and Size Over 34 (see Table 2). The goal is to find optimal subdivision criteria in replacement of the bust-underbust-difference (which determines cup size) while maintaining the structure of the band sizes.

Table 2. Band size groups and their corresponding underbust measurement ranges

#	Band size	Underbust measurement ranges (in.)	Underbust measurement ranges (cm)	Number of subjects included (j)
1	28	[27, 29)	[68.6, 73.7)	8
2	30	[29, 31)	[73.7, 78.7)	17
3	32	[31, 33)	[78.7, 83.8)	12
4	34	[33, 35)	[83.8, 88.9)	6
5	Over 34	[35, ∞)	[88.9, ∞)	2

For each band size, optimized categorizations (using k-medoid clustering and the algorithm that finds the optimal prototypes) were done j times, where j is the total number of subjects in that size group (e.g. j= 12 for Size 32). The total number of sub-groups is represented by k and satisfies the following equation (Eq. 3).

$$k = j_1 + j_2 + j_3 + j_4 + j_5 \quad \text{(Eq.3)}$$

where j_1 to j_5 corresponds to the number of sub-groups for Size 28, 30, 32, 34 and Over 34, respectively. $j_i \geq 1$ (i= 1 to 5) to maintain the structure of the band sizes (in other words, no band size is left out).

Clearly, k is at least 5, and at most 45 (when every subject forms a sub-group). Nevertheless, how to distribute k into the five j's when k falls between 6 and 44 is not intuitive and requires further calculations.

Increasing any of the j's by 1, which also means increasing k by 1, will result in a reduction in the overall aggregate-fit-loss, and there is always one particular j which corresponds to the maximum reduction in the overall aggregate-fit-loss among the five j's. Therefore, a program was developed which returns the band-size group whose j corresponds to the maximum decrease in the overall aggregate-fit-loss when j increases by 1. This program was set to begin with k= 5 (when all j's equal 1), add one

sub-group each time while keeping track of the aggregate-fit-loss value, and finally stop at k= 45 (when all j's reach their maximum). Table 3 shows part of the results.

Table 3. Optimal distribution of the total number of groups (k) into size groups (j's)

Band size		Number of sub-groups within each band-size group						
28	j_1	1	1	1	2	3	5	8
30	j_2	1	1	3	5	6	12	17
32	j_3	1	1	2	2	4	6	12
34	j_4	1	2	3	4	5	5	6
Over 34	j_5	1	1	1	2	2	2	2
Total number of groups	k	5	6	10	15	20	30	45

The green curve in Figure 6 shows the results of the hybrid AFL categorization method. There is an increase of the aggregate-fit-loss in the green curve compared with the complete AFL method (i.e. red curve). However, the decrease in the aggregate-fit-loss from the black curve and the blue curve, to the green curve are still significant.

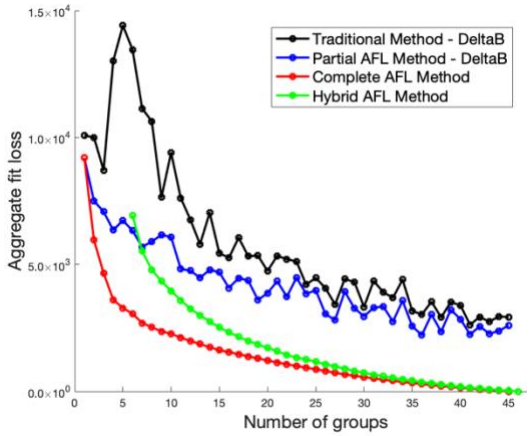

a) Traditional categorization based on Underbust circumference

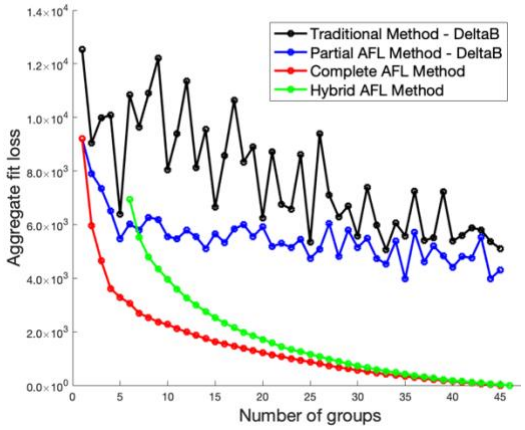

b) Traditional categorization based on DeltaB (difference between bust and underbust)

Figure 6. The results of the hybrid method (the green curves)

The hybrid method has a more realistic application for the sizing systems of bras. While the complete AFL method requires building a new sizing system from scratch, the hybrid method keeps the structure of band sizes, but can still achieve a significant improvement in sizing. The clustering results can be maintained, and new cases be added as described in Section 3.3. Furthermore, when k= 20 (which means 86.8% of decrease in the overall aggregate-fit-loss from k= 1), it requires only four cup sizes per band size on average (4 × 5 = 20). Considering the wide variety of cup sizes in the market (from A Cup to G Cup or more), four is an acceptable number.

4. Conclusions

To improve the sizing systems of bras and potentially other apparel products, in this study we investigated the breast shape of 46 non-obese (BMI < 30), Caucasian female subjects (Age 18 to 45), and proposed a novel method for minimizing the aggregate-fit-loss of a sizing system through categorization and optimized selection of prototypes. A fit-loss function was introduced that calculates the dissimilarity between

any two scans of breasts via pointwise comparisons of 9,000 points. By directly using each point's distance towards the origin (i.e. Point (0, 0, 0)) instead of body measurements, the breast morphology can be more precisely captured. One of the 46 scans was reserved for later demonstration, while a pairwise dissimilarity matrix was generated for the rest 45 scans.

The within-group aggregate-fit-loss is minimized by an algorithm that returns the optimal prototype corresponding to the lowest aggregate-fit-loss of a given group. The overall aggregate-fit-loss is reduced by breast shape categorization based on the dissimilarity matrix. Three Hierarchical clustering methods, including Ward's method, Complete-linkage, and Centroid-linkage clustering, and K-medoid clustering were used for the categorization and the results were compared. In the end, K-medoid clustering method was chosen. Compared with the traditional method and the partial AFL method, the complete AFL method shows significant reduction in the overall aggregate-fit-loss. In addition, by studying the slope decrements of the overall aggregate-fit-loss curve of the chosen clustering method, we decided that $k = 4$ should be the appropriate number of groups. The prototype breast shapes of the four groups were presented.

Additionally, we demonstrated two methods to implement the clustering results, by regarding the reserved scan as a new consumer waiting to be assigned to one of the existing groups. One method maintains the prototype of each group whereas the other allows for the prototypes to be replaced by the new case. To ensure the consistency in the fit of the products and to reduce the amount of calculation needed, maintaining the prototypes is preferable. In this method, the new case can be allocated by finding the group of which the prototype has the lowest fit-loss value with the new case among all the prototypes.

Finally, to provide a more feasible solution for the improvement of bra sizing, the

constraint of band sizes was brought into the categorization. The subjects were firstly sorted into band size groups based on their underbust measurement, then the optimization of aggregate-fit-loss was done within each size group. Furthermore, we proposed a way to decide on which band-size group should have more sub-groups than the others also using aggregate-fit-loss as the reference. The results of this hybrid categorization method show slight increase in the aggregate-fit-loss value, compared with the optimal results of the complete AFL method, but reveal significant decrease from the traditional method.

This study has several limitations. Firstly, the sample size may be too small to serve as the basis of a sizing system, especially when adding the constraint of band sizes (too few subjects were included in each band-size group). However, in more of a sense, the 46 scans were used to demonstrate our method. Future studies can adopt the same method on a national scale database of body scans. Secondly, the perception of fit is not taken into consideration in this study. It is possible that within certain threshold, the tiny differences in shape create no difference in terms of fit, and therefore the corresponding fit-loss should be evaluated as zero. In addition, a wearer might feel quite differently for a garment that is too large, in contrast for a garment that is too small. Hence, it may be more reasonable to set different penalties for a shape being larger than the prototype shape, in contrast for a shape being smaller and based on difference areas on the body, which may have different levels of sensitivity. Lastly, despite Moiré patterns' capability to reveal breast contour lines, they cannot provide information on the physical properties of the breasts. The physical properties, determined by tissue composition, are the ultimate ruling factors to distinguish the breast (dominated by fat tissue) from the chest wall (dominated by the pectoral muscles). A robust, automated and non-contact method to identify the upper boundary of breasts remains to be developed.

Although (as with any new method) limitations remain which will be the focus of further work, our novel method introduces novel parameters to evaluate breast shape in 3D. This method has potential as a replacement for the current method using 1D body measurements taken from the body surface, which have been proven in many studies to be insufficient in capturing body shape variations, preventing development of sizing systems that provide good fit. In our method we have developed a way of capturing useful data from 3D body scans overall, comparing points throughout the surface of the scan to identify shape groupings, and thereby using all the information captured in the scan. This is the first true 3D system ever developed for categorizing shape. In aid of this, we proposed a new way to align body scans, at the central axis defined by the averaged x and y coordinates of all the points on the scan, which allows us to acquire a standardized reference point which is based on more data than traditional anatomical body landmarks. This can potentially facilitate the automation of handling 3D body scan data, increasing the value of automatically detected landmarks. We also recognize the challenge of providing a feasible solution for both the industry and consumers to ensure that sizing systems developed through our method are applicable in real life. For the industry, finding ideal human fit models has always been a challenge. The general lack of a reliable selection criteria for fit models exacerbates the inconsistency of product fit among companies. Our solution facilitates selection of fit models based on body shape for the first time, and our method can associate the fit models closely with individual consumers of a company's target market. For consumers, we provided technological solutions for finding their shape-based selection of products that may best fit them. With 3D scanner becoming more accessible and the development of the technology of body scanning using personal cellphones, expecting consumers to upload their body scans to online stores or to step into the 3D scanners in physical stores is no longer implausible. With the

method proposed in this paper, revolutionary change in apparel sizing may take place in the short future.

DISCLOSURE STATEMENT

This chapter is a peer-reviewed journal paper published in 2020. Citation information is listed below. Reuse permission has been acquired from Sage.

Pei, J., Fan, J. & Ashdown, S. P. (2020). A Novel Optimization Approach to Minimize Aggregate-Fit-loss for Improved Breast sizing, *Textile Research Journal*, published online. https://doi.org/10.1177/0040517519901318

REFERENCES

Alexander, M., Connell, L. J., & Presley, A. B. (2005). Clothing fit preferences of young female adult consumers. *International Journal of Clothing Science and Technology*, *17*(1), 52-64.

Ashdown, S., & Loker, S. (2010). Mass-customized target market sizing: Extending the sizing paradigm for improved apparel fit. *Fashion Practice*, *2*(2), 147-173.

Ashdown, S. P. (2014). Creation of ready-made clothing: The development and future of sizing systems. In Faust, M. E., & Carrier, S.(Eds.), *Designing Apparel for Consumers: The Impact of Body Shape and Size* (pp. 17-33). Woodhead Publishing.

Arbutina, M., Dragan, D., Mihic, S., & Anisic, Z. (2017). Review of 3D body scanning systems. *Acta Technica Corviniensis-Bulletin of Engineering*, *10*(1), 17.

Bye, E., Labat, K. L., & Delong, M. R. (2006). Analysis of body measurement systems for apparel. *Clothing and Textiles Research Journal*, *24*(2), 66-79.

Bengtson, B. P., & Glicksman, C. A. (2015). The standardization of bra cup measurements: redefining bra sizing language. *Clinics in plastic surgery*, *42*(4), 405-411.

Cain, G. (1950). The American way of designing. Fairchild Publications.

Chun-Yoon, J., & Jasper, C. R. (1996). Key dimensions of women's ready-to-wear apparel: Developing a consumer size-labeling system. *Clothing and Textiles Research Journal*, *14*(1), 89-95.

Chun, J. (2007). Communication of sizing and fit. *Sizing in clothing: Developing effective sizing systems for ready-to-wear clothing*, 220-243.

Chung, M. J., Lin, H. F., & Wang, M. J. J. (2007). The development of sizing systems for Taiwanese elementary-and high-school students. *International Journal of*

Industrial Ergonomics, *37*(8), 707-716.

Chen, C. M., LaBat, K., & Bye, E. (2011). Bust prominence related to bra fit problems. *International Journal of Consumer Studies*, *35*(6), 695-701.

Coltman, C. E., Steele, J. R., & McGhee, D. E. (2018). Effects of age and body mass index on breast characteristics: a cluster analysis. *Ergonomics*, *61*(9), 1232-1245.

Doustaneh, A. H., Gorji, M., & Varsei, M. (2010). Using Self Organization Method to Establish Nonlinear Sizing System. *World Applied Sciences Journal*, *9*(12), 1359-1364.

Filipe, A. B., Carvalho, C., Montagna, G., & Freire, J. (2015). The fitting of plus size bra for middle aged women. *Procedia Manufacturing*, *3*, 6393-6399.

Gupta, D., & Gangadhar, B. R. (2004). A statistical model for developing body size charts for garments. *International Journal of Clothing Science and Technology*, *16*(5), 458-469.

Gribbin, E. A. (2014). Body shape and its influence on apparel size and consumer choices. In *Designing apparel for consumers* (pp. 3-16). Woodhead Publishing.

Hsu, C. H. (2009). Data mining to improve industrial standards and enhance production and marketing: An empirical study in apparel industry. *Expert Systems with Applications*, *36*(3), 4185-4191.

Han, H., Nam, Y., & Choi, K. (2010). Comparative analysis of 3D body scan measurements and manual measurements of size Korea adult females. *International Journal of Industrial Ergonomics*, *40*(5), 530-540.

Haleem, A., & Javaid, M. (2019). 3D scanning applications in medical field: a literature-based review. *Clinical Epidemiology and Global Health*, *7*(2), 199-210.

Kinley, T. R. (2003). Size variation in women's pants. *Clothing and Textiles Research Journal*, *21*(1), 19-31.

Kennedy, K. (2009), "What size am I? Decoding women's clothing standards",

Fashion Theory, Vol. 13 No. 4, pp. 511-530.

Kaufman, L., & Rousseeuw, P. J. (2009). *Finding groups in data: an introduction to cluster analysis* (Vol. 344). John Wiley & Sons.

Kim, D. E., LaBat, K., Bye, E., Sohn, M., & Ryan, K. (2015). A study of scan garment accuracy and reliability. *The journal of the Textile Institute*, *106*(8), 853-861.

Lee, H. Y., Hong, K., & Kim, E. A. (2004). Measurement protocol of women's nude breasts using a 3D scanning technique. *Applied Ergonomics*, *35*(4), 353-359.

Liu, Y., Wang, J., & Istook, C. L. (2017). Study of optimum parameters for Chinese female underwire bra size system by 3D virtual anthropometric measurement. *The Journal of The Textile Institute*, *108*(6), 877-882.

McCulloch, C. E., Paal, B., & Ashdown, S. P. (1998). An optimisation approach to apparel sizing. *Journal of the Operational Research Society*, *49*(5), 492-499.

McGhee, D. E., & Steele, J. R. (2010). Optimising breast support in female patients through correct bra fit. A cross-sectional study. *Journal of Science and Medicine in Sport*, *13*(6), 568-572.

Miao, H., Panna, A., Gomella, A. A., Bennett, E. E., Znati, S., Chen, L., & Wen, H. (2016). A universal moiré effect and application in X-ray phase-contrast imaging. *Nature physics*, *12*(9), 830.

McGhee, D. E., Ramsay, L. G., Coltman, C. E., Gho, S. A., & Steele, J. R. (2018). Bra band size measurements derived from three-dimensional scans are not accurate in women with large, ptotic breasts. *Ergonomics*, *61*(3), 464-472.

Paal, B. (1997). *Creating efficient apparel sizing systems: an optimization approach*. Cornell University, May.

Petrova, A. (2007). Creating sizing systems. *Sizing in clothing: Developing effective sizing systems for ready-to-wear clothing*, 57-87.

Pandarum, R., Yu, W., & Hunter, L. (2011). 3-D breast anthropometry of plus-sized

women in South Africa. *Ergonomics*, *54*(9), 866-875.

Pei, J., Park, H., Ashdown, S. P. & Vuruskan, A. (2017). A sizing improvement methodology based on adjustment of interior accommodation rates across measurement categories within a size chart. *International Journal of Clothing Science and Technology*, *29*(5), 716-731.

Pei, J., Park, H., & Ashdown, S. P. (2019). Female breast shape categorization based on analysis of CAESAR 3D body scan data. *Textile Research Journal*, *89*(4), 590-611.

Pei, J., Fan, J. & Ashdown, S. P. (2019). Detection and Comparison of Breast Shape Variation among Different 3D Body Scan Conditions: Nude, with a Structured Bra, and with a Soft Bra, *Textile Research Journal*, *89*(21), 4595-4606.

Peterson, A., & Suh, M. (2016). Effect of Bra Style and Size on its Fit and Comfort.

Peterson, A., & Suh, M. (2019). Exploratory Study on Breast Volume and Bra Cup Design. *Journal of Textile and Apparel, Technology and Management*, *11*(1).

Robinette, K. M., Daanen, H., & Paquet, E. (1999). The CAESAR project: a 3-D surface anthropometry survey. In *3-D Digital Imaging and Modeling, 1999. Proceedings. Second International Conference on* (pp. 380-386). IEEE.

Takasaki, H. (1970). Moiré topography. *Applied optics*, *9*(6), 1467-1472.

Tryfos, P. (1986). An integer programming approach to the apparel sizing problem. *Journal of the Operational Research Society*, 1001-1006.

Tadisina, K., Frojo, G., Plikaitis, C., & Bernstein, M. (2016). Basics of Bra Sizing. *Plastic and Reconstructive Surgery*, *138*(4).

Smathers, D. G., & Horridge, P. E. (1979). The effects of physical changes on clothing preferences of elderly women. *The International Journal of Aging and Human Development*, *9*(3), 273-278.

Shen, L., & Huck, J. (1993). Bodice pattern development using somatographic and

physical data. *International Journal of Clothing Science and Technology*, *5*(1), 6-16.

Salehi, E. M., & Shahrabi, J. (2012). Developing a new suit sizing system using data optimization techniques. *International Journal of Clothing Science and Technology*, *24*(1), 27-35.

Vinué, G., León, T., Alemany, S., & Ayala, G. (2014). Looking for representative fit models for apparel sizing. *Decision Support Systems*, *57*, 22-33.

Wit, E., & McClure, J. (2004). *Statistics for microarrays: design, analysis and inference*. John Wiley & Sons.

Wang, Z., & Suh, M. (2019). Bra Underwire Customization With 3-D Printing. *Clothing and Textiles Research Journal*, *37*(4), 281-296.

Xia, S., West, A., Istook, C., & Li, J. (2018, October). Acquiring Accurate Body Measurements on a Smartphone from Supplied Colored Garments for Online Apparel Purchasing Platforms and E-Retailers. In *Proc. 3DBODY. TECH 2018-9th Int. Conf. Exhib. 3D Body Scanning Process. Technol. Lugano, Switzerland* (pp. 126-130).

Yu, W., Fan, J., Ng, S. P., & Harlock, S. (2014). *Innovation and technology of women's intimate apparel*. Woodhead Publishing.

Zheng, R., Yu, W., & Fan, J. (2007). Development of a new Chinese bra sizing system based on breast anthropometric measurements. *International Journal of Industrial Ergonomics*, *37*(8), 697-705.

Zhu, S., Mok, P. Y., & Kwok, Y. L. (2013). An efficient human model customization method based on orthogonal-view monocular photos. *Computer-Aided Design*, *45*(11), 1314-1332.

Zakaria, N., & Gupta, D. (2014). Apparel sizing: existing sizing systems and the development of new sizing systems In Gupta, D., & Zakaria, N. (Eds.),

Anthropometry, apparel sizing and design (pp. 3-15). Elsevier.

Zhu, S., & Mok, P. Y. (2015). Predicting realistic and precise human body models under clothing based on orthogonal-view photos. *Procedia Manufacturing*, *3*, 3812-3819.

CHAPTER 7

CONCLUSIONS AND SUGGESTIONS FOR FURTHER WORK

Due to the limitation of traditional linear body measurements in representing the complicated 3D shape of the female breast, in this dissertation, alternative methods to quantifying breast shape were proposed, analyzed and examined (Research Objective 1).

In 2D, topographic contour maps were created and an Asymmetry Index was proposed to quantify the degree of asymmetry between the left and right breasts. Thirty-five non-traditional measurements were extracted from the simplified contour maps. Four critical shape factors were summarized according to the dominating measurements which present higher variance, namely: 1) the vertical position of the bust point, 2) the volume of the breast, 3) the horizontal position of the bust point, and 4) the fullness of the breast. This 2D system was then used in the aesthetic evaluation of nude breast and the shaping effects of structured-bras and soft-bras (Research Objective 4), linking the subjective evaluation methods with the objective evaluation methods (Research Objective 3). While the traditional measurements such as bust circumference are typically unable to detect the modification of breast shape introduced by a bra, eight among the thirty-five non-traditional measurements were found to be especially sensitive and indicative to this shape modification.

In 3D, two methods of handling 3D body scans were proposed, which capture data throughout the surface of the scan systematically. Heat maps that visualize the shape variations from the nude-to-bra condition via colors were plotted on the surfaces of the 3D scans of the participants in bras (Research Objective 4), and were used for qualitative analysis, again, associating the subjective evaluation methods with the

objective evaluation methods (Research Objective 3). Regression models were built to predict the in-bra shape given only the nude breast shape (Research Objective 4). Moreover, the same scan processing methods were used to handle 4D scans, which are essentially a series of 3D scans captured in time.

Both the 2D and 3D systems eliminate the use of traditional linear measurements (Research Objective 1), and also eliminate the need of palpation to find anatomical body landmarks, on which the accuracy of traditional measurements depend (Research Objective 2). The 2D and 3D systems can also be used by plastic surgeons to predict thus improve surgical outcomes. In addition, applying these methods on a national scale database of 3D scans of breasts can offer helpful information to healthcare providers to establish breast care guidelines.

In 4D, 4D body scanning technology was introduced to quantitively study breast shape under motion (Research Objective 5). A protocol to handle and analyze 4D data for application in product design was developed to inform future research (Research Objective 4). The promises and challenges of the 4D body scanning technology were also discussed. Ten breast shape related measurements were tracked in dynamic states and compared with the static state. The results can benefit product development of sports bras in particular, and female personal protective equipment (PPE) such as body armors, fall harness systems, turnout gear, etc., which require high degree of fit and mobility at the upper torso. In addition, it was further proved that anatomical landmarks should not be used (Research Objective 2), not even to align scans captured in time because: 1) they are easy to fall off or shift under motion; 2) they can be obstructed by the swinging arms or buried in skin folds; 3) without falling, shifting or obstruction, still they may be inadequate to provide accurate alignment due to soft tissue artifacts. Moreover, while the information of the upper boundary of the breasts is missing on 3D scans, it can be retrieved with the help of 4D scanning, by taking

advantage of the time delay in the vertical displacement between the breasts and the chest wall during physical activity. This non-contact method to identify breast boundary does not rely on landmarks as well (Research Objective 2). It is essential for the accurate separation of the breasts so that critical anthropometric measurements such as breast volume (which is directly related to bra cup size) can be acquired. It is also essential for completeness of the 3D breast-shape evaluation system so that the 3D system may be used for product development purposes (Research Objective 6).

Finally, the aforementioned methods and results were integrated and adjusted to provide useful information for the improvement of bra sizing (Research Objective 6). Product development of ready-to-wears, including bras, are still based on the body-shapes of the human fit models which a company hires. The body-shape difference between a consumer and the fit model of their size results in a fit-loss of certain degree. Aggregate-fit-loss is a concept attempting to estimate the accumulative fit-loss, resulting from the body-shape discrepancy, between the fit models and individual consumers. Based on the 3D evaluation system, a feasible solution to optimize the sizing system of bras was proposed, to minimize the aggregate-fit-loss by shape categorization and optimized selection of fit models (Research Objective 6). The fit-loss function calculates the dissimilarity between any two 3D body-scans, via pointwise comparisons of the point-to-origin distances of all the points on scan surface. This fit-loss function also extends the use of traditional linear measurements (Research Objective 1), and it is able to comprehensively capture the difference, even the nuances, in the 3D shape of the female breast between individuals. To make the sizing method more acceptable by the fashion industry, the constraint of band sizes was brought into the categorization. In other words, band sizes (determined by the size of the ribcage which is relatively stable and not affected by hormone levels) are kept in the sizing system, while the cup sizes are replaced by shape-based categories.

With or without the constraint of band sizes, the method overcomes the challenge of finding ideal fit models, filling the lack of reliable selection criteria which has been troubling the industry for a long time. It also associates the fit models closely with individual consumers of a company's target market. For consumers, technological solutions were also presented for finding their shape-based selection of products that may best fit them. By having her breasts scanned, a consumer no longer needs to take her own measurements (which is an exceptionally error-prone process) or to have a professional well-trained fit expert measure her breasts. Nor does she need to experience the frustration of finding her "correct" size based on sets of numbers in the size chart, which are often confusing. Her scan can be automatically allocated to the group of which the fit model has the lowest shape discrepancy (i.e. fit-loss value) with her. With 3D scanner becoming more accessible and the development of cellphone scanning, expecting consumers to upload their body scans to online stores or to step into the 3D scanners in physical stores is no longer implausible. Methods presented in this dissertation may bring revolutionary changes in apparel sizing and how bra products are made.

Suggestions for Future Work

Firstly, the methods proposed and examined in this dissertation are based on a limited number of body scans. The sample size may be too small to capture all the breast shape variation for the target population to serve as the basis for a sizing system. Future studies can adopt the same method on a national scale database of body scans. The processing of scans and the extraction of data were all done via Matlab® programs to ensure reliability and reduce human operation errors. Those programs make it possible and easier to handle large numbers of scans. Moreover, future studies can be done on a small but specific sample, for example, for the flat-chested

population who are under-studied, or for the large-breast population who are in general more frustrated with bra fit.

Secondly, by adopting the tools that associate subjective and objective evaluation methods, more studies can be done to interpret the perception of fit and aesthetics to inform product design. For example, it is possible that within certain threshold, the tiny differences in shape create no difference in terms of the perceived fit. In addition, a wearer might feel differently for a garment being too large, from a garment being too small. Therefore, to incorporate subjective perceptions to the aggregate-fit-loss method, it may be reasonable to set different weightings for a shape being larger than that of the fit-model's, in contrast for a shape being smaller. It may also be reasonable to set weightings for fit-loss values based on difference areas on the body, where different levels of sensitivity may affect fit perceptions. Furthermore, future studies can look into the material properties of bras and incorporate those information in the study of shape modification by a bra. It will also be important to test all the objective evaluation methods, especially the sizing method, on real bra products, fit models and participants, to make them truly practicable.

In terms of the 4D body scanning technology, future researchers need to figure out a way to secure landmarks on participant's body and prevent them from shifting, falling off, obstructed by the swinging arms and buried in skin folds. In addition, 4D scanning typically captures hundreds of scans within minutes, therefore, an automatic process needs to be developed to replace manual work so that this technology can effectively benefit human-centered product design. The technology can serve as a useful tool for sports bra evaluation. It can also be used to compare the degree of shape change of breasts during physical activities with and without a bra is worn, or when different types of bras are worn, to increase the understanding of breast kinematics. Moreover, studies can be done for other types of wearable products for

women as well. There are many remaining challenges for the technology, but it offers endless possibilities for research at the same time.